Performance Analysis of Hybrid ARQ

Protocols in a Slotted Code Division

Multiple-Access Network

A THESIS

Presented to

The Academic Faculty

By

Joseph M. Hanratty

In Partial Fulfillment

of the Requirements for the Degree of

Doctor of Philosophy in Electrical Engineering

Georgia Institute of Technology

25 July 1989

89 8 08 175

REPORT DOCUMENTATION PAGE	*Form Approved* OMB No. 0704-0188

1. AGENCY USE ONLY (Leave Blank)	2. REPORT DATE August 1989	3. REPORT TYPE AND DATES COVERED Final

4. TITLE AND SUBTITLE Performance Analysis of Hybrid ARQ Protocols in a Slotted Code Division Multiple Access Network

5. FUNDING NUMBERS

6. AUTHOR(S) Joseph M. Hanratty

7. PERFORMING ORGANIZATION NAME(S) AND ADDRESS(ES)
Major Joseph M. Hanratty, 4630 Abelia Ct Acworth GA 30101
Georgia Institute of Technology; Atlanta GA, 30332

8. PERFORMING ORGANIZATION REPORT NUMBER
UNK

9. SPONSORING/MONITORING AGENCY NAME(S) AND ADDRESS(ES)
U.S Army, (Signal Corps)

10. SPONSORING/MONITORING AGENCY REPORT NUMBER
UNK

11. SUPPLEMENTARY NOTES

12a. DISTRIBUTION/AVAILABILITY STATEMENT
Unlimited

12b. DISTRIBUTION CODE

13. ABSTRACT *(Maximum 200 words)*

A link throughput-delay analysis is presented for a slotted direct-sequence spread-spectrum multiple-access packet radio network (PRN) operating in the presence of background noise, multiple-access interference, and pulsed jammer noise. The PRN is comprised of an arbitrary number of full-duplex radio units arranged in a paired-off topology. Slotted ALOHA random access is used in conjunction with CDMA for channel access and a type I hybrid ARQ is used for error control. Expression are derived for the link throughput-delay in terms of the channel cutoff rate and capacity. With the friendly objective of maximizing the link throughput, and the enemy objective of minimizing the link throughput, the dependency of the *optimal* retransmission probability, processing gain, code rate, and jamming fraction on the population size, traffic intensity, bit energy-to-background-noise ratio, and bit energy-to-jammer-noise ratio is examined in detail. It is shown that a properly designed (optimized) PRN using random-access CDMA offers a significantly larger heavy load throughput than a random-access PRN.

14. SUBJECT TERMS Spread Spectrum Multiple Access, Anti-Jamming, Error Control Coding, Packet Radio Networks

15. NUMBER OF PAGES 155

16. PRICE CODE

17. SECURITY CLASSIFICATION OF REPORT UNCLASSIFIED	18. SECURITY CLASSIFICATION OF THIS PAGE UNCLASSIFIED	19. SECURITY CLASSIFICATION OF ABSTRACT UNCLASSIFIED	20. LIMITATION OF ABSTRACT UL

GENERAL INSTRUCTIONS FOR COMPLETING SF 298

The Report Documentation Page (RDP) is used in announcing and cataloging reports. It is important that this information be consistent with the rest of the report, particularly the cover and title page. Instructions for filling in each block of the form follow. It is important to *stay within the lines* to meet *optical scanning requirements*.

Block 1. Agency Use Only (Leave blank).

Block 2. Report Date. Full publication date including day, month, and year, if available (e.g. 1 Jan 88). Must cite at least the year.

Block 3. Type of Report and Dates Covered. State whether report is interim, final, etc. If applicable, enter inclusive report dates (e.g. 10 Jun 87 - 30 Jun 88).

Block 4. Title and Subtitle. A title is taken from the part of the report that provides the most meaningful and complete information. When a report is prepared in more than one volume, repeat the primary title, add volume number, and include subtitle for the specific volume. On classified documents enter the title classification in parentheses.

Block 5. Funding Numbers. To include contract and grant numbers; may include program element number(s), project number(s), task number(s), and work unit number(s). Use the following labels:

C	- Contract	PR	- Project
G	- Grant	TA	- Task
PE	- Program Element	WU	- Work Unit Accession No.

Block 6. Author(s). Name(s) of person(s) responsible for writing the report, performing the research, or credited with the content of the report. If editor or compiler, this should follow the name(s).

Block 7. Performing Organization Name(s) and Address(es). Self-explanatory.

Block 8. Performing Organization Report Number. Enter the unique alphanumeric report number(s) assigned by the organization performing the report.

Block 9. Sponsoring/Monitoring Agency Name(s) and Address(es). Self-explanatory.

Block 10. Sponsoring/Monitoring Agency Report Number. (If known)

Block 11. Supplementary Notes. Enter information not included elsewhere such as: Prepared in cooperation with...; Trans. of...; To be published in.... When a report is revised, include a statement whether the new report supersedes or supplements the older report.

Block 12a. Distribution/Availability Statement. Denotes public availability or limitations. Cite any availability to the public. Enter additional limitations or special markings in all capitals (e.g. NOFORN, REL, ITAR).

DOD - See DoDD 5230.24, "Distribution Statements on Technical Documents."
DOE - See authorities.
NASA - See Handbook NHB 2200.2.
NTIS - Leave blank.

Block 12b. Distribution Code.

DOD - Leave blank.
DOE - Enter DOE distribution categories from the Standard Distribution for Unclassified Scientific and Technical Reports.
NASA - Leave blank.
NTIS - Leave blank.

Block 13. Abstract. Include a brief (*Maximum 200 words*) factual summary of the most significant information contained in the report.

Block 14. Subject Terms. Keywords or phrases identifying major subjects in the report.

Block 15. Number of Pages. Enter the total number of pages.

Block 16. Price Code. Enter appropriate price code (*NTIS only*).

Blocks 17. - 19. Security Classifications. Self-explanatory. Enter U.S. Security Classification in accordance with U.S. Security Regulations (i.e., UNCLASSIFIED). If form contains classified information, stamp classification on the top and bottom of the page.

Block 20. Limitation of Abstract. This block must be completed to assign a limitation to the abstract. Enter either UL (unlimited) or SAR (same as report). An entry in this block is necessary if the abstract is to be limited. If blank, the abstract is assumed to be unlimited.

Performance Analysis of Hybrid ARQ

Protocols in a Slotted Code Division

Multiple-Access Network

Approved:

Dr. Gordon L. Stüber, Chairman

Dr. Aubrey M. Bush

Dr. Stephen B. Wicker

Date approved by Chairman _8-1-89_

This dissertation is dedicated to

my mother,

Virginia C. Hanratty

and

to the memory of

my father,

Eugene J. Hanratty.

Acknowledgments

There are many individuals who have contributed to the present work. I am especially gratefull to Dr. Gordon L. Stüber, my thesis advisor, for his patience, assistance, and encouragement during the course of this work. He has been a true friend as much as he has been my mentor.

I wish to also extend a special thanks to Dr. Aubrey M. Bush for his guidance and many helpful insights into all aspects of the research.

I am grateful to Drs. S. Wicker, T-C Lea, and M. Ammar for their stimulating comments and valuable suggestions concerning this research.

I am pleased to acknowledge the support of the United States Army that provided the opportunity for advanced schooling.

Finally and most importantly, I wish to acknowledge the commitment, sacrifice, and support of my wife, Cathy, and children, Cameron and Jessica. I deeply appreciate their love and understanding. This thesis is as much theirs as it is mine.

Contents

List of Figures

List of Tables

Glossary of Symbols

a Product of the code rate and the bit energy-to-total noise ratio

b Product of the jamming fraction, code rate, and the bit energy-to-jammer noise ratio

C Channel capacity

C^* Optimal channel code rate assuming that the code rate equals C

D Average packet delay

D_d Deterministic packet delay

D_r Average packet retransmission delay

D_{BN} Delay resulting from the use of the binomial composite traffic arrival distribution

D_{NBN} Delay resulting from the use of a nonbinomial composite traffic arrival distribution

E Average number of packet retransmissions required per successfully transmitted packet

E_b Bit energy

E_S Code symbol energy

$E\{\cdot\}$ Expectation operator

$f_M(l)$ Probability distribution function for the number of attempted packet transmission made in a given time slot

$g_{\{R_o,C\}}(P_S)$ Functional relationship between the probability of symbol error and the channel cutoff rate and capacity

$H[\cdot]$ Binary entropy function

m Number of allowable packet transmissions during a given time slot

$\hat{m}$ Maximum allowable number of simultaneous packet transmissions in a time slot

M Number of attempted packet transmissions made during a given time slot

M_R Maximum number of active receivers in a time slot

M_T Maximum number of active transmitters in a time slot

n Number of backlogged user

$n(t)$ Number of backlogged users as a function of time

$\bar{n}$ Average number of backlogged users

$\hat{n}$ Estimate of the number of backlogged users

N Population size in terms of the number of transmitter-receiver pairs

N_j Equivalent one-sided noise Power Spectral Density for the jth transmitter

N_o Background noise power spectral density

N_t Total additive noise at the front end of the nth receiver

N_R Maximum number of potential receivers in a time slot

N_T Maximum number of potential transmitters in a time slot

p_{ij} State transition probability for the number of backlogged users

p_o Probability of original packet transmission in the next time slot

p_r Probability of packet retransmission in the next time slot

p_r^* Optimal probability of packet retransmission

$p(x)$ Probability that event x occured

P Transmitted power

P_b Probability of bit error

P_C Probability that a received packet is correctly decoded

P_S Probability of symbol error

$\mathbf{P}$ State transition matrix for the number of backlogged users

r Code rate

R_o Channel cutoff rate

R_o^* Optimal code rate assuming that the code rate equals R_o

S Number of successful packets per slot

T_{in} Input transmission rate

T_{out}	Output transmission rate
T	Throughput
T_b	Data bit duration
T_{BN}	Throughput resulting from the use of the binomial composite traffic arrival distribution
T_C	Spreading sequence chip duration
$T_{D=1}$	Maximum(maximin) normalized throughput at unity delay
T_{NBN}	Throughput resulting from the use of a nonbinomial composite traffic arrival distribution
$T_{\{R_o,C\}}$	Maximum(maximin) normalized throughput evaluated with respect to the channel cutoff rate or channel capacity
$T_{\{R_o,C\},NN}$	Maximum(maximin) nonnormalized throughput evaluated with respect to the channel cutoff rate or channel capacity
T_S	Code symbol duration
U	Total number of radio units in the network
γ_j	Signal attenuation factor for the jth signal
η	Processing gain
$\eta^{\{R_o,C\}}$	Optimal processing gain
λ_J	Bit energy-to-jammer noise ratio
λ_o	Bit energy-to-background noise ratio
λ_t	Bit energy-to-total noise ratio
$\lambda_{o,J}^{\{R_o,C\}}$	Noise limit for the background and jammer noise cases, respectively
$\hat{\lambda}_{o,J}^{\{R_o,C\}}$	Asymptotic noise limit for the background and jammer noise cases, respectively
$\tilde{\lambda}_{o,J}$	Bit energy-to-{background, jammer} noise ratio for $\eta = 1$
ν	Average composite traffic intensity
ν_o	Average new traffic intensity
ν_r	Average retransmission traffic intensity
$\nu^{\{R_o,C\}}$	Cutoff traffic intensity

$\hat{\nu}$ Estimate of the average composite traffic intensity

π Equilibrium state probability distribution for the number of backlogged users

ρ Jamming fraction

$\rho^{\{R_o,C\}}$ Optimal jamming fraction

$\rho_{L,U}^{\{R_o,C\}}$ Lower and upper bounds on the range for the optimal jamming fraction

$\triangle_x$ Channel component x

Summary

In the area of communications there is a general interest in designing multiple-access protocols which provide for fair and efficient use of the network channel, and error control protocols which provide for high throughput efficiency and reliability. This thesis examines and optimizes the performance of a slotted random access code division multiple-access (CDMA) packet radio network (PRN). The PRN is comprised of an arbitrary number of full-duplex radio units arranged in a paired-off topology. Slotted ALOHA random access is used in conjunction with CDMA for channel access and a type I hybrid ARQ is used for error control.

Performance is evaluated in terms of link-level throughput-delay for channels stressed by multiple-access interference, background noise, and jammer noise. Throughput-delay expressions are derived in terms of the channel's cutoff rate and capacity. Performance bounds are achieved by using error detecting/correcting codes with rates operating arbitrarily close to the channel's cutoff rate and capacity. The mathematical model accounts for the effects of multiple-access interference, background noise, and jammer noise. The stochastic nature of the multiple-access interference is modeled by means of a Markov chain with the state being the number of backlogged users. Jammer noise is modeled as a worst case pulse jammer. Both the steady-state and dynamic performance of the network is analyzed.

Performance is optimized over network design parameters such as the retransmission probability, code rate, and processing gain. For channels operating in the presence of jammer noise, the optimization involves a worst case jamming scenario where an enemy pulse jammer chooses its jamming fraction based on complete knowledge of the spread spectrum system except for the exact spreading code. The effects of jammer state availability on network performance is considered in particular.

Performance results show that for a given population size, traffic intensity, and bit

energy-to-noise ratio, there is an optimal retransmission probability, code rate and processing gain that maximizes the network utilization. Numerical results also indicate that, at high traffic loads and/or at high jammer noise levels, it is more efficient in terms of network utilization to use CDMA in conjunction with random access than to use random access alone. Important descriptive parameters such as the cutoff traffic intensity, noise limits, and asymptotic noise limits arising from this analysis help illustrate when it is best to use one of the various error control techniques considered in this study (ARQ, Hybrid ARQ, CDMA).

CHAPTER 1

Introduction

1.1 Problem Description

Packet radio networks are communication systems which apply packet switching techniques to multiple-access radio channels. The need for packet radio networks is driven by the requirement for a general purpose data communications capability among a community of geographically dispersed and mobile users who sporadically desire the use of a high data rate channel, and by the physical/economic constraints which make it difficult/costly to provide the desired level of service by some alternate means of communications (e.g., wire, optical fiber).

Since the introduction of packet radio networks in the early 1970's, a considerable amount of work has been done in developing multiple-access protocols and error control protocols to meet the increasing demands of an ever growing number of network applications. The challenge has been to design multiple-access protocols which provide for fair and efficient use of the network channel, and error control protocols which provide for high throughput efficiency and reliability. This thesis examines the efficiency of random access protocols used in conjunction with code division multiple-access (CDMA) for channel access, and the efficiency of hybrid automatic-repeat-request (ARQ) for error control, in packet radio networks.

A multiple-access communication network consists of a number of terminals which communicate over the same communication channel for reasons of efficiency or the nature of the application. Satellite and terrestrial packet radio networks are examples of such

networks. Channel access protocols provide coordination among users in order to minimize contention on the channel. The amount of coordination may range from complete coordination as in fixed access schemes such as time division multiple-access (TDMA), frequency division multiple-access (FDMA), or code division multiple-access (CDMA), to little or no coordination as in random access schemes such as the ALOHA protocol. For this study, network users are characterized as having a high peak-to-average data rate requirement (i.e., bursty). Each user sporadically desires the use of a high data rate channel. In this case, random access is the most efficient protocol. However, with random access, throughput efficiency decreases significantly at the higher traffic loads due to the increased number of colliding packets. CDMA, on the other hand, allows for the possibility of colliding packets to be successfully recovered when the network is operating at these high traffic loads or when the network is being stressed with either unintentional or intentional (jamming) interference. It appears, therefore, that a combination of random access and CDMA may provide reasonable throughput performance at the higher traffic intensities and/or at high interference noise levels.

The key performance measures of random access networks are their throughput-delay characteristics. Hybrid ARQ schemes are often used to improve these characteristics and to increase network reliability. They achieve this improvement by using a combination of forward error detection combined with repeat transmissions (ARQ) and forward error correction (FEC). This thesis determines what combination of ARQ and FEC results in the best network performance.

Most of the research conducted in the area of spread spectrum multiple access to date has focused on the physical level issues [24,25,49,56,72,73,79,80,97] , with few works considering issues at the link [15,70,75] and network levels [16,85,90]. Tractable analytic results exist for only a few special cases (eg., regular topologies) where symplifying assumptions (eg., operation in a benign environment) are made to further ease the analysis. The primary reason for the lack of more general results at the link and network levels is the difficulty in analyzing arbitrary network topologies under general network operating conditions. The analysis of arbitrary topologies would require the knowledge of the joint probability distribution for the number of active receivers and transmitters. The combinatorial complexity

of the arbitrary topology alone makes a general analytical optimization computationally infeasible. Including such factors as actual radio propagation effects, node motion, and dynamic jamming strategies further complicates the analysis. As a result, a general theory of network operation has yet to be developed which incorporates arbitrary network topologies and a full range of network operating conditions. The goal of the present work is to advance, however modestly, the general understanding of CDMA network modeling, analysis, and design.

1.2 Problem Solution

The objective of the proposed research is to examine and optimize the performance of a slotted random access code division multiple-access (CDMA) packet radio network (PRN). The PRN is comprised of an arbitrary number of full-duplex radio units arranged in a paired-off topology. Slotted ALOHA random access is used in conjunction with CDMA for channel access, and a Type I Hybrid ARQ is used for error control.

Performance is evaluated in terms of link-level throughput and average packet delay for channels exposed to multiple-access interference, background noise, and jammer noise. Expressions for the throughput and corresponding average packet delay are derived in terms of the channel's cutoff rate and capacity. Performance bounds are achieved by using error detecting/correcting codes with rates operating arbitrarily close to the channel's cutoff rate or capacity. Thus, for hard decision decoding, throughput-delay characteristics achieved by using the capacity limit represent a *theoretical* performance limit, while characteristics achieved by using the cutoff rate limit represent the *practical* performance limit. The mathematical model accounts for the effects of multiple-access interference, background noise, and jammer noise. The stochastic nature of the multiple-access interference is modeled by means of a Markov chain with the state being the number of backlogged users. Enemy jamming is modeled by a worst case pulse jammer. Both the steady-state and dynamic performance of the network is analyzed.

Performance is optimized over network design parameters such as the retransmission probability, code rate, and processing gain. For channels operating in the presence of jamming noise, optimization involves a worst case jamming scenario where an enemy pulse

jammer chooses its jamming fraction based on complete knowledge of the spread spectrum system except for the exact spreading code. How optimal design parameter values depend on network parameters such as the population size, traffic intensity, bit energy-to-background noise ratio, and bit-energy-to-jammer noise ratio is examined.

Throughput-delay performance also depends upon the availability of network side information at the receiver (and transmitter). For this work, two degrees of side information are examined:

1. *Complete Side Information* Transmitters and receivers have knowledge of the population size, traffic intensity, bit energy-to-background noise ratio, bit energy-to-jammer noise ratio, and jammer state. For this analysis, jammer state is simply knowledge of whether the jammer is on or off during a particular code symbol duration.

2. *Partial Side Information* Same as (1) above, except that the jammer state is unknown to the transmitters and receivers.

1.3   Outline of the Dissertation

Chapter 2   This chapter provides an overview of channel access and error control protocols. The basic concepts of conventional and code division multiple-access, and ARQ, hybrid ARQ, and adaptive hybrid ARQ error control are described. Related research in these areas is also discussed.

Chapter 3   This chapter examines the steady-state and dynamic performance of Type I Hybrid ARQ protocols in a slotted direct-sequence CDMA network operating in the presence of multiple-access interference and background noise. A Markov model is used to account for the stochastic nature of the multiple-access interference. Throughput-delay expressions are derived in terms of the channel cutoff rate and capacity. These performance bounds assume the use of error detecting/correcting codes operating arbitrarily close to the channel cutoff rate or capacity. The stability of the network is evaluated for the finite population case. It is shown that, for a given population size, traffic intensity, and bit energy-to-noise ratio, there is an optimal retransmission probability, code rate and processing gain that maximizes network performance. Numerical results also indicate that, at high traffic

intensities, it is more efficient in terms of network utilization to use CDMA in conjunction with random access than to use random access alone. Important descriptive parameters such as the cutoff traffic intensity, noise limit, and asymptotic noise limit arising from this analysis help illustrate when it is best to use one of the various error control techniques considered in this study (ARQ, Hybrid ARQ, CDMA).

Chapter 4 This chapter examines the throughput-delay performance the CDMA network operating in a hostile jamming environment. The approach taken in this chapter parallels that of the last chapter. The network model accounts for the presence of multiple-access interference, background noise, and jammer noise. Enemy jamming is modeled by means of a worst case pulse jammer. As in Chapter 3, throughput-delay performance bounds are derived in terms of the channel cutoff rate and capacity. It is shown that, for a given population size, traffic intensity, and bit energy-to-noise ratio, there is an optimal probability of retransmission, code rate, and processing gain that maximizes network performance in the presence of worst case pulse jamming. It is also shown that, at high traffic intensities and/or jammer noise levels, it is more efficient in terms of network utilization to use CDMA in conjunction with random access than to use random access alone. The effect of pulse jamming, with and without jammer state information, is also examined.

Chapter 5 This chapter discusses ideal network operation and issues related to practical network operation.

Chapter 6 This chapter summarizes the results of this work and draws conclusions which are of general use.

Chapter 7 This chapter gives recommendations for further study.

CHAPTER 2

Background

2.1 Channel Access Protocols

The fundamental characteristic of a multiple-access network is that many transmitters compete for access to a single communication channel. When two or more stations transmit packets simultaneously, their packets overlap and may be destroyed. To prevent these collisions, channel access protocols are used to provide the necessary coordination among the many potentially conflicting transmitters. How well protocols manage contention on the channel is usually measured in terms of the network's throughput-delay performance. Protocol performance depends primarily on how well the protocol is matched to networks characteristics such as the traffic arrival process, topology, population size, channel propagation delay-to-transmission delay ratio, etc.

2.1.1 Conventional Multiple-Access

In general, protocols can be categorized by the amount of coordination they provide among network transmitters. Three major categories are possible: fixed access, demand access, and random access.

- *fixed access*: Fixed or scheduled access protocols such as Frequency Division Multiple Access (FDMA) and Time Division Multiple Access (TDMA) provide complete coordination among network transmitters. Channel contention is completely avoided by assigning each transmitter a particular sub-band of the network's overall bandwidth as in FDMA, or a particular time slot within each of the network's time frames as

in TDMA. Note that a frequency sub-band or a time slot is available to each transmitter whether they use it or not. Thus, if packet arrival rates are steady and the offered traffic load is moderate-to-heavy, then network efficiency is high. However, if transmitters are bursty (i.e., they have high peak-to-average packet arrival rates) then most slots remain idle while the few busy transmitters have packets waiting to be transmitted. As a result, network efficiency is low [38].

- *demand access*: Demand access (reservation-based) protocols attempt to maximize network performance over the entire range of traffic loading by dynamically allocating channel capacity as a function of the current traffic load condition in an optimum manner. Contention is eliminated by allowing each transmitter to make a reservation to transmit its packet in some future time slot. As slot reservations are made, the corresponding information packets form a network wide common queue from which they are transmitted without fear of collisions. Reservation packets are typically much smaller than information packets and are either interleaved with information slots on the network channel or transmitted on a separate reservation side channel [77]. Note that reservations are made on a contention basis. Ideally, demand access protocols operate like ALOHA (with low delay) at low traffic loads and like TDMA (with high throughput) at high traffic loads. In [77], Roberts showed that performance characteristics near this ideal could be achieved, but at the expense of significant network overhead and highly centralized control. Other more decentalized schemes are possible [37].

- *random access*: At the other extreme of network coordination, random access protocols provide little or no coordination at all. The simplest of the random access protocols, the ALOHA protocol, allows each terminal to transmit its packet as soon as it has one to send. All transmitters are allowed to contend freely for access to the network channel. Should a collision occur, each terminal involved in the collision retransmits its packet after some random delay. Random access protocols provide short packet delay when the network is comprised of bursty transmitters and the average offered traffic load is low. As the offered traffic load increases, however, throughput decreases

due to increased collisions and delay becomes large. Additional protocol coordination is necessary at these higher traffic loads.

This study considers the use of the slotted ALOHA random access protocol which is described in more detail below.

Related Work on Random Access ALOHA Protocol: The first example of a communication network which used the idea of random access in sharing a multiple-access radio channel for data transmission was the experimental ALOHA system at the University of Hawaii in the early 1970's. The system got its name from the ALOHA protocol which was first introduced by Abramson [2]. As mentioned earlier, the ALOHA protocol allows a sender to transmit its packet as soon as it has one to send. There is zero access delay. If after a given delay (positive time out period) an acknowledgement is not received, or if a negative acknowledgement is received, then a retransmission is sent after some random delay. A random delay is used to prevent previously collided packets from recolliding. The ALOHA protocol is well suited to the peculiar (bursty) statistics of digital data. Abramson [2] determined the capacity or maximum throughput of the network to be $1/2e = 0.184$. Roberts [76] later improved upon the throughput performance of the ALOHA protocol by introducing its slotted version. In a slotted system, the time axis is divided into equally sized slots. Slotted ALOHA is identical to nonslotted or pure ALOHA except that packet transmissions start at the beginning of a time slot. For our purposes, packet length equals slot duration. Throughput performance improves to $1/e = 0.368$ because collisions can now occur only within the period of a time slot, whereas with pure ALOHA, packets are vulnerable over a two slot time interval.

While initial experimental successes with the ALOHA protocol were encouraging, its unstable nature limited its maximum available throughput to 0.184 and 0.368, respectively, for its pure and slotted versions. Early work was, therefore, aimed at further characterizing network behavior and solving the instability problem. Kleinrock and Lam [39] characterized the network's dynamic behavior by the use of fluid approximation techniques and demonstrated three possible system behaviors: stable, bistable, and saturation. Stable systems have one stable operating point with relatively high throughput and low delay. Bistable systems exhibit two possible networks operating points; one having high throughput and

low delay, the other having low throughput and high delay. Similar bistable behavior was reported by Carleial and Hellman [9] who based their results on expected drift analysis. Saturated system have low throughput and unbounded delay. Kleinrock and Lam investigated the fundamental tradeoffs between network stability, throughput, and average packet delay in terms of system parameters such as population size, traffic intensity, and retransmission probability. From their initial results [39], they developed control procedures which stabilized the network by dynamically controlling the retransmission probability [45]. They used a single-level control limit policy based on Howard's policy iteration method. Here, one of two possible probabilities of retransmission (p_1, p_2) are selected depending on whether the current estimate of the number of backlogged transmitters $\hat{n}$ is above or below a certain control limit n_c (i.e., choose p_1 if $\hat{n} \leq n_c$, choose p_2 if $\hat{n} > n_c$). Estimates on the number of backlogged transmitters were made based on the number of previous idle slots. Near optimum throughput-delay performance was reported. Since Kleinrock and Lam's work, multi-level control policies and more decentralized control schemes have been proposed and analyzed [21,28,34,65].

Collision resolution algorithms (splitting algorithms) are an alternate technique which can be used to maintain network stability. Basically, these algorithms resolve network contention by systematically splitting those terminals involved in a collision into smaller and smaller groups until retransmission success is guaranteed. Examples include the first-come first-serve algorithm introduced by Gallager [23] and the tree algorithm introduced by Capetanakis [8]. These algorithms achieve maximum throughputs of 0.487 and 0.430, respectively, for slotted ALOHA.

Concurrent with the above efforts to improve ALOHA protocol performance, work was also being done to analyze and exploit the effects of capture. So far, the analysis of the ALOHA protocol assumes that when any part of two or more packets overlap all packets that are involved in the collision are destroyed and must be retransmitted. With capture, however, there is some probability that one of the packets may arrive at the receiver with sufficient power to capture it and thus be received correctly. Because not all colliding packets are destroyed, capture improves network performance. The effects of capture were first investigated by Roberts [76] for the case of perfect capture (i.e., capture

occurs with probability one). Later studies investigated the effects of both natural and man-made capture. Capture occurs naturally due to channel fading, and due to the varying distances of mobile radio units [3,43,69]. Capture can be induced by varying signal power levels in a prioritized or random manner [47,63]. In [63], for example, Metzner showed that by simply dividing transmitters into two groups; one transmitting at high power, the other at low power, the maximum throughput of slotted ALOHA could be increased from 0.368 to as high as 0.530. Lee shows in [47] that for multiple power level systems, throughputs approaching 0.660 can be obtained as the number of levels approaches infinity.

With the ALOHA protocol, the transmitter must know which packets need to be re-transmitted. Typically, acknowledgements are used for this purpose. Positive or negative acknowledgements are sent by the receiver back to the transmitter to indicate whether the packet was received correctly or not. The performance results reported so far assume that acknowledgements are made over a seperate return channel at no cost in channel capacity and with complete reliability. In reality, however, acknowledgements are not free and their presence significantly degrades the throughput-delay performance of the network. The effects of acknowledgement traffic on network performance were first analyzed by Tobagi and Kleinrock [89] for a fully connected, slotted network. They showed how performance suffered due to acknowledgement traffic and proposed two different channel configurations in order to cope with the problem. A common channel configuration was proposed in which acknowledgements share the same channel as the data, and a split channel configuration was proposed in which the acknowledgements and data are transmitted on separate channels. Channel capacities for both configurations were evaluated. Elsanadidi and Chu [20] performed a similar analysis for a network having a star topology. Results from both [89] and [20] indicate that the split configuration tends to be the more efficient of the two.

2.1.2 Code Division Multiple-Access

Code division multiple-access (CDMA) permits contention free access to the network with no access delay. The particular CDMA technique considered in this study is spread spectrum multiple-access (SSMA). SSMA is characterized by the use of a high rate pseudorandom code (many code symbols per data bit) which has the effect of spreading the bandwidth

of the data signal beyond what is needed for narrow-band transmission. Spread spectrum operation may be achieved by using any one of three basic modulation techniques: direct-sequence, frequency hopping, or time hopping [56]. Hybrid modulation schemes which use various combinations of these basic schemes are also possible. For this analysis, direct-sequence modulation is employed whereby the carrier is phase modulated by the data sequence and the pseudorandom spreading sequence. Contention free access is achieved by selecting orthogonal code sequences so that the mutual interference between simultaneous transmissions is minimized. There is no channel access delay if the code family size is large enough so that each transmitter has its own spreading code.

The benefits of using spread spectrum signaling are primarily due to its multiple-access, delay-capture, anti-multipath, and narrow-band inteference rejection properties [74]. The first two properties relate directly to its effectiveness as a multiple-access technique. Multiple-access refers to the ability of a receiver to reject transmissions which are addressed to other receivers. Discrimination between multiple arriving packets is based on the spreading code as opposed to packet power levels or arrival times. Spreading code sequences are selected that are mutually orthogonal so that they may overlap with little or no interference. Delay-capture refers to the ability of a receiver to successfully recover one of many time-overlapping packets addressed to it. Discrimination between multiple arriving packets is based on a combination of packet arrival times and power levels, and not entirely on packet power levels as in narrow-band systems. It is the multiple-access and delay-capture properties that allow for colliding packets to be successfully recovered. Anti-multipath refers to the ability to communicate reliably over a network link which has multiple transmission paths and is, therefore, susceptible to the effects of fading and intersymbol interference. Narrow-band interference rejection refers to the ability to successfully receive a packet in the presence of narrow-band interference (e.g., jamming). It is the narrow-band interference rejection property that allows CDMA to provide useful throughput levels while operating in the presence of hostile enemy jamming, where narrow-band slotted ALOHA usually cannot.

For successful spread spectrum operation, code coordination between receiver and transmitter is necessary. Code coordination can be achieved by any one of three possible spreading code protocols: common codes, transmitter-directed codes, and receiver-directed

codes [85].

- *common code* : The common code protocol is the simplest protocol to implement because the same spreading code is used by all terminals. Addressing information is typically placed at the beginning of the packet. Because only one code is used, this protocol must rely on the delay-capture properties of spread spectrum to discriminate between two or more incoming packets. Since only one code channel is used, this protocol is most like the ALOHA protocol. In fact, if all terminals are perfectly synchronized and propagation delay is zero, then colliding packets destroy one another and this protocol is exactly the ALOHA protocol.

- *transmitter-directed code* : With the transmitter-directed protocol, each transmitter is assigned a unique transmitting code. While this eliminates the possibility of contention, a key disadvantage of this protocol is that receivers must anticipate which transmitter to monitor. This protocol is best suited to broadcast applications where only a few terminals are transmitting large amounts of data to a large number of 'receiving' terminals.

- *receiver-directed code* : When the receiver-directed protocol is used, each receiver is assigned a unique spreading code. With this protocol, the burden is on the transmitter to encode transmissions with the address code of the intended receiver. A drawback of this scheme is that the possibility of contention does exists since multiple transmissions may be addressed to the same receiver. Packets are destroyed if there is insufficient phase offset among arriving packets. This protocol is well suited to applications where receivers may not necessarily know packet origination.

In this study, we consider a packet radio network which employs receiver-directed direct-sequence SSMA.

Related Work on Code Division Multiple-Access: Early work in the area of CDMA focused primarily on physical level issues such as spread spectrum format selection, spreading code design, and corresponding bit error rate performance. Most notable are works by

Pursley and Sarwate who investigated the effects of spreading cross-correlation and partial-correlation functions on system performance [73,79]. These works resulted in the design and optimization of code sets with good correlation properties which are necessary in multiple-access systems. System performance was evaluated in terms of performance bounds based on the number of supportable simulatneous transmissions at a given bit error rate (BER) and signal-to-noise ratio (SNR) [13,31,72,93,97]. In [93], for example, Weber et. al. showed that system performance degrades gradually with an increased number of simultaneous transmissions, and that there is a pronounced threshold region above which performance degrades quickly. Hui [31] investigated the throughput performance in terms of the channel cutoff rate and capacity for a binary symmeteric channel. He determined that coding schemes with low processing gain (short spreading sequences) and low rate codes are optimum in terms of system throughput.

In most of the aboves analyses, BER performance evaluation assumed a worst case scenario where all transmitters in the network are active all of the time. In reality, however, the multiple-access interference is not constant but is a random variable. Thus, an analysis which considers this stochastic nature of the multiple-access interference can provide more realistic performance analysis. In [75], Raychaudhuri's analysis of slotted CDMA systems incorporates the stochastic nature of the multiple-access interference by using various models for the traffic arrival process. A transmitter-directed protocol was used and both infinite (Poisson arrivals) and finite (Binomial arrivals) population models were considered. For the finite population model, the performance was also evaluated in terms of a general arrival model where the probability of original packet transmission p_o was not equal to the probability of packet retransmission p_r. The stability of the finite population system was also investigated. In [70], Polydoros and Silvester provided a generic model for the study of local throughput in slotted spread spectrum networks, that accounts for the stochastic nature of the multiple-access interference, various capture and retention models, topologies, spread spectrum protocols, and channel conditions. Stability was also discussed.

While numerous results have been obtained for slotted CDMA systems, few results exist for the unslotted (asynchronous) case because of the difficulty in modeling the multiple-access intereference. For the slotted case, the multiple-access interference varies from slot to

slot, but remains constant during the slot interval. Thus, the code symbol error probability due to multiple-access interference also remains constant. For the unslotted case, however, the number of interfering transmissions changes as the packet (codeword) is being received resulting in a time-varying symbol error probability within a codeword. This time varying symbol error probability makes the exact evaluation of the codeword error probability very difficult to compute. Most analyses have either solved for upper and lower bounds on the codeword error probability [71,88], or have computed the codeword error probability exactly by determining the joint distribution of interfering transmissions for particular codes and network operating conditions [1,68]. Note that the performance of unslotted systems is upper bounded by the performance of slotted systems and that only slotted systems are considered in this study.

Capture can occur in our CDMA system 1) when a packet arrives at the receiver with sufficiently greater power than the other contending packets (power-capture) or 2) when a packet arrives earlier than the other packets (delay-capture). The delay-capture effect is manifested during the synchronization phase when many packets are competing for the attention of a particular receiver. This effect is a direct result of the spreading codes used. It is assumed that spreading codes do not repeat themselves within a packet duration so that packets contending for the same receiver and arriving with a certain time offset have pseudoorthogonal code sequences. This allows the first arriving packet to capture the receiver and the remaining packets to be rejected as noise. Note that as the first packet is being received, other later arriving packets may have power levels greater than the first but may still be rejected depending upon the interference rejection margin of the system. As such, delay-capture plays a more significant role than power-capture in CDMA system performance.

The effects of delay-capture on network performance have not been extensively investigated because of the difficulty in accurately modeling the delay-capture phenomena [15,70]. In [15], Davis and Gronemeyer investigated the delay-capture effect in a slotted CDMA system where a randomized time of arrival procedure was used to prevent discrimination as a function of range. A receiver-directed spreading protocol was used with a star type topology. The stochastic nature of the multiple-access intereference was modeled by a

Markov chain with the state being the number of backlogged transmitters, and capture was shown to have a semi-exponential probability distribution function with capture parameter c. It was shown how capture effects tend to improve the throughput-delay performance and stability of the system. More recently, Polydoros and Silvester [70] provided a more detailed model of the reception process which accounts for capture as well as the retention of a packet. Packet retention refers to the probability of correctly decoding a packet once it is captured. The probability of correct packet decoding depends upon the level of background noise, multiple-access noise due to the rejected packets, and possibly jammer noise. [70] investigated the effects of network traffic load, capture parameter c, and receiver population size on local throughput for various exponential capture models. Retention analysis investigated the effects of code rate, processing gain, and the probabilities of original packet transmission and packet retransmission on throughput performance. Various traffic arrival models for finite and infinite population were used. Optimal code rate and transmission strategies were determined. Note that most of the analysis presented earlier in this section assumed that either capture occurs with probability one (perfect capture) or that capture does not occur at all. Retention was assumed to occur with probability one.

As with narrow-band multiple-access systems, the presence of acknowledgement traffic can also adversely effect the performance of CDMA systems. Sastry [81] investigated these effects on the performance of a slotted ALOHA-CDMA network. A paired-off topology was used with a receiver-directed spread spectrum protocol. Acknowledgements were made on the same channel (common channel) as the data in the next immmediate time slot. To account for the effects of acknowledgement traffic, their presence was included in determining the composite arrival distribution function. It was shown that the introduction of acknowledgement traffic did not cause performance to degrade as much as in the narrow-band case. This improved performance is due to the multiple-access capability of CDMA. Later studies showed similar results and analyzed various schemes to further reduce the effect of acknowledgement traffic to include to use of split slot and mini-slot techniques [48], and the use of dedicated code channels [16].

2.2   Error Control Protocols

There are two fundamental techniques for error control in digital communication systems: forward error correction (FEC) and forward error detection combined with automatic repeat-request (ARQ). In either case, a codeword is formed by appending a certain number of parity bits to a packet to form the coded packet or codeword. For this discussion a packet will be composed of a single codeword. FEC involves the use of an error correcting code in order to correct errors caused by poor channel conditions. Erroneous data is delivered to the receiver whenever errors are either undetectable or uncorrectable by the code being used [12,52,57]. ARQ, on the other hand, relys on the use of a good error detecting code. When a codeword is detected in error, the receiver requests a retransmission of the codeword in question. Retransmissions continue until the codeword is received successfully. Erroneous data is delivered to the receiver only when an undetectable error has occured.

The performance of these techniques is usually measured in terms of throughput efficiency and network reliability. Throughput efficiency is defined as the ratio of the average number of information bits successfully accepted by the receiver per unit time per unit bandwidth to the total number of bits that could be transmitted per unit time per unit bandwidth. Reliability is usually measured in terms of probability of decoding error. Since no retransmissions are required for FEC, throughput efficiency is relatively constant regardless of the channel conditions. However, the reliability of the packet sent decreases significantly as the channel condition degrades beyond the error correcting capabilities of the code being used. ARQ, on the other hand, provides high reliability for all channel conditions. However, throughput efficiency decreases dramatically with the channel quality as the number of retransmissions increase. By using the proper combination FEC and ARQ, hybrid ARQ schemes offer the potential of achieveing both high throughput efficiency and high reliability. To meet the wide range of possible channel conditions, various forms of hybrid ARQ have been developed, including Type I, Type II, and adaptive hybrid ARQ.

2.2.1   Automatic Repeat Request

There are three basic ARQ modes: stop-and-wait (SAW), go-back-N (GBN), and selective repeat (SR). These modes are based on how retransmissions are made.

- *stop-and-wait (SAW)*: With the SAW mode, a sender waits for either a positive or negative acknowledgement of the packet just sent before sending another. A positive acknowledgement from the receiver indicates that the packet was received without error and that the next packet may be sent. A negative acknowledgement from the receiver indicates that the transmitted packet has been received in error. In this case, the transmitter resends the packet. Although this is the simplest of the three modes, it is also the most inefficient due to the idle time wasted waiting for acknowledgements.

- *go-back-N (GBN)*: The GBN mode of operation allows packets to be transmitted continuously. Idle time is reduced because the transmitter does not wait for an acknowledgement before sending another packet. However, transmitted packets must be stored at the transmitter until they are acknowledged. Acknowledgements are received after a round-trip delay. During this period, $N - 1$ succeeding packets have been transmitted. Should a negative acknowledgement be received for packet i, then the transmitter must go back N packets to packet i and retransmit it and the $N - 1$ succeeding packets. At the receiver, when packet i was found in error, it and all $N - 1$ succeeding packets are discarded, regardless if any of the $N - 1$ packets were received correctly. Retransmissions continue until packet i is received without error. The primary disadvantage of the GBN mode of operation is that $N - 1$ packets are discarded with each retransmission.

- *selective repeat (SR)*: The SR mode of operation also allows the transmitter to send packets continuously, but only resends those packets that are negatively acknowledged. Because packets are normally delivered to the receiver in consecutive order, buffering must be provided at the receiver to store error free packets received while the negatively acknowledged packet is being retransmitted. Buffer capacity must be sufficient to prevent buffer overflow. SR is the most efficient of the three modes, but is also the most complex.

Related Work on ARQ: Most of the work in ARQ has involved analyzing performance in terms of bounds on the probability of undetected decoding error [36,40,51,59], and investi-

gating the relative efficiency of the three basic ARQ modes [5,6]. Shortcomings have been overcome by using various combinations of the basic modes [64,66,94]. In [66], for example, Miller and Lin employed a combination of SRT and GBN ARQ to help solve the buffer overflow problem experienced in the SRT ARQ. Here, the retransmission of codeword i is handled as in the SRT ARQ. Retransmission requests for subsequent codewords are handled as per the GBN ARQ until codeword i is correctly acknowledged. Once codeword i is positively acknowledged, the system reverts to the SRT mode. The use of the GBN ARQ mode for these subsequent retransmission request guarantees no buffer overflow.

2.2.2 Hybrid ARQ

When faced with both high channel error rates and stringent reliability requirements, hybrid ARQ may have to be used. Hybrid ARQ protocols combine the forward error detecting capability of plain ARQ with the use of a forward error correcting code to achieve improved network performance. There are basically two forms of hybrid ARQ: type I and type II. With either type, the ARQ portion of the protocol may be any one of the basic modes disscussed earlier. In a Type I Hybrid ARQ, FEC reduces the number of retransmissions by correcting those error patterns that occur most frequently, while FED detects those remaining error patterns that occur infrequently. The degree of throughput efficiency and reliability depend on how well the combination of FED/FEC is matched to the channel requirements. Type I Hybrid ARQ works well as long as the channel conditions remain fairly constant. Should the channel error rate decrease significantly, the Type I Hybrid ARQ becomes less efficient because the extra FEC parity bits are wasted. Alternately, if the channel error rate increases beyond the error correcting capabilities of the code employed, then retransmissions increase and throughput efficiency decreases. For time-varying channel conditions, it is better to use the Type II Hybrid ARQ protocol which uses only FED when the channel conditions are good (plain ARQ) and uses both FED and FEC when the channel conditions are poor [52].

Related Work on Hybrid ARQ: Work in the area of Type I Hybrid ARQ has primarily involved analyzing the performance of various block and convolutional coding schemes. Most of the early work evaluated the performance of block coding schemes [7,22,67,78,82] where

the Bose-Chaudhuri-Hocquenghem (BCH) class of codes were typically used. More recently, convolutional codes have received increased interest because of their good error detecting and error correcting capabilities. Both Viterbi and sequential decoding of convolutional codes have been investigated [17,18,50,83,96].

The Viterbi algorithm provides maximum likelihood decoding for convolutional codes. The error probability becomes smaller as the constraint length of the code becomes longer, but the complexity of the decoding operation grows exponentially. Work in this area has focused on trellis path truncation techniques. In [96], Yamamoto and Itoh proposed a decoding scheme whereby retransmissions are requested based on the reliability of surviving paths in the trellis diagram. Paths were deemed unreliable if, at any node, their partial path metric is too close to any that of any other surviving path. Should all paths be deemed unreliable before decoding is complete, then a retransmission is requested. A two-fold improvement in throughput efficiency over plain FEC with Viterbi decoding was achieved. Wicker [95] used a similar approach whereby path reliability was based on partial path metrics exceeding an absolute threshold. Significant improvement in reliability was achieved at little expense in increased network complexity.

With sequential decoding, decoding proceeds in a sequential manner until the codeword is decoded or an erasure is declared when decoding time becomes too long [18,33]. In the latter case, decoding is halted and a retransmission is requested. Two techniques have been developed to improve throughput efficiency with respect to decoding time; the time-out algorithm (TOA) where retransmissions are requested after an optimum decoding time-out limit is reached, and the slope control algorithm (SCA) where retransmission requests are based on whether the decoding path metric has fallen below some optimum threshold. The SCA is more efficient because it does not wait the entire time-out period, but predicts before the TOA limit has elapsed whether the packet is too noisy to be decoded.

When channel condition are time-varying, it is more effective to use the Type II Hybrid ARQ protocol which uses only plain ARQ when channel conditions are good, and uses hybrid ARQ when channel conditions are poor. Metzner [62] was the first to propose a Type II Hybrid ARQ which used parity retransmissions. His basic scheme has since been improved upon by many authors [53,54,55,91,92] with Lin and Yu's version becoming the most widely

accepted and analyzed [53]. Their version involves the use of two linear block codes. One is a high rate error detecting code C_0, and the other is a rate one-half invertible code C_1 designed for simultaneous error detection and error correction. Invertibility allows information bits to be decoded by simply knowing their parity bits. When decoding fails, retransmissions alternate between C_0 and C_1 until the packet is decoded correctly. In [53,91], the Lin and Yu version of Type II Hybrid ARQ was analyzed with a SR ARQ and a finite buffer size. Analysis showed that, even with a finite buffer size, throughput performance exceeds that of the ideal SR ARQ case when a code correction capability of $t = 5$ or more was used. Reliability was comparable to that of pure ARQ. Additionally, the complexity of the above scheme is only slightly greater than for the corresponding Type I Hybrid ARQ scheme.

Wang and Lin [55,92] investigated the use of convolutional codes in Type II Hybrid ARQ protocols. The error detection code is still a high rate block code, but the error correction code is now a rate one-half convolutional code. In [92] it is shown that, when the channel bit error rate is high, this scheme offers significantly better throughput performance than pure SR ARQ with infinite buffer size. Throughput efficiency drops to 0.5, however, when the channel noise is great enough to cause retransmissions. In [55], higher rate convolutional codes were shown to be an effective remedy for poor channel conditions, but at the expense of increased receiver complexity.

2.2.3 Adaptive Hybrid ARQ

Should channel conditions degrade beyond the capabilities of the Type I or Type II Hybrid ARQ, additional coding must be introduced in order to ensure successful communications. Adaptive Hybrid ARQ can be used for these highly nonstationary channels. Adaptability refers to the use of packet (codeword) combining techniques which achieve progressively lower rate codes by combining unreliable packets. Recall that Type II Hybrid ARQ combines only the two most current packets and discards all previous packets. Performance was therefore limited to the error correction capability of the two packet combination. Because adaptive hybrid ARQ uses a combination of all previous packets, it is possible to more efficiently match the code rate to the existing channel conditions so that throughput efficiency can be optimized for all channel conditions.

Related Work on Adaptive Hybrid ARQ: A full range of packet combining techniques have been proposed and analyzed. Sindhu [84] proposed a very simple scheme which uses the same codeword for all retransmissions (memory ARQ). Enough FEC is used so that repeated codewords contain sufficient collective information to allow correct decoding. Although the decoding algorithm is complex, significant improvement over plain ARQ is achieved, especially at high channel error rates. Modified memory ARQ schemes improve upon this basic scheme by sending codewords which contain additional incremental redundancy [54,58,62]. Other variations to the modified memory ARQ scheme are discussed below.

In [4], Benelli extended the basic idea of memory ARQ and proposed a symbol-by-symbol diversity combining scheme. Here, a reliability weight is assigned to each codeword symbol. With each retransmission, this weight is used to update a decision accumulator for each symbol in the codeword (packet). Retransmissions continue until decoding is complete. This technique is further analyzed in [46] for the case of a fixed number of retransmissions. Optimal thresholds and weighting factors are found which minimize the bit error rate.

Krishna and Morgera [42] proposed a generalized hybrid ARQ scheme where a variable number of parity blocks (packets) are transmitted until there are no detected errors. The code being used (Krishna Morgera, KM code [41]) is designed such that the greater the number of combined parity blocks, the greater the error correcting capability of the resulting code. A key feature of the KM code is that the same decoder is used to receive each successive retransmitted parity block.

Finally, Chase [10] proposed to combine packets on a packet-by-packet basis. Packets are combined based on a weighted hard or soft decision maximum-likelihood packet combining metric. The weighting of each packet is made based on an estimate of the packet's reliability which depends on the quality of the channel when the packet was sent. Channel quality is estimated by counting the number of errors in a known header sequence or measuring the instantaneous signal-to-noise ratio. Noisy packets are combined to obtain a code rate of $r/k + 1$, where r is the original code rate and k is the number of retransmissions.

Most of the hybrid ARQ schemes mentioned above were analyzed for benign environments. The same is true for work in the area of code division multiple-access. Most work has isolated on the effects of either background noise or multiple-access interference, with

few works considering them both and even fewer considering the effects of jamming. None have considered the combined effects of all three. In this study, an analytical framework is developed to study the combined effects of all three on system performance.

CHAPTER 3

Performance Evaluation in the Presence of Background Noise with Complete Side Information

This chapter examines the steady-state and dynamic performance of Type I Hybrid ARQ protocols in a slotted direct-sequence CDMA network operating in the presence of background noise and multiple-access interference. In the first section, the network and channel model is described in terms of its physical and link level characteristics. In Section 3.2, throughput-delay expressions are derived in terms of the channel cutoff rate and capacity. These performance bounds assume the use of error detecting/correcting codes operating arbitrarily close to the channel cutoff rate or capacity. The stochastic nature of the multiple-access interference is modeled by means of a Markov model for the number of backlogged transmitters. The stability of the network is evaluated for the finite population case. In Section 3.3, numerical results show how network design parameters such as the retransmission probability, code rate, and processing gain should be chosen in order to optimize network performance. It is also shown how the above design parameters depend on the uncontrolled network parameters such as population size, traffic intensity, and bit energy-to-background noise ratio. Numerical results indicate that, at high traffic intensities, it is more efficient in terms of network utilization to use CDMA in conjunction with random access than to use random access alone. Important descriptive parameters such as the cutoff traffic intensity, background noise limit, and asymptotic background noise limit arising from this analysis help illustrate when it is best to use one of the various error control techniques considered

in this study (ARQ, Hybrid ARQ, CDMA).

3.1 Network and Channel Model

3.1.1 Topological Considerations

The network consists of U radio units arranged in a paired-off topology similar to that discussed in [70 75]. Following their notation, let N_T and N_R be the maximum number of *potential* transmitters and receivers, respectively. N_T and N_R are fixed for a given network. Also, let M_T and M_R be the number of *active* transmitters and receivers, respectively, in a given time slot. M_T and M_R remain fixed for a slot duration but are are random variables from slot to slot. In our terminology, a receiver can receive only one packet at a time, and a transmitter can transmit only one packet at a time. A radio unit, however, may have multiple receivers/transmitters in order to receive/transmit multiple packets. Note that the term topology does not refer to the spatial aspects of the network but to the logical connectivity between receivers and transmitters. In SSMA networks, the topology depends strongly on the spreading protocol used. For this analysis, we assume that the sender of a message knows its intended destination so that a receiver-directed protocol will be used.

With the paired-off topology, $U/2 = N_T = N_R$ and $M_T = M_R$. In this case there are $M = M_T = M_R$ paired-off radio units, each with one transmitter and one receiver as shown in Fig. 3.1.a. In the sequel, $N = N_T = N_R$ is called the population size, and $M = M_T = M_R$ is the number of simultaneous packets transmitted during a particular slot interval. Note, in this case, that when a transmitter is active there is complete receiver availability of the corresponding receiver. There is no topological competition among transmitters for the attention of a particular receiver. Thus, the channel is not susceptible to the effects of capture, and the only disruptive interaction between concurrent packet transmissions is due to multiple-access interefrence of the other $M - 1$ interfering packets. Another example of a paired-off topology occurs when M radio units each having one transmitter are paired-off with the M receivers of a single radio as shown in Fig. 3.1.b . A practical example of this more centralized paired-off topology is the up-link of a satellite radio relay network where N terrestrial transmitters transmit to N satellite receivers. Note, in this case, that the

physical layout is in the form of a star, but the topology is paired-off.

For this analysis, we assume a homogeneous network where the effects of multiple-access interference, background noise, and jammer noise are felt equally at each receiver. This assumes that the probability distribution of the multiple-access interference is the same at each receiver, that each interferer contributes an equal amount to the total interfering power at a given receiver, that interfering packet power levels are equal to the desired signal power level, and that all receivers are effected by the same jamming strategy and power levels. Without the homogeneity assumption, we are faced with the more general problem of determining how the total interfering power is divided among the interfering signals. This is a very complicated problem, even for our simple paired-off topology, because it requires an elaborate description of the network architecture and the propagation environment.
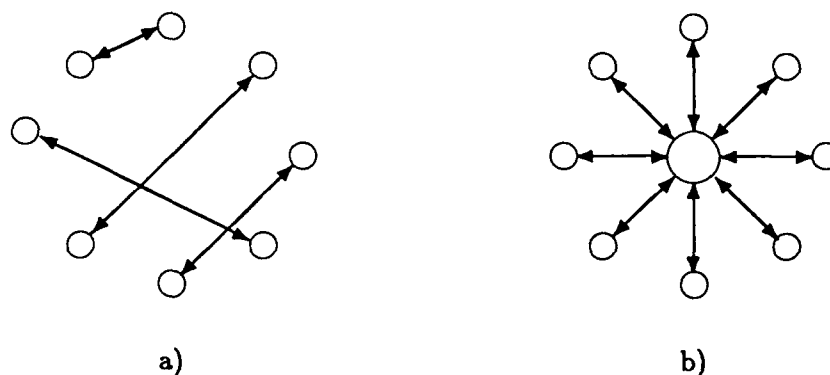
Figure 3.1: Examples of Paired-off Topologies

a) Decentralized Single Receiver/Transmitter Radio Units

b) Centralized Multiple Receiver/Transmitter Radio Unit

With the star topology, any number of transmitters N_T compete for the attention of a single receiver $(N_R = 1)$. In the above example, the central base station of Fig. 3.1.b . would have only one receiver. In CDMA networks having a star topology, capture effects (power capture and delay capture) have a significant effect on network performance. Although the present work considers only paired-off topologies and does not consider the

effects of capture, the analyses of star topologies with capture can be performed within the analytic framework of the present study (cf. [15]).

Finally, note that the paired-off and star topologies are special cases of the more general case, the fully connected topology ($N = N_T = N_R = M_T = M_T$). Although the fully connected topology is a more general and, in some cases, a more realistic topology, its representation would require the joint probabilistic description of the number of active transmitters M_T and active receivers M_R. This joint probabilistic description is extremely difficult to obtain. Including such factors as the actual radio propagation effects, radio unit motion, dynamic jamming strategies, etc., further complicates the analysis and makes a numerical solution extremely difficult, if not intractable. As a result, no general theory yet exists which incorporates arbitrary network topologies operating under a full range of network operating conditions.

3.1.2 Packet Flow

Transmitters access the network by using direct-sequence CDMA with a standard slotted ALOHA protocol. Information is transmitted in the form of packets, one packet per time slot. Packet flow for the network is shown in Fig. 3.2. Each of the network's transceivers can
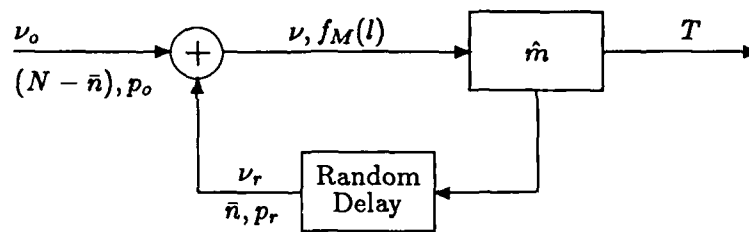
Figure 3.2: CDMA Network Packet Flow Model

be in one of two modes: origination or blocked. In the origination mode, the probability of transmitting a packet in the ith future time slot is geometrically distributed with parameter p_o, where p_o is the probability that the transmitter will transmit the packet in the next

time slot.

$$\text{Prob} \{ \text{ packet transmission in the } i^{th} \text{ future time slot } \} = p_o(1 - p_o)^{i-1} \qquad (3.1)$$

When either multiple-access interference or background noise causes a packet to be received in error, a transmitter enters the blocked mode. In this mode, the probability of retransmission is also geometrically distributed but with parameter p_r, where p_r is the probability that a transmitter will retransmit its packet in the next time slot. While a transmitter is waiting to retransmit, it is considered blocked or backlogged because it cannot transmit (but may receive) a new packet until the retransmitted packet is received without error. In practice, limits are set on the maximum number of retransmissions allowed for a given packet.

The traffic intensity is defined as the average number of packets transmitted per slot, and the new and retransmitted traffic intensities are denoted by ν_o and ν_r, respectively. At the input to the CDMA channel, new packet transmissions combine with packet retransmissions to form the composite channel traffic. The composite channel traffic can be characterized by its intensity and steady-state arrival distribution. The composite traffic intensity ν simply equals the sum of the new and retransmitted traffic intensities ($\nu = \nu_o + \nu_r$). The composite arrival distribution $f_M(l)$ is the steady-state probability distribution for the number of attempted transmissions M in a given time slot. The form of this distribution depends primarily upon the relative values of p_o and p_r, and on the population size N. Significant simplification in its form results when $p_o = p_r = p$, in which case the distribution becomes binomial with parameters p and N. Further simplification occurs when $p_o = p_r \to 0$ and $N \to \infty$, in which case the binomial distribution approaches the Poisson distribution with arrival rate equal to the composite traffic intensity ν. When $N < \infty$ and $p_o \neq p_r$, then the general composite arrival distribution is derived by means of a Markov model as described in Section 3.2.

3.1.3 Error Control

A Type I Hybrid ARQ protocol is used for error control. This protocol combines the forward-error-detecting (FED) capability of plain (conventional) ARQ with the use of

forward-error-correcting (FEC) codes to achieve improved network performance. An example of a Type I Hybrid ARQ channel (hereafter referred to as Hybrid ARQ) is shown in Fig. 3.3. The ARQ portion of this protocol is of the stop-and-wait (SAW) variety where the
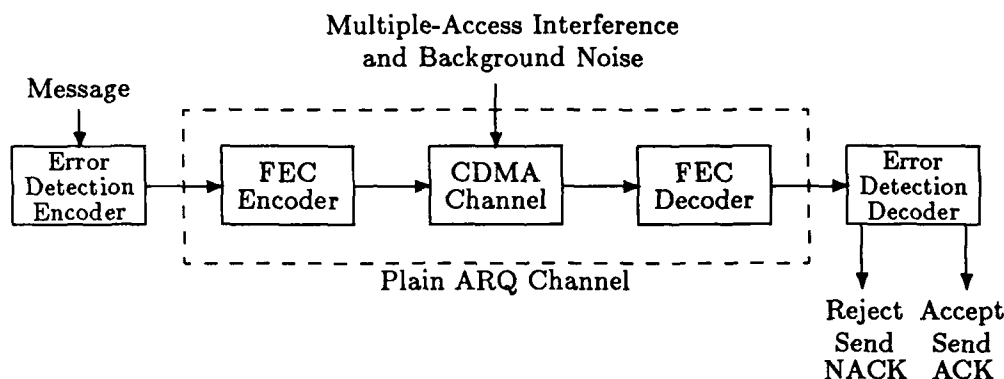
Figure 3.3: Type I Hybrid ARQ System

transmitter waits for either a positive (ACK) or negative (NAK) acknowledgement of the packet just sent before sending the next new or retransmitted packet, respectively. When a negative acknowledgement is received at the transmitter, the sender retransmits the requested packet in the ith future slot with probability $(1 - p_r)^{i-1}p_r$. It is assumed that acknowledgements are made instantaneously over a separate, noiseless return channel. As a result, acknowledgements are assumed to be costless and fully reliable. The FEC portion of the protocol is used to combat the effects of poor channel conditions and tends to reduce the number of retransmissions. Together, the proper combination of FEC and ARQ provide higher network reliability and throughput than could otherwise be achieved by them separately. All transmitters are assumed to use the same error detecting/correcting codes.

For this analysis, we assume that the channel conditions (i.e., background noise power spectral density (PSD) excluding the multiple-access interference) remain constant. Otherwise, the Type I Hybrid ARQ protocol becomes less efficient as the channel error rate decreases because the extra error correction parity bits are wasted. For time-varying channel

conditions, it is better to use a Hybrid ARQ protocol with a variable code rate [14]. Code combining techniques (adaptive Hybrid ARQ) can be employed as a further improvement [10,11].

3.1.4 Coding Channel

Each packet that is transmitted over the Hybrid ARQ channel of Fig. 3.3 is comprised of one or more code words. Each code word is used for simultaneous error detection and error correction. The CDMA channel portion of Fig. 3.3 corresponds to the coding channel for the network. The coding channel is assumed to be a a binary symmetric channel having crossover probability P_S and the following cutoff rate and capacity:

$$R_o = 1 - \log_2\left(1 + \sqrt{4P_S(1 - P_S)}\right), \tag{3.2}$$

$$C = 1 - H[P_S], \tag{3.3}$$

where $H[P_S]$ is the binary entropy function given by

$$H[P_S] = -P_S \log_2 P_S - (1 - P_S)\log_2(1 - P_S). \tag{3.4}$$

Observe from (3.2) and (3.3) that R_o and C can be expressed in the form $R_o = g_{R_o}(P_S)$ and $C = g_C(P_S)$, respectively. For convenience, these functions can be expressed in the union form $R_o, C = g_{\{R_o,c\}}(P_S)$. Likewise, these functions can be inverted to obtain expressions for the probability of symbol error as a function of the cutoff rate and capacity, $P_S = g_{\{R_o,C\}}^{-1}(R_o, C)$. For the cutoff rate case, the probability of symbol error is

$$P_S = \frac{(1 - \sqrt{1 - \alpha^2})}{2}, \tag{3.5}$$

where

$$\alpha = 2^{1-R_o} - 1, \tag{3.6}$$

and for the capacity case

$$P_S = H^{-1}[1 - C], \tag{3.7}$$

where $H^{-1}[\cdot]$ is the inverse operator of $H[\cdot]$. The probability of symbol error P_S depends upon many factors, including the type of modulation used. For this analysis, we consider

the use of binary modulation, e.g. BPSK or DPSK, and results are developed for the DPSK case. The uncoded bit error probability in the presence of additive white Gaussian noise (AWGN) is $P_b = f(\lambda_t)$ where λ_t is the bit energy-to-total noise ratio. For DPSK, $f(\lambda_t) = \frac{1}{2}\exp\{-\lambda_t\}$, and for BPSK $f(\lambda_t) = Q(\sqrt{2\lambda_t}))$ where

$$Q(x) = \int_x^\infty \frac{1}{\sqrt{2\pi}} e^{-\frac{\xi^2}{2}} d\xi. \tag{3.8}$$

When coding is used, the above code symbol error probability becomes

$$P_S = f(r\lambda_t), \tag{3.9}$$

where r is the code rate.

3.1.5 Code Division Multiple Access

The particular CDMA technique considered in this study is spread spectrum multiple-access (SSMA) which, in the sequel, will generally be referred to as CDMA. SSMA is characterized by the use of high rate (many chips per code symbol) pseudonoise (PN) spreading sequences. Spreading sequences are selected from code families having low off peak autocorrelations and low cross-correlations. It is assumed that the period of the spreading sequence is much greater than the code symbol duration. Although well known sets of deterministic sequences are available (e.g., Gold codes), the analysis in this study assumes completely random spreading sequences. For direct-sequence SSMA, the multiple-access interference at the front end of the receiver matched to the desired signal can be modeled as additional broad-band Gaussian noise [72]. A rigorous justification of this Gaussian approximation via comparison with the exact error probability has been provided for deterministic sequences [25] , and random sequences [49] , under the assumption of coherent detection. Similar results for differentially coherent detection (DPSK) have also been obtained [24] .

Following the above Gaussian approximation, and the network homogeneity assumption, the equivalent one-sided noise PSD due to the ith interferer is $N_i = PT_C = E_S = rE_b$ where P is the transmitted power, T_C is the PN chip duration, E_S is the code symbol energy, and E_b is the bit energy. Because the transmitted signals are mutually noncoherent,

their PSD's add and the total additive noise at the front end of the nth receiver is [93]

$$N_t = N_o + \eta^{-1} \sum_{\substack{j=1 \\ j \neq n}}^{M} r E_b \gamma_j, \tag{3.10}$$

where N_o is the background noise PSD, $\eta = T_S/T_C$ is the processing gain, M is the number of simultaneous transmitters, and γ_j is the attenuation of the jth signal. The attenuation can be used to account for fading, or transmitters having unequal transmitted power. From the homogeneity assumption, all packets arrive at each receiver with equal powers so that the bit energy-to-*total* noise ratio for the nth receiver is

$$\lambda_t = \frac{E_b}{N_o + \eta^{-1} r E_b \sum_{\substack{j=1 \\ j \neq n}}^{M}} \tag{3.11}$$

$$= \frac{\lambda_o}{1 + \eta^{-1} r \lambda_o \sum_{\substack{j=1 \\ j \neq n}}^{M}} \tag{3.12}$$

$$= \frac{\lambda_o}{1 + \eta^{-1} r \lambda_o (M - 1)}, \tag{3.13}$$

where λ_o is the bit energy-to-*background* noise ratio.

Finally, it is assumed that all transmitters employ the same carrier frequency, code symbol duration T_S, modulation technique, processing gain η, and that all receivers are synchronized in frequency, phase, chip, and bit epoch of the desired signal.

3.2   Network Analysis

In this section, the steady-state and dynamic performance of the Type I Hybrid ARQ protocol in slotted direct-sequence CDMA systems is analyzed. Expressions for the throughput and corresponding average packet delay are developed for the steady-state performance. To evaluate the dynamic performance, expressions are developed for the input-output packet flow rates of the network.

3.2.1   Steady-State Throughput-Delay Analysis

The throughput T at the output of the Hybrid ARQ channel is defined as the expected number of successful packets S per slot;

$$T = E\{S\}. \tag{3.14}$$

By the chain rule of expectation, (3.14) can be expressed as

$$T = E\{E\{S \mid M\}\}, \tag{3.15}$$

where

$$E\{S \mid M\} = \sum_{k=1}^{l} k p_{S|M}(k \mid l) \tag{3.16}$$

and

$$
\begin{aligned}
p_{S|M}(k \mid l) &= \mathrm{Prob}\{S = k \text{ successful packets} \mid M = l \text{ attempted transmissions}\}, \\
&= \binom{l}{k} P_C^k(l)[1 - P_C(l)]^{l-k}. \tag{3.17}
\end{aligned}
$$

Here, $P_C(l)$ is the probability of a correctly received packet when there are l simultaneous packet transmissions. Using (3.16) and (3.17), the throughput expression in (3.15) becomes

$$T = \sum_{l=1}^{N} \left\{ \sum_{k=1}^{l} k \binom{l}{k} P_C^k(l)[1 - P_C(l)]^{l-k} \right\} f_M(l), \tag{3.18}$$

where $f_M(l)$ is the probability distribution function for the number of attempted transmissions (composite arrivals) during a particular slot interval. Since

$$\left\{ \sum_{k=1}^{l} k \binom{l}{k} P_C^k(l)[1 - P_C(l)]^{l-k} \right\} = l P_C(l), \tag{3.19}$$

then

$$T = \sum_{l=1}^{N} l P_C(l) f_M(l). \tag{3.20}$$

Among other factors, throughput depends upon the channel's code rate r, processing gain η, and the bit energy-to-background noise ratio λ_o. By combining equations (3.9) and (3.13), the following expression can be obtained for the number of allowable simultaneous packet transmissions in a time slot;

$$m = \frac{\eta}{r} \left(\frac{r}{f^{-1}(g_{\{R_o, C\}}^{-1}(R_o, C))} - \frac{1}{\lambda_o} \right) + 1. \tag{3.21}$$

where $f^{-1}(\cdot)$ and $g^{-1}(\cdot)$ are the inverse operators of $f(\cdot)$ and $g(\cdot)$, respectively.

Suppose that the code being used has the property that the packet error probability is zero if $r \leq C$ and one if $r > C$. This ideal threshold effect occurs because it is possible to achieve arbitrarily reliable communication for all code rates up to channel capacity, while it

is impossible to achieve reliable communication with a code having a rate exceeding capacity. In practice, it is extremely difficult to operate with a code rate near capacity. The cutoff rate R_o has been proposed by Massey [60], and others, as a more realistic upper bound on the achievable rate. For sequential decoding of convolutional codes, R_o is the computational cutoff rate, and is usually viewed as the practical limit on the highest rate at which a sequential decoder can operate. If $r > R_o$, then frequent buffer overflows occur resulting in many decoding errors. On the other hand, it has been demonstrated that it is possible to operate very close to the cutoff rate. In [33], for example, two constraint length 21 rate 4/5 convolutional codes were used over a channel such that $r = 0.988R_o$. In 1000 packets, each consisting of 1000 bits, there were no observed decoding errors. As the constraint length of the code and/or the buffer size in the sequential decoder is increased, this threshold effect becomes even more pronounced [12]. Stüber [87] evaluated a Layland Lushbaugh constraint length 32 rate $\frac{1}{2}$ convolutional code [19], where Fano sequential decoding was used under a time out condition. The computer simulation consisted of transmitting 400 packets, each consisting of $L = 1000$ bits, over a BSC. The decoder used hard decision decoding without channel state information. The probability of correct packet reception was obtained as a function of the channel crossover probability for various time out limits. It was shown that the ideal decoder threshold approximation is quite accurate in terms of the network optimization, for convolutionally encoded packets with a Fano sequential decoder. Thus, for our purpose, an ideal decoder threshold is assumed, where the packet error probability is zero if $r \leq R_o$ and one if $r > R_o$. Results derived under the assumption of an ideal decoder threshold at capacity are included for comparison purposes.

For the limiting case as $r \to \{R_o, C\}$ and for fixed values of N, $\{R_o, C\}$, η, and λ_o, (3.21) gives the maximum number of allowable simultaneous packet transmissions as $\hat{m} = \lfloor m \rfloor$. If the actual number of packets l exceeds $\hat{m}$, then information is being transmitted at a rate above the cutoff rate or capacity of the channel. As a result, all packets are incorrectly received and must be retransmitted ($P_C(l) = 0, l > \hat{m}$). If the number of packets is less than or equal to $\hat{m}$, then all packets are received successfully ($P_C(l) = 1, l \leq \hat{m}$). The

throughput expression in (3.20) becomes

$$T = \sum_{l=1}^{\min(\hat{m},N)} l f_M(l).$$

(3.22)

In order to compare throughputs of different systems on an equal basis, we need to account for $\{R_o, C\}$ and η. The normalized throughput or network utilization becomes

$$T(p_r, \{R_o, C\}, \eta) = \frac{\{R_o, C\}}{\eta} T = \frac{\{R_o, C\}}{\eta} \sum_{l=1}^{\min(\hat{m},N)} l f_M(l).$$

(3.23)

This is the average number of successful packets (per slot) per unit time per unit bandwidth. Note that the normalized throughput is a function of the probability of retransmission, the code rate, and the processing gain. The normalized throughput is also a function of the population size, the composite traffic intensity, and the bit energy-to-background noise ratio. However, this dependency is not shown explicitly because these parameters are assumed to be uncontrolled. The maximum normalized throughput is

$$T_{\{R_o, C\}} = \max_{\substack{0 < p_r \leq 1}} \max_{\substack{0 < \{R_o, C\} \leq 1 \\ 1 \leq \eta}} T(p_r, \{R_o, C\}, \eta),$$

$$= \max_{\substack{0 < p_r \leq 1}} \max_{\substack{0 < \{R_o, C\} \leq 1 \\ 1 \leq \eta}} \frac{\{R_o, C\}}{\eta} \sum_{l=1}^{\min(\hat{m},N)} l f_M(l).$$

(3.24)

For the cutoff rate case, (3.24) represents the practically achievable limit on the maximum normalized throughput T_{R_o}. For the capacity case, (3.24) represents the theoretical upper limit on the maximum normalized throughput, T_C. The optimal probability of retransmission, code rate, and processing gain are denoted by p_r^*, $\{R_o^*, C^*\}$, and $\eta^{\{R_o, C\}}$, respectively.

The composite packet arrival distribution $f_M(l)$ is derived by using a Markov model similar to that developed in [39]. The channel is viewed as a discrete-time system where $n(t)$ represents the number of backlogged transmitters n during a particular slot interval. The network may then be in any one of $N + 1$ possible states. A geometric distribution for the probability of retransmission results in the retransmission delay also being geometrically distributed with an average

$$D_r = E/p_r,$$

(3.25)

where E is the average number of packet retransmissions per successfully transmitted packet. The memoryless property of the geometric distribution allows for a simple, sin-

gle state description. Assuming N and p_o to be time-invariant, $n(t)$ represents a Markov process with state transition matrix $\mathbf{P} = [p_{ij}]$ where the state transition probabilities are defined as

$$p_{ij} = \text{Prob}\{n(t+1) = j \mid n(t) = i\}. \tag{3.26}$$

Calculation of the above state transition matrix is more complicated than in the narrow-band case [39], but is simpler than in [75] because $P_C(l)$ is binary in value ($P_C(l) = 1$ for $l \leq \hat{m}$ and $P_C(l) = 0$ for $l > \hat{m}$). From this simplification, the following expressions for the one-step state transition probabilities can be derived (Appendix A);

$$p_{ij} = \begin{cases}
\text{(for } j < i) \\[1mm]
0, & i - j > \hat{m} \\[2mm]
\sum_{k=0}^{\min(\hat{m}-i+j,N-i)} b(k, N-i, p_o)b(i-j, i, p_r), & i - j \leq \hat{m} \\[3mm]
\text{(for } j = i) \\[1mm]
\sum_{k=0}^{\min(N-i,\hat{m})} b(k, N-i, p_o)b(0, i, p_r), & i \leq \hat{m} \\[2mm]
\sum_{k=0}^{\min(N-i,\hat{m})} b(k, N-i, p_o)b(0, i, p_r) \\
\quad + \sum_{k=\hat{m}+1}^{i} b(k, i, p_r)b(0, N-i, p_o), & \hat{m} < i < N \\[2mm]
\sum_{k=\hat{m}+1}^{N} b(k, N, p_r) + b(0, N, p_r), & i = N \\[3mm]
\text{(for } j > i) \\[1mm]
0, & j \leq \hat{m}, j - i \leq \hat{m} \\[2mm]
b(j-i, N-i, p_o)[1 - \sum_{k=0}^{\hat{m}-j+i} b(k, i, p_r)], & \hat{m} < j \leq N, j - i \leq \hat{m} \\[2mm]
b(j-i, N-i, p_o), & \hat{m} < j \leq N, j - i > \hat{m}
\end{cases} \tag{3.27}$$

where the terms in the summation represent the binomial distribution function such that

$$b(\alpha, n, p) = \binom{n}{\alpha} p^\alpha (1-p)^{n-\alpha}. \tag{3.28}$$

When $\hat{m} = 1$, (3.27) reduces to the standard narrow-band slotted ALOHA case as in [39]. For the infinite population model, if we let $N \to \infty$ and $p_o \to 0$ such that $Np_o = T_{\{R_o, C\}}$,

then (3.27) becomes

$$
p_{ij} = \begin{cases}
\text{(for } j < i) \\[4pt]
0, & i - j > \hat{m} \\[6pt]
\sum_{k=0}^{\min(\hat{m}-i+j,N-i)} \frac{T^k}{k!} e^{-T} b(i-j,i,p_r), & i - j \leq \hat{m} \\[10pt]
\text{(for } j = i) \\[4pt]
\sum_{k=0}^{\min(N-i,\hat{m})} \frac{T^k}{k!} e^{-T} b(0,i,p_r), & i \leq \hat{m} \\[8pt]
\sum_{k=0}^{\min(N-i,\hat{m})} \frac{T^k}{k!} e^{-T} b(0,i,p_r) \\
\quad + \quad e^{-T} \sum_{k=\hat{m}+1}^{i} b(0,N-i,p_o), & \hat{m} < i < N \\[8pt]
\sum_{k=\hat{m}+1}^{N} b(k,N,p_r) + b(0,N,p_r), & i = N \\[10pt]
\text{(for } j > i) \\[4pt]
0, & j \leq \hat{m}, j - i \leq \hat{m} \\[6pt]
\frac{T^{j-i}}{(j-i)!} e^{-T} [1 - \sum_{k=0}^{\hat{m}-j+i} b(k,i,p_r)], & \hat{m} < j \leq N, j - i \leq \hat{m} \\[8pt]
\frac{T^{j-i}}{(j-i)!} e^{-T}, & \hat{m} < j \leq N, j - i > \hat{m}
\end{cases}
\tag{3.29}
$$

With $\mathbf{P}$, we can solve for the equilibrium state probability distribution $\underline{\pi}$ in the following equation:

$$
\underline{\pi} = \underline{\pi} \mathbf{P}, \tag{3.30}
$$

where

$$
\underline{\pi} = [\pi(0), \pi(1), \ldots, \pi(N)], \tag{3.31}
$$

and

$$
\sum_{n=0}^{N} \pi(n) = 1. \tag{3.32}
$$

Using the above solution for $\underline{\pi}$, we can now express $f_M(l)$ in terms of the number of back-logged transmitters as

$$
f_M(l) = \sum_{n=0}^{N} f_M(l \mid n) \pi(n), \tag{3.33}
$$

where

$$
f_M(l \mid n) = \sum_{k=\max(l-n,0)}^{\min(l,N-n)} b(k, N-n, p_o) b(l-k, n, p_r). \tag{3.34}
$$

Substituting (3.33) into (3.24), the normalized throughput equation becomes

$$T_{\{R_o,C\}} = \max_{0 < p_r \leq 1} \max_{\substack{0 < \{R_o,C\} \leq 1 \\ 1 \leq \eta}} \frac{\{R_o,C\}}{\eta} \sum_{l=1}^{\min(\hat{m},N)} l \sum_{n=0}^{N} \pi(n) \sum_{k=\max(l-n,0)}^{\min(l,N-n)} b(k,N-n,p_o)b(l-k,n,p_r).$$

(3.35)

For the special case when $N = \infty$, $p_o = p_r = 0$ and $p_o N = T_{\{R_o,C\}}$, (3.35) becomes

$$T_{\{R_o,C\}} = \max_{0 < p_r \leq 1} \max_{\substack{0 < \{R_o,C\} \leq 1 \\ 1 \leq \eta}} \frac{\{R_o,C\}}{\eta} \sum_{l=1}^{\min(\hat{m},N)} \frac{l\nu^l \exp\{-\nu\}}{l!}$$

(3.36)

which is the same as the throughput expression derived in [86] where FEC is employed without retransmissions.

The average packet delay D of a network is often modeled as the sum of a random delay component D_r, a deterministic component D_d, and a one slot transmission time:

$$D = D_r + D_d + 1.$$

(3.37)

The deterministic component can be used to model any fixed delay inherent in the network. For this analysis, it is assumed that the deterministic component is zero. As such, equation (3.37) becomes

$$D = D_r + 1.$$

(3.38)

The random delay component D_r is the average retransmission delay defined earlier and represents the average rescheduling delay or the average backlog time experienced by a transmitter. This random component is necessary to prevent backlogged transmitters from contending with other transmitters blocked during the same time slot. From Little's result [38], D_r can be expressed as

$$D_r = \frac{\bar{n}}{T_{\{R_o,C\}}},$$

(3.39)

where $\bar{n}$ is the average number of backlogged transmitters which can be calculated from

$$\bar{n} = \sum_{n=0}^{N} n\pi(n).$$

(3.40)

By using (3.38) and (3.39), the throughput can be directly related to the average packet delay (3.37) as

$$T_{\{R_o,C\}} = \frac{\bar{n}}{D-1}.$$

(3.41)

This alternate expression for the throughput is the one that is actually used in the maximization required by (3.24), while (3.24) provides a convenient check during the analysis.

Throughput can also be related to E, the average number of packet retransmissions per successfully transmitted packet, by the following expression

$$E = \frac{\nu}{T_{\{R_o,C\}}} - 1, \qquad (3.42)$$

where $\nu/T_{\{R_o,C\}}$ is the average number of times a packet must be transmitted until it is successfully received. This expression can be used with the data from Section 3.3 (Fig 3.5) to obtain a plot of E against $T_{\{R_o,C\}}$. Substituting (3.42) and (3.39) into (3.25), the probability of retransmission can be expressed as

$$p_r = \frac{\nu - T_{\{R_o,C\}}}{\bar{n}}. \qquad (3.43)$$

A similar expression for the probability of original packet transmission can be obtained as

$$\begin{aligned} p_o &= \frac{\nu_o}{\sum_{n=1}^{N}(N-n)\pi(n)} \\ &= \frac{T}{N - \bar{n}} \end{aligned} \qquad (3.44)$$

These expressions for p_r and p_o are used in computing the $\mathbf{P}$ matrix (3.27) and are key in performing the maximization in (3.24).

3.2.2 Dynamic Throughput-Delay Analysis

The analysis presented so far is not sufficient to fully characterize the performance of our CDMA network. Up to this point, we have assumed that the network is in equilibrium. That is, for a given number of backlogged transmitters n, the input transmission rate T_{in} is equal to the output or delivered transmission rate T_{out}. The channel input transmission rate is defined as the number of new packet transmissions per time slot. The normalized input transmission rate is

$$T_{in} = \frac{\{R_o,C\}}{\eta}(N-n)p_o. \qquad (3.45)$$

Note that if we take the expectation over n in (3.45), then T_{in} becomes the input traffic intensity ν_o. The channel output transmission rate is defined as the probability of up to $\hat{m}$

successful packet transmissions per time slot. The normalized output transmission rate is given by

$$T_{out} = \frac{\{R_o, C\}}{\eta} \left[\sum_{k=0}^{\hat{m}} \sum_{l=0}^{\hat{m}-k} b(k, N - n, p_o) b(l, n, p_r) - (1 - p_o)^{N-n} (1 - p_r)^n \right]. \qquad (3.46)$$

Note that if we take the expectation over n in (3.46), then the output transmission rate becomes the normalized throughput in (3.23). When N and p_o are stationary with time, (3.45) and (3.46) are referred to as the channel load line and equilibrium contour, respectively.

A channel is said to be stable when its load line intersects (nontangentially) the equilibrium contour in exactly one place. Points where the load line intersects the equilibrium contour are defined as channel operating points. For stable channels with a large population size, analysis has shown that networks actually operate close to these channel operating points [44]. In Fig. 3.4, (3.46) is plotted against three different channel load lines (3.45) to show the effects of changing network operating conditions on the network's stability. Load line A represents a stable channel having an operating point (T_1, n_1) with relatively high throughput and a low number of backlogged transmitters (low delay). Load line C also represents a stable channel, but in this case the network is overloaded with a channel operating point having relatively low throughput and a high number of backlogged transmitters (high delay). Load line B represents an unstable channel having three possible channel operating points with the most desirable operating point being at (T_3, n_3). Assuming that the network is currently operating in the vicinity of this point, it will not remain there because $n(t)$ is a random process. That is, there is a nonzero probability that the number of backlogged transmitters will exceed n_2. When this occurs, $T_{in} > T_{out}$ which causes the operating point to drift (accelerate) up the load line to the overloaded equilibrium point (low throughput and high delay). While there is also a nonzero probability that the channel operating point will return below the $\{T_2, n_2\}$ point, simulations show that the channel tends to remain near the overloaded equilibrium point instead [44].

For the finite population case, if the channel is stable, then the network operating point can reside in the vicinity of the channel operating point indefinitely. For an unstable channel, however, network operation around the desired operating point is achievable for only a finite amount of time before the channel saturates. Finite population channels can

be stabilized by decreasing p_r (at the expense of increasing delay), by decreasing N, or by employing external stabilizing measures which include various retransmission control strategies [45]. For the infinite population case, channels are inherently unstable and can operate near their desirable operating points for only a finite amount of time [35,39]. This operational time can be increased by the methods mentioned above to achieve performance close to the theoretical optimum [45].

3.3 Performance Evaluation

In this section, the dependency of the network's throughput-delay performance on N, ν, λ_o, p_r, $\{R_o, C\}$, and η is examined in detail for both the steady-state and dynamic cases. The optimal probabilities of retransmission, processing gains, and code rates are identified. The results obtained here for DS/DPSK signaling can also be obtained for DS/BPSK signaling within the same framework.

3.3.1 Steady-State Throughput-Delay Performance

Figs. 3.5 and 3.6-3.7 are plots of the maximum normalized throughtputs, T_{R_o} and T_C, against traffic intensity ν and against average delay D, respectively. These plots illustrate the combined effects of maximizing throughput over the probability of retransmission p_r, and the code rate and processing gain $\{R_o, C; \eta\}$. The first maximization required by (3.24) is performed by fixing D in (3.41), allowing p_r to vary ($0 \leq p_r \leq 1$) in (3.30), and solving for a $(\bar{n}, \pi(n))$ solution which maximizes (3.41). This procedure is repeated for all possible values of $\hat{m}$ ($1 \leq \hat{m} \leq N$) and results in N optimal $(p_r, T_{\{R_o,C\}})$ pairs for each fixed value of D. An alternate procedure, whereby the throughput is fixed and the delay is minimized, produces the same optimal $(p_r, T_{\{R_o,C\}}, \hat{m}, D)$ combinations. For the second maximization required by (3.24), D is again fixed for a given level of background noise. The code rate and processing gain $\{R_o, C; \eta\}$ are allowed to vary in (3.21) yielding $\hat{m}$ values for which the corresponding throughputs are known from step one. Each value of throughput is then normalized and the maximum normalized value is selected. Note that (3.21) requires a solution for P_S. For the cutoff rate case, a solution for P_S is found in a straight forward

manner by using (3.5) and (3.6). For the capacity case, a P_S solution is found by solving (3.3) and (3.4) simultaneously.

Results in Figs. 3.5 and 3.6-3.7 are shown for population sizes $N = 10, 30$, and ∞ ; and for background noise levels of $\lambda_o = \infty$ and $\lambda_o = 10.34$ dB. The background noise level of 10.34 dB was chosen because it results in a bit error probability of 10^{-5} for uncoded DPSK in the absence of multiple-access interference. Although the infinite population case may be an unrealistic population size, it does provide a useful bound on system performance.

Optimization of Throughput-Delay Performance over Probability of Retransmission

Optimal values for probability of retransmission p_r^* exist for all values of traffic intensity as shown in Fig. 3.8. For the low range of traffic intensities ($\nu < 1.0$) in Fig. 3.8, there are two distinct p_r^* values for each value of ν. Selecting the lower p_r^* value for a given traffic intensity results in the maximum possible value for $T_{\{R_o,C\}}$ (Fig. 3.5) but with nonminimal delay (Figs. 3.6-3.7). In Figs. 3.6-3.7, these lower p_r^* values correspond to the upper branch of the throughput-delay curve. Here, ν is increasing along the curve from A to B and back to C. Points on the A-B portion of the curve correspond to stable operating points, whereas those on the B-C portion of the curve do not. A maximal $T_{\{R_o,C\}}$ value is achieved under the following conditions: $p_r^* \ll 1.0$, $p_o \to 1.0$, and $\bar{n} \to N$. As a result, the throughput is closely approximated by the equation $T_{\{R_o,C\}} = \nu$ for low ν ($\nu < 0.5$) in Fig. 3.5, and by the equation $T_{\{R_o,C\}} = N/D$ for the upper branch (A-B) in Figs. 3.6-3.7. These two throughput expressions are related through Little's result (3.39) by applying the above conditions to (3.43) and (3.41), respectively.

Selecting the higher p_r^* value for a given traffic intensity ($\nu < 1.0$) in Fig. 3.8 results in a nonmaximal $T_{\{R_o,C\}}$ value (not shown in Fig. 3.5) but at minimal delay (Figs. 3.6-3.7). The higher p_r^* values correspond to the lower right-hand branch of the throughput-delay curve in Figs. 3.6-3.7 (increasing ν from E to F). This throughput-delay curve agrees with the results from earlier throughput-delay analyses for conventional narrow-band slotted ALOHA [44]. Furthermore, simulation results obtained by Lam [44] agree very well with these analytic results. For these nonmaximal $T_{\{R_o,C\}}$ values, $p_r^* > p_o$ and $\bar{n}$ is relatively

low.

Note in Fig. 3.8 that for the low range of traffic intensities ($\nu < 1.0$), the upper and lower curves for p_r^* are separate and distinct. For a given traffic intensity, this separation represents the change in p_r^* that is necessary to move the network from an operating point having maximal throughput to one having minimal delay, and vice-versa. In Fig. 3.6, for example, the throughput-delay points for traffic intensities of $\nu = 0.525$ and 1.00 are plotted for comparison purposes for the two values of p_r^*. Note in this example, that for $\nu = 1.0$ it seems that an improvement in throughput can be had for a modest increase in delay by operating on the upper branch (B-C). However, the upper branch (B-C) operating point is not stable, whereas, the lower branch (E-F) operating point is. Stability issues are discussed further in Section 3.3.2.

For the upper range of traffic intensities ($\nu > 1.0$) in Fig. 3.8, there are also two distinct p_r^* values for most values of ν as indicated by the solid and dashed lines. The solid lines correspond to the case where either plain or Hybrid ARQ is the optimal protocol ($\hat{m} = 1$). Here, p_r^* can be approximated by $p_r^* = \nu/N$. Because p_r^* is independent of λ_o, the same value of p_r^* is used for both plain and Hybrid ARQ for a given traffic intensity. The dashed lines correspond to the case when Type 1 Hybrid ARQ is used with CDMA (hereafter referred to as CDMA) ($\hat{m} \geq 2$). The dashed lines correspond to when $p_r^* = \nu/N$ exactly, which is usually the case when CDMA is used as explained below.

Fig. 3.9 depicts, in more detail, p_r^* against ν for a population size of $N = 10$. All p_r^*-ν curves are shown ($1 \leq \hat{m} \leq 10$) and are numbered accordingly. For a given N,ν, and λ_o, only one of the $\hat{m}$ values will be optimal, and, therefore, only one of the p_r^*-ν curves will provide the optimal retransmission probability p_r^*. In general, higher ν and/or lower λ_o values require higher optimal $\hat{m}$ values. Note that when CDMA is used ($\hat{m} \geq 2$) each of the p_r^*-ν curves has that $p_r^* = \nu/N$ exactly over a relatively large range of ν. See, for example, dashed line 5 ($\hat{m} = 5$) where $p_r^* = \nu/N$ for $3.2 < \nu < 6.0$. When this occurs, $p_r^* = \nu/N = p_o$ and the composite arrival distribution $f_M(l)$ is binomial. Whether the network operates on this linear portion of the curve depends on ν and λ_o through a parameter called the cutoff traffic intensity (discussed below). As mentioned earlier, operation on this linear portion of the curve is usually the case. Let $p_{r,BN}$ denote the retransmission probability

when the composite arrival distribution is binomial (i.e., $p_r = \nu/N$), and $p_{r,NBN}$ denote the retransmission probability when the composite arrival distribution is not binomial (i.e., $p_r \neq \nu/N$). Accordingly, $p^*_{r,BN}$ and $p^*_{r,NBN}$ denote the optimal retransmission probabilities in either case. For very high ν, $p_{r,BN}$ is no longer optimal but is still a good approximation for $p^*_{r,NBN}$ because using $p_{r,BN}$ results in only slightly lower throughput and increased delay. This effect is shown in Fig. 3.10 for ($\hat{m} = 3$). Note that $p_{r,BN}$ is a good estimate for p^*_r over the entire range of traffic intensity with respect to throughput performance.

In Fig. 3.5, the plain/Hybrid ARQ p^*_r values correspond to the plain/Hybrid ARQ curves and the CDMA p^*_r values correspond to the upper branches which break away from the plain ARQ curves at various traffic intensities. In Figs. 3.6-3.7, the B-C-A branch of the throughput-delay curve (ν increasing from B to C then toward A) corresponds to the plain/Hybrid ARQ p^*_r values and the C-D branch corresponds to the CDMA p^*_r values.

Optimization of Throughput-Delay Performance over Code Rate and Processing Gain

Note, in Fig. 3.5, for the plain/Hybrid ARQ case, that throughput becomes vanishingly small and delay in Figs. 3.6-3.7 becomes unbounded as the traffic intensity increases. However, when CDMA is used, this degradation in performance does not occur. Instead, the maximum normalized throughput decreases to some minimal value, at a particular traffic intensity, and then increases again. The corresponding delay decreases. The traffic intensity at which CDMA achieves this improved performance over plain/Hybrid ARQ is defined as the *cutoff traffic intensity* which is denoted as $\nu^{\{R_o,C\}}$ and is described as follows. If $\nu < \nu^{\{R_o,C\}}$, then the optimal processing gain $\eta^{\{R_o,C\}}$ is unity for all bit energy-to-background noise ratios ($\lambda_o \leq \infty$). If $\nu > \nu^{\{R_o,C\}}$, then $\eta^{\{R_o,C\}} > 1$ with the actual value depending on the traffic intensity, population size, and the bit energy-to-background noise ratio as described below. In Fig. 3.5, the cutoff intensities occur at the intersection of the CDMA curves with the plain/Hybrid ARQ curves. Observe that for $\lambda_o = \infty$ and $\nu < \nu^{\{R_o,C\}}$, T_{R_o} and T_C are identically equal. For $\lambda_o < \infty$ and $\nu < \nu^{\{R_o,C\}}$, $T_{R_o} \neq T_C$, but these differences are usually too small to show graphically, the only exception being for T_{R_o} at $\lambda_o = 10.34$ dB. In Figs. 3.6-3.7, point C is an example of a throughput-delay

point which corresponds to a cutoff intensity. Note how the delay drops precipitously (C-D) when CDMA is used. Recall that these delay results must be adjusted for any fixed delay inherent in the network being considered. Any additional fixed delay would cause the curves in Figs. 3.6-3.7 to be shifted upward by a corresponding amount.

Fig. 3.11 illustrates the effect of bit energy-to-background noise ratio λ_o and population size N on the cutoff traffic intensity $\nu^{\{R_o,C\}}$. In general, $\nu^{\{R_o,C\}}$ increases to its maximum value (N) as λ_o decreases. Note that for each $\nu^{\{R_o,C\}}$ there is a corresponding λ_o which is defined as the *background noise limit* for that cutoff intensity, denoted by $\lambda_o^{\{R_o,C\}}$. Also, for each λ_o there is a corresponding cutoff traffic intensity. The $\{6.82 \text{ dB}, 4.81 \text{ dB}\}$ background noise limits are defined as the network *asymptotic background noise limits* and are denoted $\hat{\lambda}_o^{\{R_o,C\}}$. The network cannot operate at bit energy-to-background noise ratios below these asymptotic background noise limits, because they represent the smallest λ_o that can be present for reliable coded communications in the absence of multiple-access interference [86].

Figs. 3.12-3.13 show how the optimal processing gain $\eta^{\{R_o,C\}}$ depends on the traffic intensity for different population sizes N and bit energy-to-background noise ratios λ_o. For the $N = \infty$ case, $\eta^{\{R_o,C\}}$ depends on ν in a nearly linear fashion. The effect of finite population size is a 'staircase' type curve which tends to the $N = \infty$ curve as $N \to \infty$.

Fig. 3.14 shows how the optimal processing gain $\eta^{\{R_o,C\}}$ depends on the bit energy-to-background noise ratio λ_o for particular traffic intensities $\nu = 5, 10$ and population sizes $N = 10, 30$, and ∞. In general, the optimal processing gain increases with decreasing λ_o. Recall that, for each traffic intensity, there is a corresponding background noise limit. Thus, for a given traffic intensity, as $\lambda_o \to \lambda_o^{\{R_o,C\}}$, $\eta^{\{R_o,C\}}$ increase to some finite maximum value at $\lambda_o^{\{R_o,C\}}$. Observe how $\eta^{\{R_o,C\}}$ increases drastically as λ_o nears $\lambda_o^{\{R_o,C\}}$. Should λ_o become less than the background noise limit for a given ν, then $\nu < \nu^{\{R_o,C\}}$ and CDMA is no longer the optimal protocol. For this case, $\hat{\lambda}_o^{\{R_o,C\}} < \lambda_o < \lambda_o^{\{R_o,C\}}$, the optimal processing gain is unity.

Fig. 3.15 summarizes the dependency of the optimal code rate $\{R_o^*, C^*\}$ on the bit energy-to-background noise ratio λ_o and population size N. Note that the selection of the optimal code rate depends primarily upon ν and λ_o, and does not depend directly on

N. When $\lambda_o = \infty$ and $\nu < \nu^{\{R_o,C\}}$, the optimal code rate $\{R_o^*, C^*\}$ is unity. Hence, the optimal protocol is plain ARQ. In fact, plain ARQ is used *only* when $\lambda_o = \infty$ and $\nu < \nu^{\{R_o,C\}}$. When $\lambda_o < \infty$ and $\nu < \nu^{\{R_o,C\}}$, $\{0.48, 0.50\} < \{R_o^*, C^*\} < 1.0$. In this case, Hybrid ARQ is used. For $\lambda_o \leq \infty$ and $\nu > \nu^{\{R_o,C\}}$, the optimal code rate $\{R_o^*, C^*\}$ is constant at $\{0.48, 0.50\}$. CDMA is the optimal protocol in this case. For a given level of background noise, the optimal code rate can be determined as the traffic intensity varies by using Figs. 3.11 and 3.15 . For a given λ_o, Fig. 3.11 gives the corresponding $\nu^{\{R_o,C\}}$. As the traffic intensity varies above and below this particular $\nu^{\{R_o,C\}}$, the optimal code rate is given by the lower branch and upper branch of Fig. 3.15, respectively.

It should be noted that, for the entire range of traffic intensities, it is possible to operate CDMA with a delay $D = 1.0$. Unity delay is achieved by selecting the appropriate code rate and processing gain combination so that $\hat{m} = N$. In most cases, however, unit delay is achieved at the expense of a far from optimal throughput. Unit delay curves are shown in Fig. 3.5 for the cutoff rate and capcity cases at $\lambda_o = \infty$. Note that the throughput at unit delay $T_{D=1}$ is very small for $0 < \nu < \nu^{\{R_o,C\}}$. At $\nu = \nu^{\{R_o,C\}}$, there is a step increase in $T_{D=1}$, after which $T_{D=1} \to T_{\{R_o,C\}}$ as $\nu \to N$. These unity delay curves together with the corresponding $T_{\{R_o,C\}}$ curves represent a bounded region of operation where throughput and delay may be traded off between one another.

Finally, recall that the maximum normalized throughput $T_{\{R_o,C\}}$ is defined as the average number of successful packets per time slot per unit bandwidth. Throughput results are normalized (r/η) so that CDMA and narrow-band results can be compared fairly. As a result, $T_{\{R_o,C\}}$ is always less or equal to unity. That is, at most one packet can be successfully transmitted per time slot per unit bandwidth. For example, at $\nu = 5.0$, $\lambda_o = \infty$, and $N = 10$; $T_{R_o} = 0.0212$ and $D = 407.0$ for narrowband operation and $T_{R_o} = 0.158$ and $D = 6.71$ for CDMA operation. For actual network operation, however, throughputs are not normalized, and it is possible to successfully transmit more than one packet per slot. Throughputs greater than one packet per slot usually occur when operating with CDMA at the higher traffic intensities. When comparing nonnormalized performance, narrow-band results should be scaled by a factor of η/r for fairness. Let $T_{\{R_o,C\},NN}$ denote the maximum nonnormalized throughput. In the above example, $\eta = 13.9$ and $r = 0.480$

so that $T_{R_o,NN} = 0.614$ and $D = 15.0$ for the narrowband case and $T_{R_o,NN} = 4.58$ and $D = 1.20$ for the CDMA case. Delays decrease uniformly by a factor of r/η due to Little's Result $(D = r\bar{n}/\eta T_{\{R_o,C\}} + 1)$. Fig. 3.16 gives complete throughput $(T_{R_o,NN})$ versus traffic intensity results for the above example. Note that for the narrow-band curve and for traffic intensities above cutoff, $T_{R_o,NN}$ remains small and decreases to zero with increasing traffic intensity because the throughput for the narrow-band case decreases to zero for this range of traffic intensities.

3.3.2 Dynamic Throughput-Delay Performance

When the traffic intensity of our network rises to a level at or above the cutoff intensity, the employment of CDMA stabilizes what would otherwise be an unstable network. This effect is shown in Fig. 3.17 for a traffic intensity $\nu = 3.0$, a population size of $N = 10$, and no background noise $(\lambda_o = \infty)$. The cutoff intensity in this case is $\nu^{R_o} = 2.85$. Note that the plain ARQ curves display an unstable characteristic whereas the CDMA curves display a stable characteristic. Average operating points generated by numerical analysis are shown for each case. Points G $(T_{R_o} = 0.129, \bar{n} = 7.417)$ and H $(T_{R_o} = 0.151, \bar{n} = 2.70)$ correspond to the plain ARQ and CDMA cases, respectively. For the CDMA case, note that the relatively large distance between the average operating point H and the channel operating point J can be attributed to the small population size. The vertical CDMA curve is due to the binomial arrival distribution $(p_r = p_o)$. In Fig. 3.6, throughput-delay points corresponding to $\nu = 3.0$ and $N = 10$ for both the plain ARQ $(T_{R_o} = 0.129, D = 56.0)$ and CDMA $(T_{R_o} = 0.151, D = 19.0)$ cases are shown for reference. In Fig. 3.7, a throughput-delay point for $\nu = 3.0$ and $N = 30$ is also shown. Observe that for the $(T_{R_o}, \lambda_o = \infty)$ curve, there is no $\nu = 3.0$ throughput-delay point on the CDMA curve (C-D) because $\nu = 3.0$ is less than the cutoff intensity for $N = 30$, $\lambda_o = \infty$ $(\nu^{R_o} = 3.17)$. Thus, for a given traffic intensity and λ_o, an increase in N causes a corresponding increase in $\nu^{\{R_o,C\}}$ which, in this case, destabilizes the network.

Finally, note that CDMA achieves a similar stabilizing effect for $\lambda_o < \infty$ and $\nu > \nu^{\{R_o,C\}}$. For this case, Hybrid ARQ operates at some code rate less than unity depending on the background noise level. In the above example $(N = 10, \nu = 3.0)$, if λ_o is high

enough so that $R_o \approx 1.0$ then R_o is close to unity and η is unity in (3.45) and (3.46) and the resulting Hybrid ARQ stability curves are very close to those shown for the plain ARQ case in Fig. 3.17. That is , the Hybrid ARQ case exhibits the same unstable characteristic (ie., multiple network operating points). If 15.25 dB $\leq \lambda_o < \infty$ then $R_o < 1.0$ and $\eta = 1.0$ and the resulting equilibrium curves generally shift to the left but maintain the same unstable form. For the CDMA case, 15.25 dB $\leq \lambda_o < \infty$ causes the CDMA stability curves to shift in a similar manner while maintaining the same stable form.
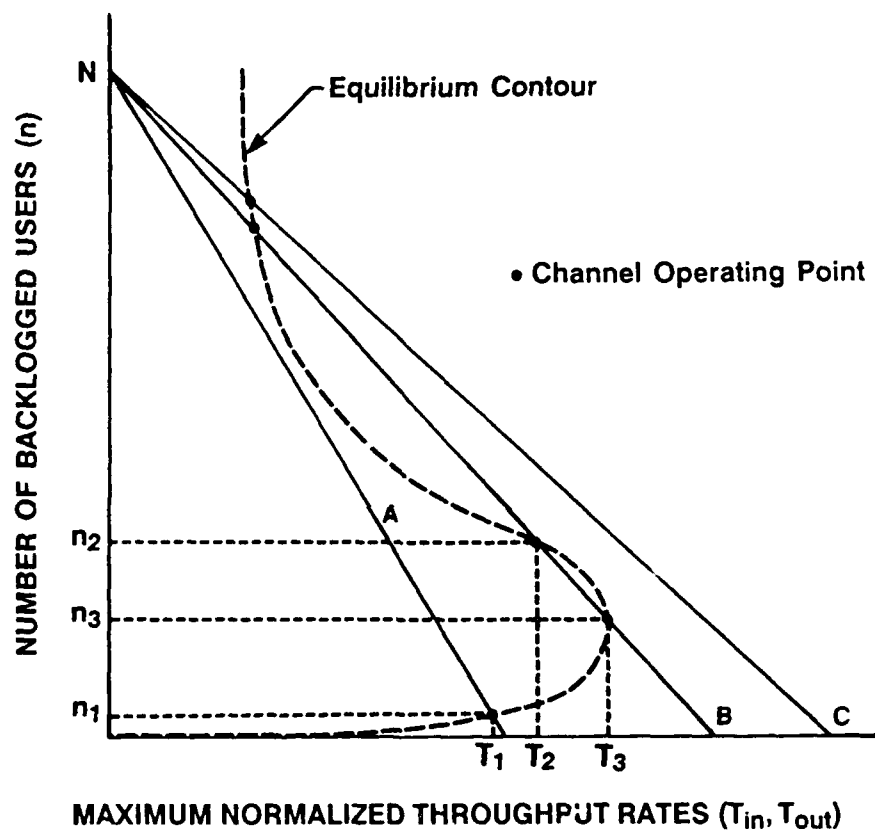
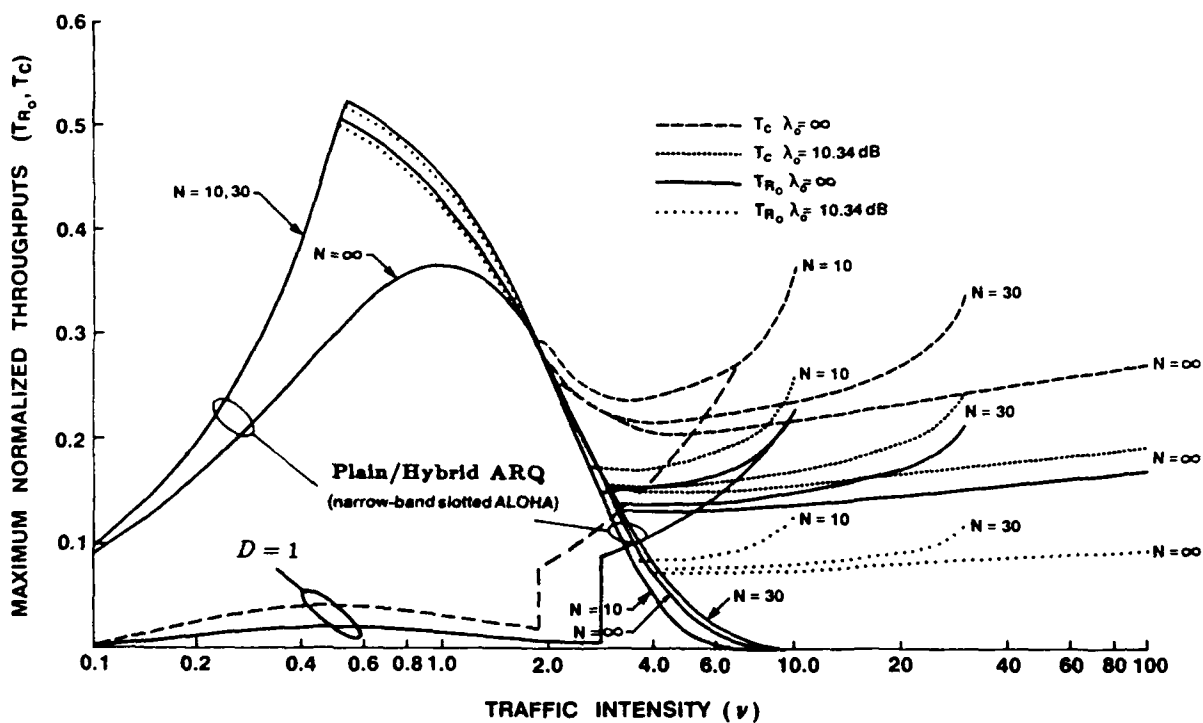Figure 3.4: CDMA Network Stability for Different Network Operating Conditions

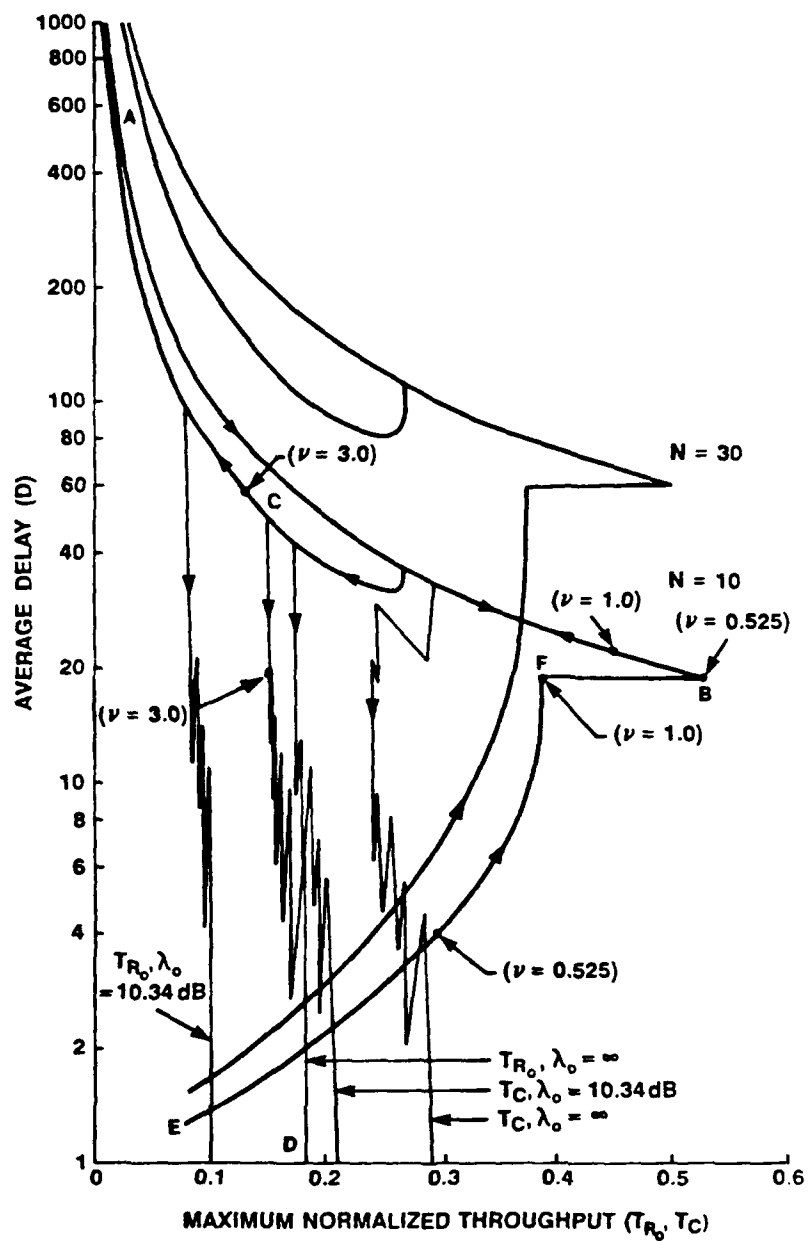Figure 3.5: Maximum Normalized Throughput ($T_{\{R_o,C\}}$) versus Traffic Intensity (ν)

Figure 3.6: Average Delay (D) versus Maximum Normalized Throughput $(T_{\{R_o,C\}})$ for N = 10 (N = 30 results are overlayed)
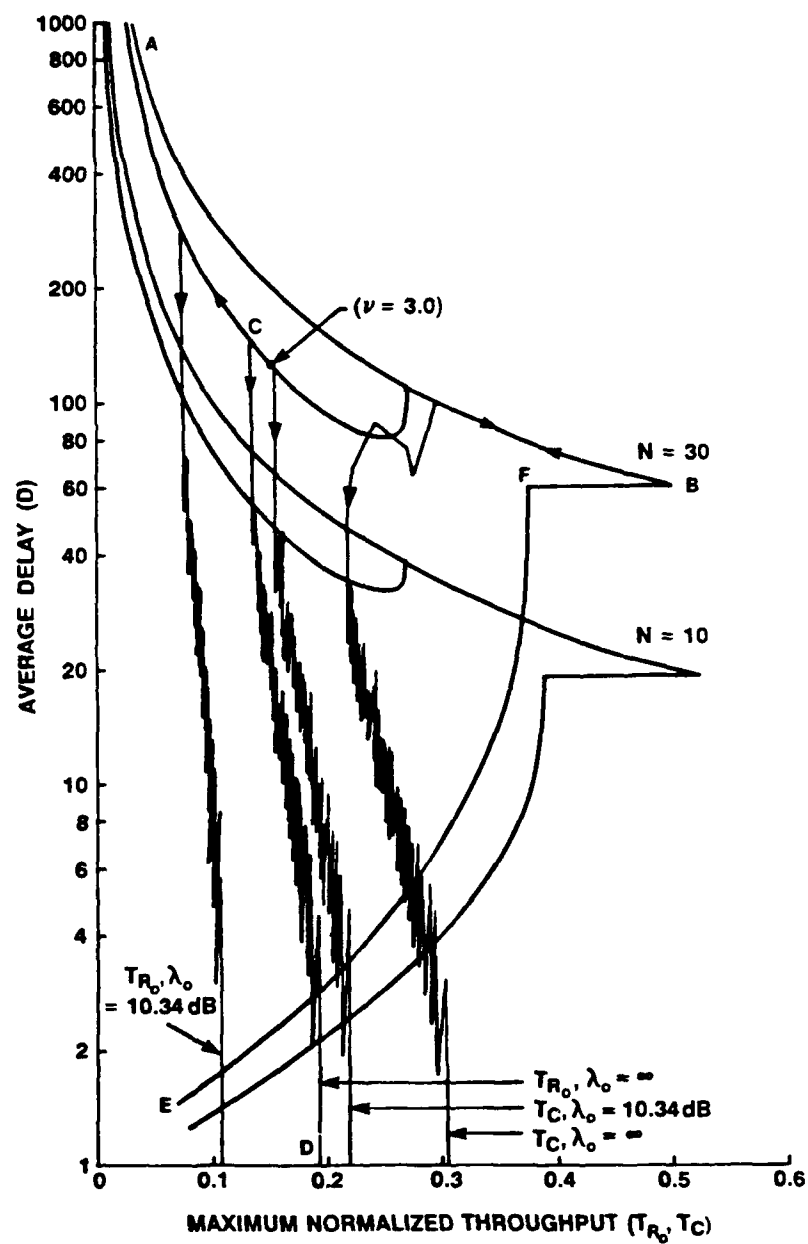
Figure 3.7: Average Delay (D) versus Maximum Normalized Throughput $(T_{\{R_o,C\}})$ for N = 30 (N = 10 results are overlayed)
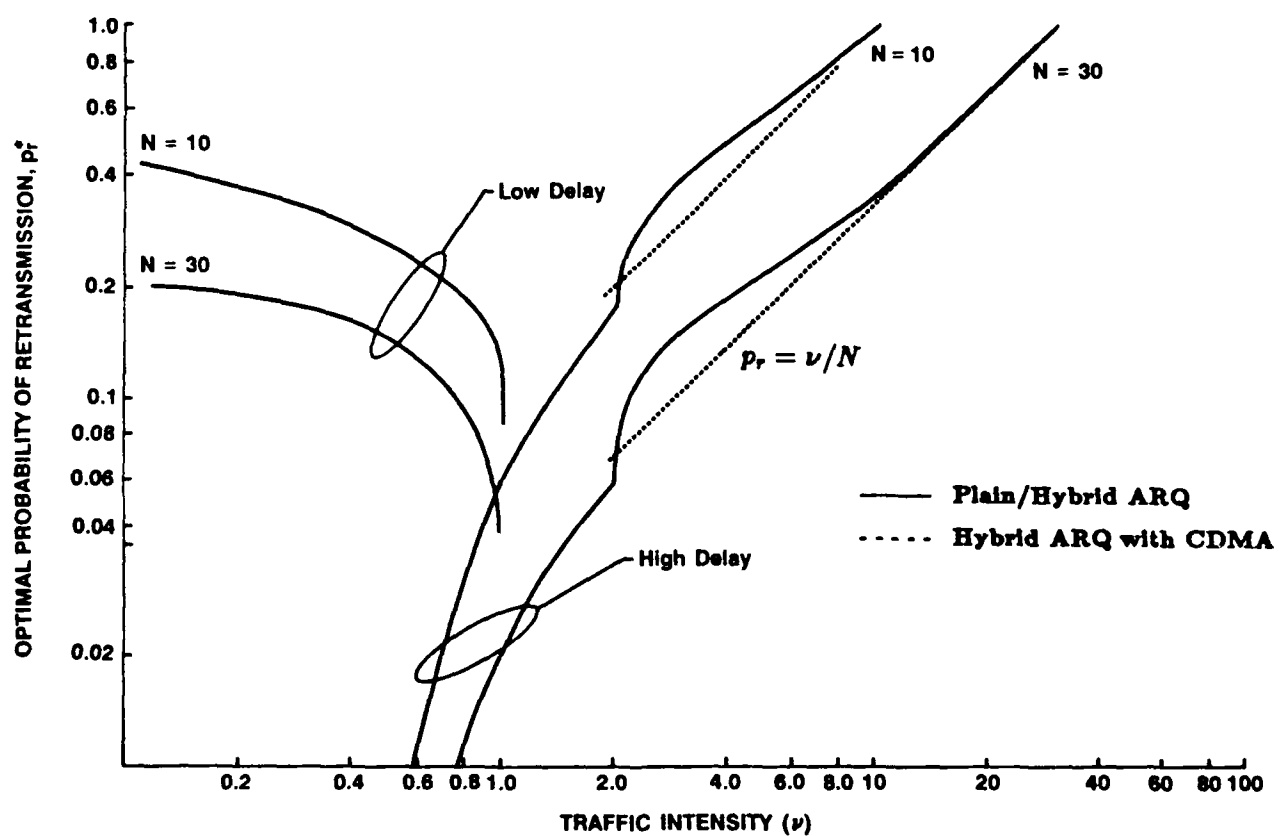
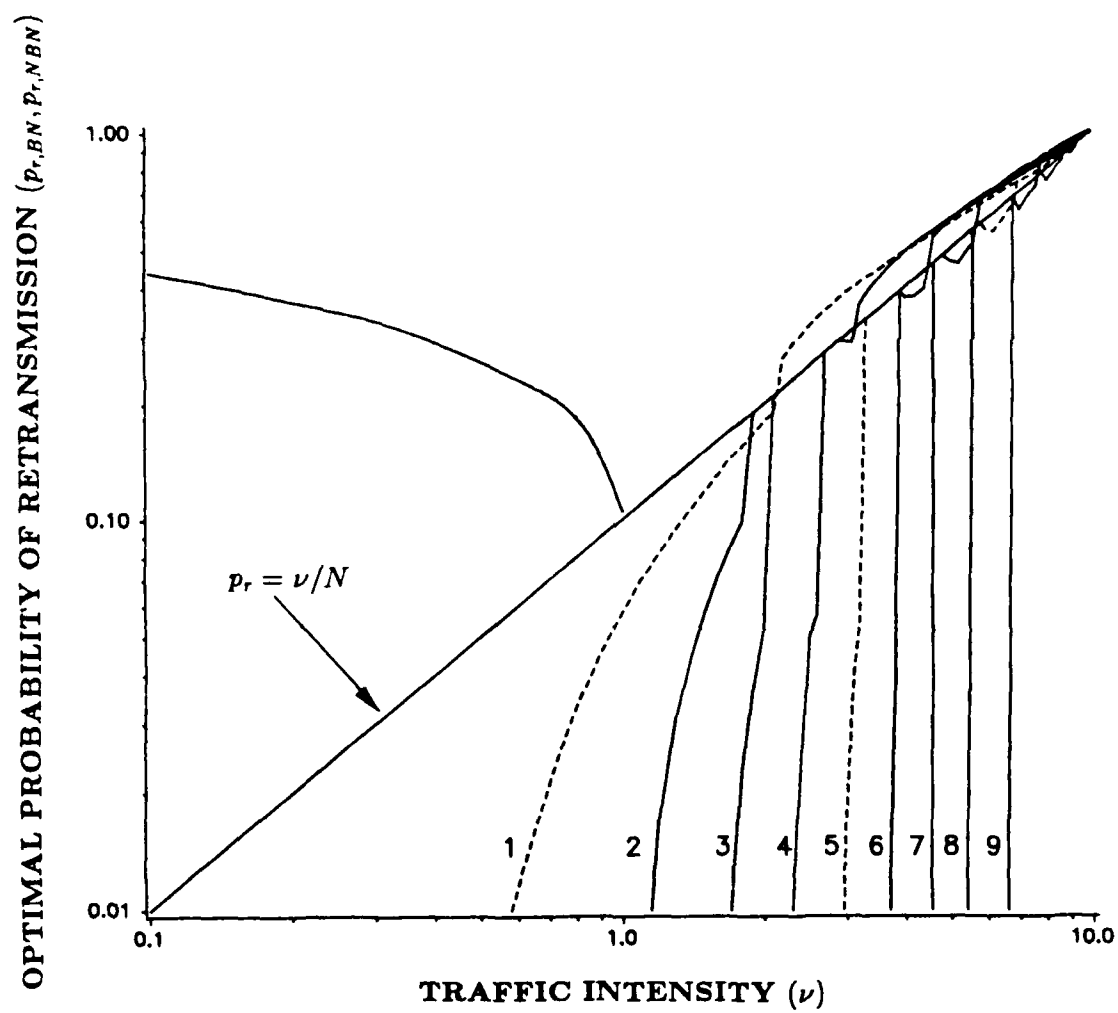Figure 3.8: Optimal Probability of Retransmission (p_r^*) versus Traffic Intensity (ν) for $N = 10, 30$

Figure 3.9: Optimal Probability of Retransmission (p_r^*) versus Traffic Intensity (ν) for $N = 10$
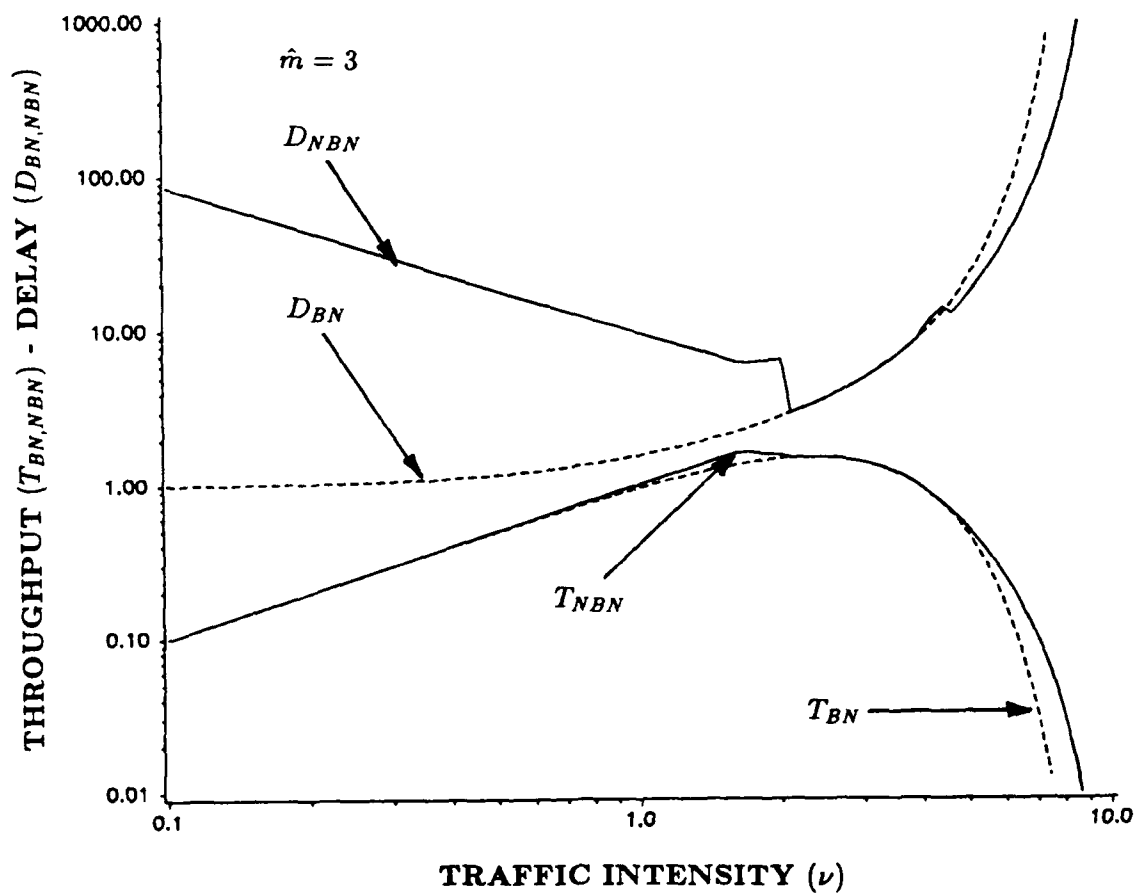
Figure 3.10: Throughput (T_{BN}, T_{NBN}) - Delay $(D_{BN,NBN})$ versus Traffic Intensity (ν), $N = 10$
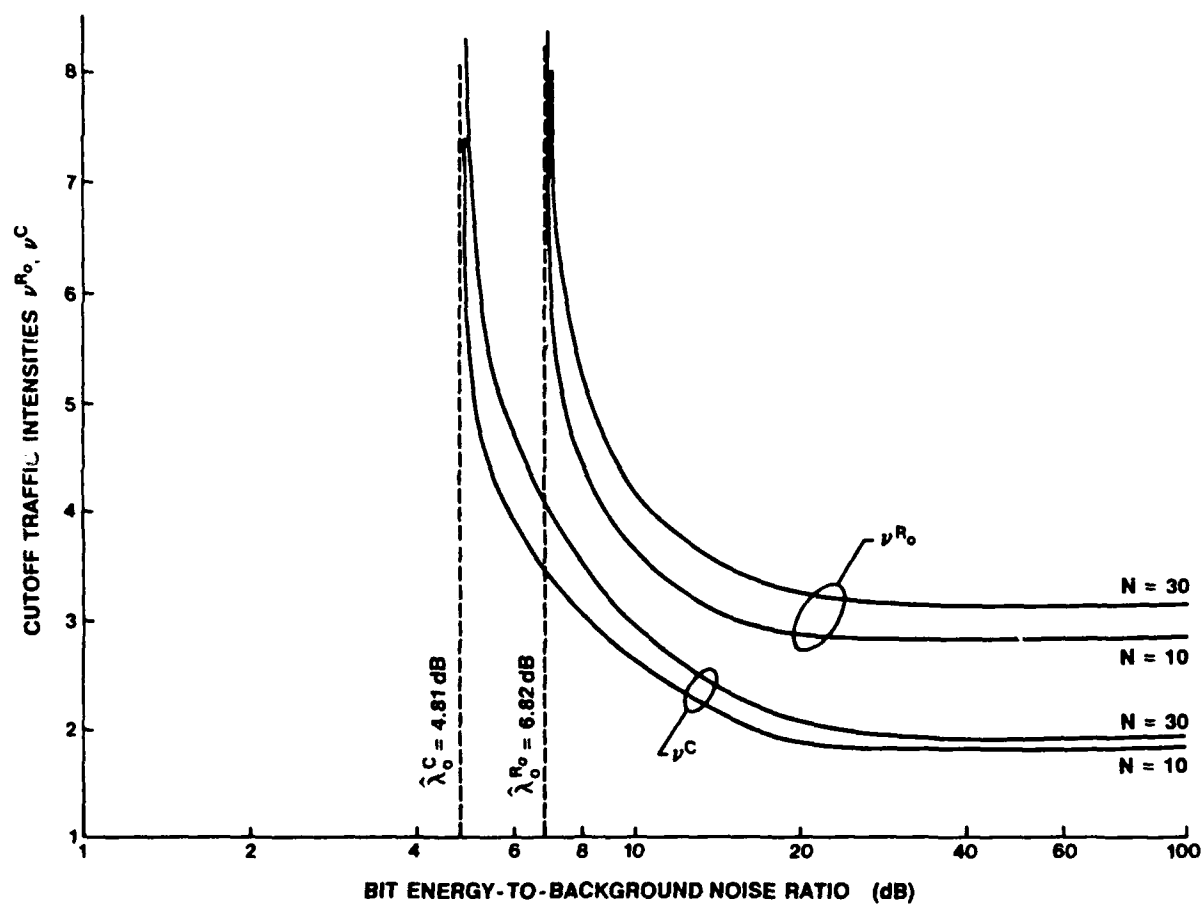
Figure 3.11: Cutoff Traffic Intensity (ν) versus Bit Energy-to-Background Noise Ratio (λ_o)
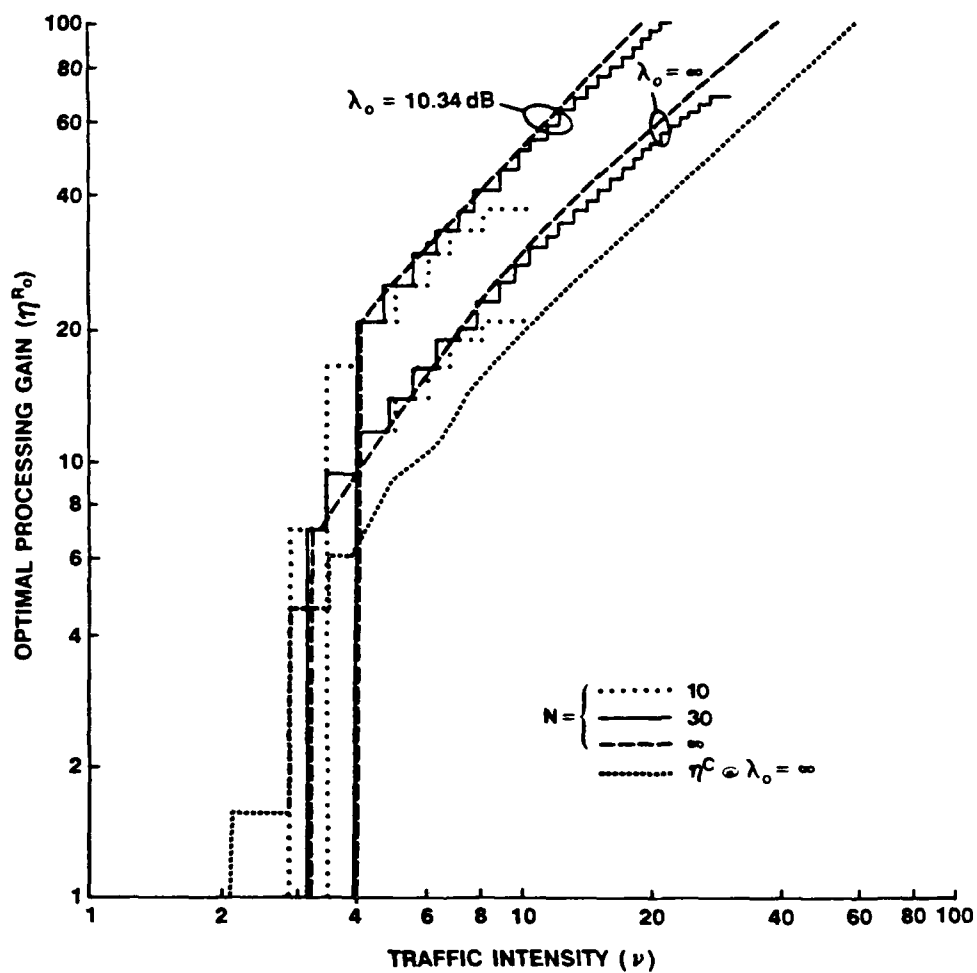
Figure 3.12: Optimal Processing Gain (η^{R_o}) versus Traffic Intensity (ν) for the Cutoff Rate Case (Capacity Case at $\lambda_o = \infty$ is shown for reference)
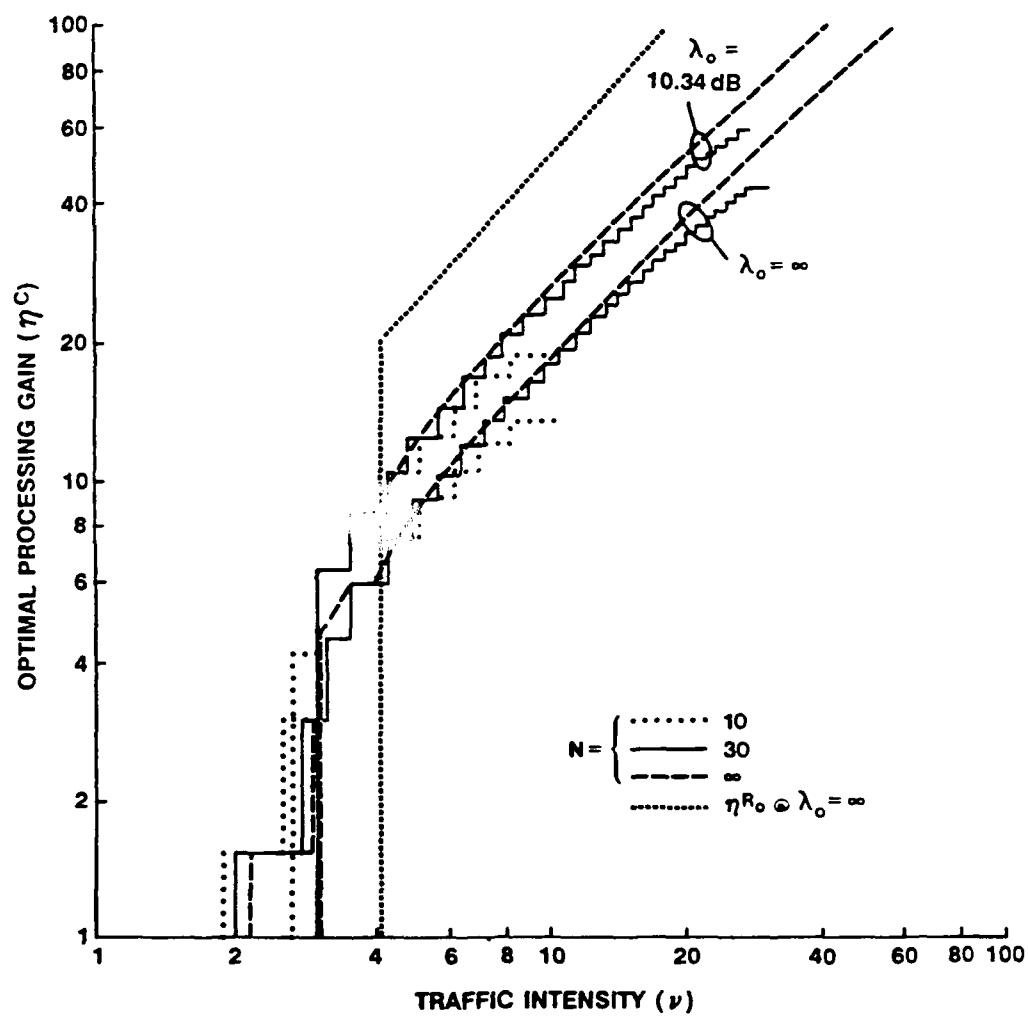
Figure 3.13: Optimal Processing Gain (η^C) versus Traffic Intensity (ν) for the Capacity Case (Cutoff Rate Case at $\lambda_o = \infty$ is shown for reference)
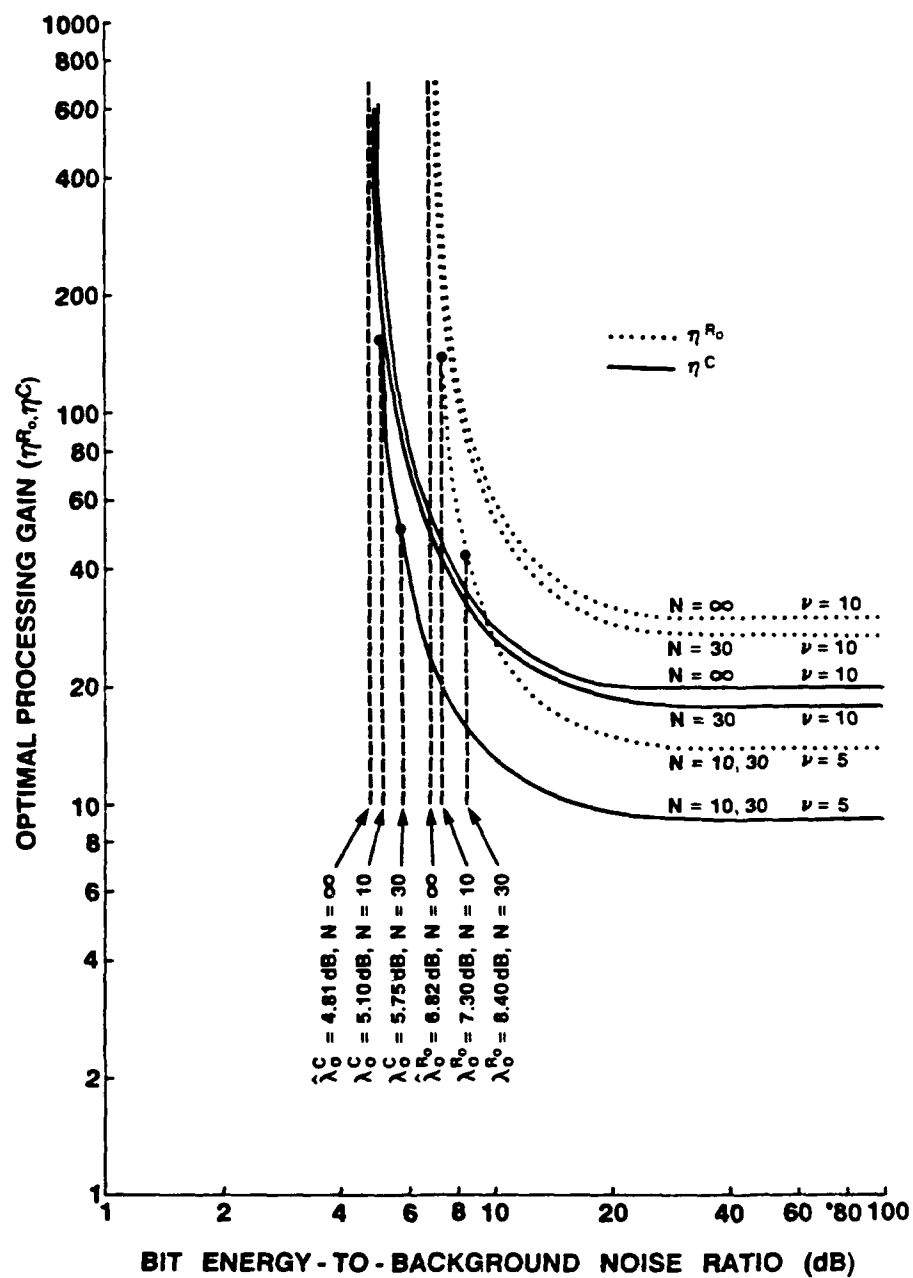
Figure 3.14: Optimal Processing Gain $(\eta^{\{R_o,C\}})$ versus Bit Energy-to-Background Noise Ratio (λ_o)
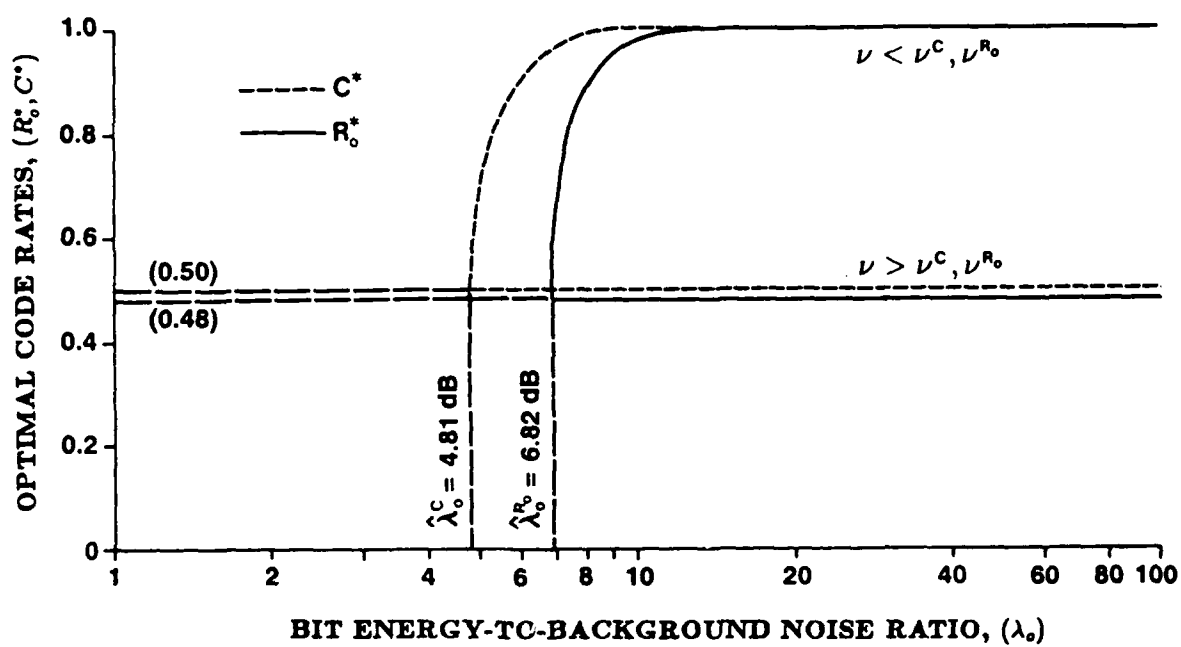
Figure 3.15: Optimal Code Rate (R_o^*, C^*) versus Bit Energy-to-Background Noise Ratio (λ_o)

Figure 3.16: Maximum Nonnormalized Throughput ($T_{R_o,NN}$) versus Traffic Intensity (ν)

Figure 3.17: Number of Backlogged Users (n) versus Input/Output Rate Equations for CDMA Network Stability Analysis

CHAPTER 4

Performance Evaluation in the Presence of Jammer Noise with Partial and Complete Side Information

This chapter examines the throughput-delay performance of Type I hybrid ARQ protocols in a slotted direct-sequence CDMA network operating in a hostile jamming environmen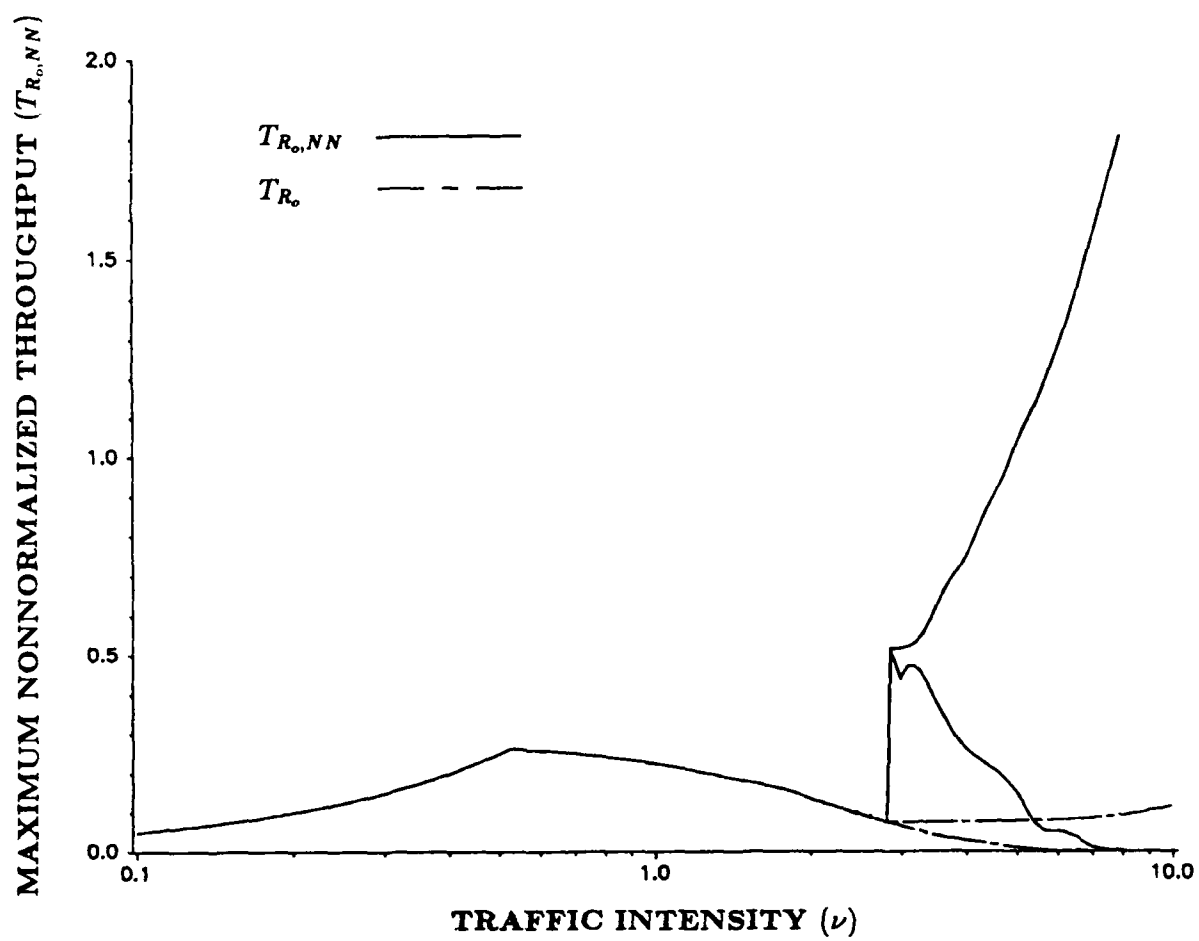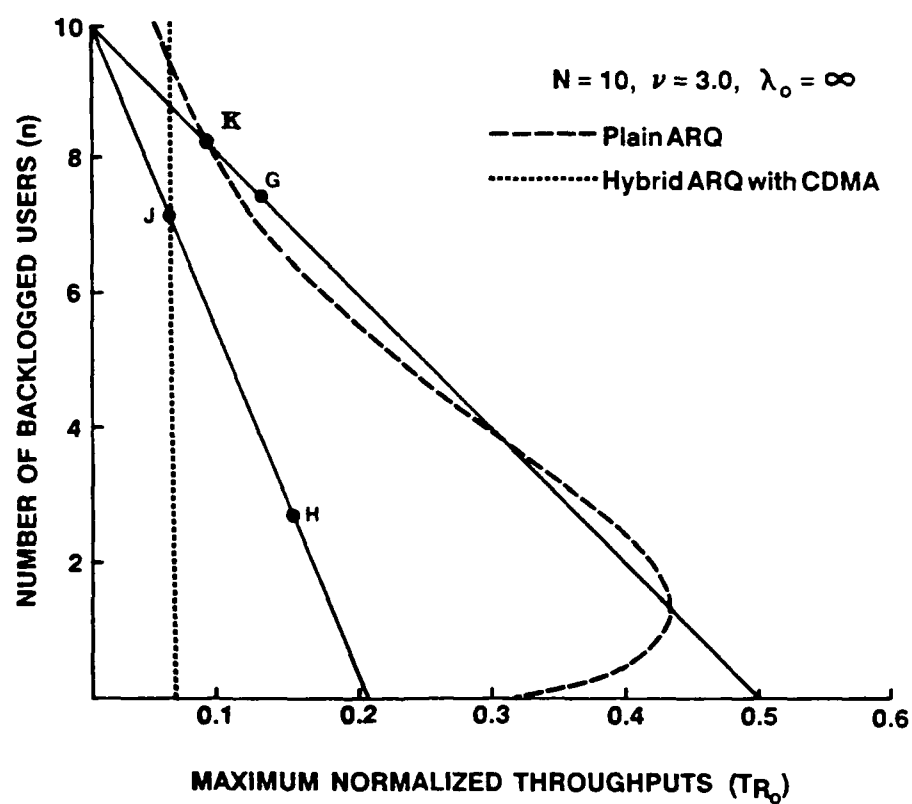t. The approach taken in this chapter parallels that of the last chapter. In the first section, the network and channel model is described in terms of its physical and link level characteristics. The model accounts for the presence of multiple-access interference, background noise, and jammer noise. The stochastic nature of the multiple-access interference is modeled by means of a Markov model for the number of backlogged transmitters. Enemy jamming is modeled as worst case pulse jamming. In Section 4.2, throughput-delay performance bounds are derived in terms of the channel cutoff rate and capacity. The effect of background noise is included in the formulation, but not included in the numerical analysis because it was discussed in detail in Chapter 3. Numerical results in Section 4.3 show how network design parameters such as the retransmission probability, code rate, and processing gain should be chosen in order to maximize system performance. It is shown that, for a given population size, traffic intensity, and bit energy-to-jammer noise ratio, there is an optimal probability of retransmission, code rate, and processing gain that maximizes network performance in the presence of worst case pulse jamming. It is also shown that, at high traffic intensities and/or high noise levels, it is more efficient in terms of network utilization to use CDMA in conjunction with random access than to use random access alone. The effects of pulse

jamming, with and without jammer state information, are also examined.

4.1   Network and Channel Model

The network and channel model is the same as described in Chapter 3 with modifications made to account for the presence of an enemy jammer. An arbitrary number of radio units are arranged in a paired-off topology and vie for access to a single network channel. Transmitters become backlogged due to the effects of background noise, multiple-access interference, and jammer noise. In a hostile jamming environmennt, CDMA becomes an even more attractive multiple accessing technique because of its good narrowband interference rejection capabilities [74]. Depending on the level of jammer noise, CDMA may be necessary at all traffic intensities if any appreciable throughput is to be obtained.

4.1.1   Enemy Jammer Model

The enemy jammer is assumed to employ pulse jamming which is an effective counter measure against direct-sequence spread-spectrum systems. For our purpose, the pulse jammer is modeled as having a two-level on-off power distribution. With probability ρ, a code symbol is jammed with additive white Gaussian noise (AWGN) having a one-sided power spectral density (PSD) N_J/ρ. With probability $1 - \rho$, a code symbol is uneffected by jamming. The average one-sided jammer noise PSD is N_J. For simplicity, it is assumed that a code symbol is either completely jammed or not jammed at all. Also, the jammer is assumed to have complete knowledge of the multiple-access network except for the exact set of spreading sequences being used. Furthermore, each receiver in the network is assumed to be affected by the same jamming strategy. A practical example of such a network is the uplink of a satellite relay network, where the satellite has N receivers (one for each of N earth-based transmitters) and where power control is used to maintain about the same power level from each transmitter.

4.1.2 Error Control

Recall that a Type I Hybrid ARQ protocol is used for error control. A more detailed description of the Type I Hybrid ARQ system is shown in Fig. 4.1. For this analysis, it
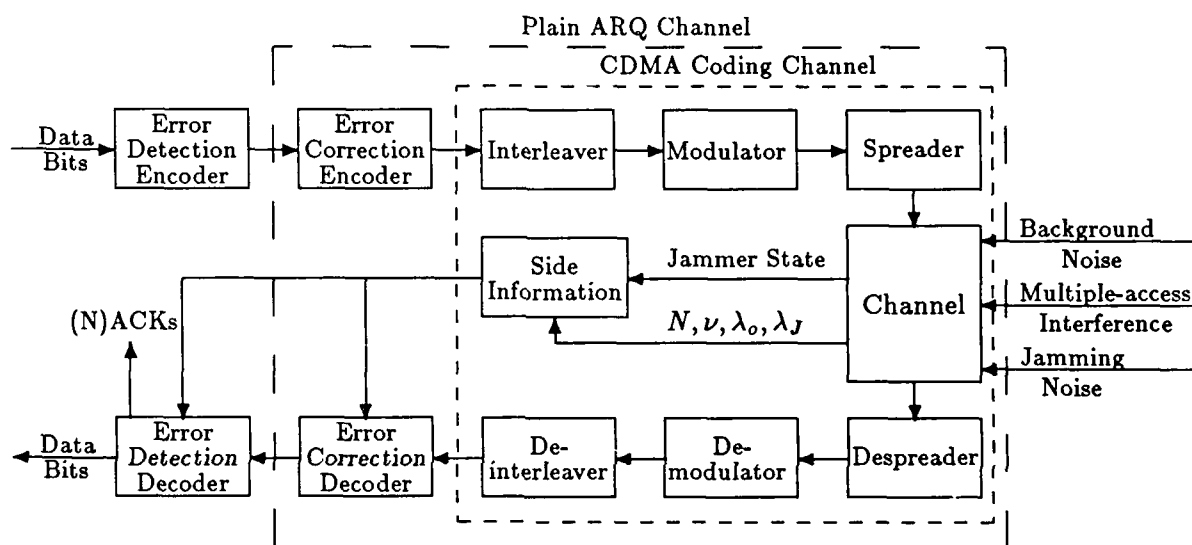
Figure 4.1: Type I Hybrid ARQ System

is assumed that acknowledgements (ACKs) and negative acknowledgements (NACKs) are made at no cost in performance over a separate return channel in the next immediate time slot. Cost free and completely reliable (N)ACKs are obtained by transmitting each (N)ACK with a very large processing gain over an entire time slot. Large processing gains are used rather than optimal code rate-processing gain combinations. This allows (N)ACK packet power levels to be reduced so that their contribution to the multiple-access interference is negligible. Thus, (N)ACKs are assumed not to decrease network utilization.

4.1.3 Coding Channel

Each data packet that is transmitted over the Type I Hybrid ARQ system in Fig. 4.1 is comprised of one or more code words. As in earlier analysis, each code word is used for simultaneous error detection and error correction. Intrapacket interleaving is used to randomize the effects of pulse jamming, in an attempt to make the coding channel appear memoryless within a time slot. The coding channel is not memoryless from slot-to-slot because the multiple-access interference changes. Recall that when binary modulation is used, the code symbol error probability in the presence of AWGN is $P_S = f(r\lambda_t)$ where r is the code rate and λ_t is the bit energy-to-*total*-noise ratio. For DPSK, $f(r\lambda_t) = \frac{1}{2}\exp\{-r\lambda_t\}$, and for BPSK $f(r\lambda_t) = erfc(\sqrt{2r\lambda_t})$. If we define $b := r\lambda_t$ and $a := \rho r\lambda_J$, where λ_J is the bit energy-to-jammer noise ratio, then with probability $1-\rho$, $P_S = f(b)$ and with probability ρ, $P_S = f(\frac{ab}{a+b})$. For binary modulation with hard decision decoding, the coding channel is modeled as a binary symmetric channel (BSC) with crossover probability P_S, under the assumption of ideal interleaving.

The cutoff rate and the capacity of the BSC depends upon the availability of jammer state information. Without jammer state information, the cutoff rate and capacity are:

$$R_o = 1 - \log_2\left(1 + \sqrt{4P_S(1 - P_S)}\right), \tag{4.1}$$

$$C = 1 - H[P_S], \tag{4.2}$$

where $H[P_S] = -P_S \log_2 P_S - (1 - P_S)\log_2(1 - P_S)$ is the binary entropy function and

$$P_S = (1 - \rho)f(b) + \rho f\left(\frac{ab}{a + b}\right). \tag{4.3}$$

If jammer state information is available, then the BSC is comprised of two component channels; $\triangle_1$, when a code symbol is not jammed with probability $1 - \rho$ and, $\triangle_2$, when a code symbol is jammed with probability ρ cutoff rate of $\triangle_1$ is

$$R_{o,1} = 1 - \log_2\left(1 + \sqrt{4f(b)(1 - f(b))}\right), \tag{4.4}$$

and the cutoff rate of $\triangle_2$ is

$$R_{o,2} = 1 - \log_2\left(1 + \sqrt{4f\left(\frac{ab}{a + b}\right)\left(1 - f\left(\frac{ab}{a + b}\right)\right)}\right). \tag{4.5}$$

The cutoff rate of the composite channel is [61]

$$R_o = -\log_2 E_i \left\{ 2^{-R_{o,i}} \right\},\tag{4.6}$$

where the expectation is over the probability distribution of the component channels. The corresponding component channel capacities are

$$C_1 = 1 - H[f(b)], \qquad C_2 = 1 - H\left[f\left(\tfrac{ab}{a+b}\right)\right],\tag{4.7}$$

and the capacity of the composite channel is [61]

$$C = E_i\{C_i\} = 1 - H[f(b)] + \rho\left(1 - H\left[f\left(\frac{ab}{a+b}\right)\right] - 1 + H[f(b)]\right).\tag{4.8}$$

4.2   Network Analysis

In this section, expressions for the throughput and corresponding average packet delay are derived in terms of the channel cutoff rate and capacity. This derivation parallels the derivation in Chapter 3. The impact of jammer state information is considered.

4.2.1   Throughput-Delay Analysis with Partial Side Information

The throughput T of our CDMA system is defined as the expected number of successful packets per slot $T = E\{S\}$, and can be expressed in terms of the composite packet arrival probability distribution function $f_M(l)$ and the probability of correct packet reception $P_C(l)$ as

$$T = \sum_{l=1}^{N} l P_C(l) f_M(l).\tag{4.9}$$

The throughput in the presence of jamming is dependent upon the availability of jammer state information. Jammer state information will increase throughput by increasing the cutoff rate and capacity of the coding channel. First, consider the case of no jammer state information. Recall that expressions for the probability of symbol error as a function of the cutoff rate and capacity can be expressed as $P_S = g^{-1}_{\{R_o, C\}}(R_o, C)$. For the cutoff rate,

$$P_S = \frac{(1 - \sqrt{1 - \alpha^2})}{2}, \quad \alpha = 2^{1 - R_o} - 1,\tag{4.10}$$

and for the capacity

$$P_S = H^{-1}[1 - C], \tag{4.11}$$

where $H^{-1}[\cdot]$ is the inverse binary entropy function. By equating (4.3) and (4.10, 4.11), and recalling that $a := \rho r \lambda_J$ and $b := r \lambda_t$, the following expression can be obtained for the bit energy-to-jammer noise ratio;

$$\lambda_J = \frac{a(f(\frac{ab}{a+b}) - f(b))}{r(g_{\{R_o,C\}}^{-1}(R_o,C) - f(b))}. \tag{4.12}$$

Substituting (3.13) into (4.12) and rearranging gives the following expression;

$$g_{\{R_o,C\}}^{-1}(R_o,C) \;+\; \left(\frac{a}{\lambda_J r} - 1\right) f\left(\frac{r\lambda_o}{1 + \eta^{-1} r\lambda_o(m-1)}\right) \tag{4.13}$$
$$-\; \frac{a}{\lambda_J r} f\left(\frac{ar\lambda_o}{a[1 + \eta^{-1} r\lambda_o(m-1)] + r\lambda_o}\right) = 0$$

The objective of the pulse jammer is to minimize the throughput for a given p_r, r, η, λ_o, and λ_J. Therefore, a worst case pulse jammer chooses a so that m in (4.13) is minimized.

If the optimal jamming fraction is unity, which usually occurs for sufficiently low code rates, then (4.12) reduces to

$$\lambda_J = \frac{\lambda_t f^{-1}(g_{\{R_o,C\}}^{-1}(R_o,C))}{r\lambda_t - f^{-1}(g_{\{R_o,C\}}^{-1}(R_o,C))}, \tag{4.14}$$

where $f^{-1}(\,\cdot\,)$ is the inverse operator of $f(\,\cdot\,)$. By using (3.13) and (4.14), an expression similar to (3.21) can be obtained for the number of allowable simultaneous packet transmissions;

$$m = \frac{\eta}{r}\left(\frac{r}{f^{-1}(g_{\{R_o,C\}}^{-1}(R_o,C))} - \frac{1}{\lambda_o} - \frac{1}{\lambda_J}\right) + 1. \tag{4.15}$$

As in earlier analyses, suppose that the code being used has the property that the packet error probability is zero if $r \leq \{R_o,C\}$ and one if $r > \{R_o,C\}$. Now consider the limiting case as $r \to \{R_o,C\}$ and suppose that the values of N, $\{R_o,C\}$, η, λ_o, and λ_J are fixed. If the optimal ρ is unity, then (4.15) gives the maximum allowable number of simultaneous packet transmissions in a time slot as $\hat{m} = \lfloor m \rfloor$. If the actual number of packets l exceeds $\hat{m}$, then information is being transmitted at a rate above the cutoff rate (capacity). As a result, all packets are incorrectly received and must be retransmitted

$(P_C(l) = 0, l > \hat{m})$. If the number of packets is less than or equal to $\hat{m}$, then all packets are received successfully ($P_C(l) = 1, l \le \hat{m}$). The throughput expression in (4.9) becomes

$$T = \sum_{l=1}^{\min(\hat{m},N)} l f_M(l). \tag{4.16}$$

To compare networks with different processing gains and code rates on a fair basis, the throughput must be normalized by a factor of r/η. The average normalized throughput or network utilization becomes

$$T(p_r, \{R_o, C\}, \eta, \rho) = \frac{\{R_o, C\}}{\eta} T = \frac{\{R_o, C\}}{\eta} \sum_{l=1}^{\min(\hat{m},N)} l f_M(l). \tag{4.17}$$

This is the average number of successful information packets (per slot) per unit time per unit bandwidth. Note that the normalized throughput is a function of the probability of retransmission, the code rate, the processing gain, and the jamming fraction, and is always less than one. The normalized throughput is also a function of the population size, the composite traffic intensity, the bit energy-to-background noise ratio and the bit energy-to-jammer noise ratio. However, these latter dependencies are not shown explicitly because these parameters are assumed to be uncontrolled. The maximin normalized throughput is

$$\begin{aligned}
T_{\{R_o,C\}} &= \max_{0 < p_r \le 1} \max_{\substack{0 < \{R_o,C\} \le 1 \\ 1 \le \eta}} \min_{0 < \rho \le 1} T(p_r, \{R_o, C\}, \eta, \rho), \\
&= \max_{0 < p_r \le 1} \max_{\substack{0 < \{R_o,C\} \le 1 \\ 1 \le \eta}} \min_{0 < \rho \le 1} \frac{\{R_o, C\}}{\eta} \sum_{l=1}^{\min(\hat{m},N)} l f_M(l), \tag{4.18}
\end{aligned}$$

and the corresponding average packet delay as given by equations (3.38 , 3.39) is

$$D = \frac{\bar{n}}{T_{\{R_o,C\}}} + 1. \tag{4.19}$$

As earlier, the link utilization derived from the capacity limit will represent a *theoretical* performance limit, whereas that derived from from the cutoff rate will represent a *practical* performance limit. The optimal probability of retransmission, code rate, processing gain, and jamming fraction are denoted by p_r^*, $\{R_o^*, C^*\}$, $\eta^{\{R_o,C\}}$, and $\rho^{\{R_o,C\}}$, respectively.

4.2.2   Throughput-Delay Analysis with Complete Side Information

If jammer state information is available, it is expected that throughput can be increased. In this case, expressions for the bit energy-to-jammer noise ratio can be obtained by performing

the expectations in (4.6) and (4.8) and manipulating the results. For the cutoff rate case, the following expression can be obtained;

$$\lambda_J = \frac{2a\left(\sqrt{f\left(\frac{ab}{a+b}\right)\left(1 - f\left(\frac{ab}{a+b}\right)\right)} - \sqrt{f(b)(1 - f(b))}\right)}{r\left(\alpha - \sqrt{4f(b)(1 - f(b))}\right)} \tag{4.20}$$

Substituting $b = R_o\lambda_t$ into (4.20) results in

$$\lambda_J R_o\left(\alpha - \sqrt{4f(R_o\lambda_t)(1 - f(R_o\lambda_t))}\right) = \\ 2a\left(\sqrt{f\left(\frac{aR_o\lambda_t}{a+R_o\lambda_t}\right)\left(1 - f\left(\frac{aR_o\lambda_t}{a+R_o\lambda_t}\right)\right)} - \sqrt{f(R_o\lambda_t)(1 - f(R_o\lambda_t))}\right) \ . \tag{4.21}$$

where λ_t is given by (3.13). Once again, a pulse jammer chooses a in (4.21) so that m is minimized.

If the optimal jamming fraction ρ is unity, then $a = r\lambda_J$ and (4.20) reduces to (4.12). For a given N, $r = R_o$, η, λ_o, and λ_J, this gives the same m (4.15) that would result if the receiver did not have jammer state information. This makes sense because when $\rho = 1$ the coding channel is comprised of only one component coding channel. Once again, the maximin normalized throughput is given by (4.18) with $\hat{m} = \lfloor m \rfloor$.

For the capacity case, the following expression for the bit energy-to-jammer noise ratio can be obtained;

$$\lambda_J = \frac{a\left(H[f(b)] - H\left[f\left(\frac{ab}{a+b}\right)\right]\right)}{r(C + H[f(b)] - 1)}. \tag{4.22}$$

By using $b = C\lambda_t$ and (3.13) in (4.22), m satisfies

$$1 - C + \left(\frac{a}{\lambda_J r} - 1\right)H\left[f\left(\frac{r\lambda_o}{1 + \eta^{-1}r\lambda_o(m-1)}\right)\right] - \frac{a}{\lambda_J r}H\left[f\left(\frac{ar\lambda_o}{a[1 + \eta^{-1}r\lambda_o(m-1)] + r\lambda_o}\right)\right] = 0. \tag{4.23}$$

As earlier, the jammer chooses ρ to minimize m in (4.23). If $\rho = 1$, then the coding channel consists of one state and the expression in (4.15) gives the value of m. The maximin normalized throughput is given by (4.18) with $\hat{m} = \lfloor m \rfloor$.

4.3 Performance Evaluation

In this section, the dependency of the network's throughput-delay performance on N, ν, λ_J, p_r, $\{R_o, C\}$, η and ρ is examined in detail. The dependency of p_r, $\{R_o^*, C^*\}$, $\eta^{\{R_o, C\}}$,

and $\rho^{\{R_o,C\}}$ on N, ν, and λ_J is discussed. The effect of jammer state information is also considered. Throughout the analysis, background noise is neglected in order to isolate the effect of jamming. The effect of background noise is considered in Chapter 3.

Figs. 4.2-4.3 are plots of the maximin normalized throughput, $T_{\{R_o,C\}}$ against the traffic intensity ν. Figs. 4.4-4.7 are plots of $T_{\{R_o,C\}}$ against average packet delay D. These plots illustrate the combined effects of maximizing throughput over probability of retransmission p_r, code rate $\{R_o, C\}$, and processing gain η, while minimizing the throughput over the jamming fraction ρ. The first maximization required by (4.18) is performed for a given level of jammer noise by fixing D in (3.41), allowing p_r to vary ($0 \leq p_r \leq 1$) in (3.30), and solving for a $(\bar{n}, \pi(n))$ solution which maximizes the throughput (3.41). Note that the usual bursty user assumption ($p_r > p_o$) is relaxed, and that most of the throughput-delay results reported below require that $p_o \geq p_r$. This procedure is repeated for all possible values of $\hat{m}$ ($1 \leq \hat{m} \leq N$) and results in N optimal ($p_r, T_{\{R_o,C\}}$) ⌐airs for each fixed value of D. An alternate procedure, whereby the throughput is fixed and the delay is minimized, produces the same optimal ($p_r, T_{\{R_o,C\}}, \hat{m}, D$) combinations. For the second maximization required by (4.18), D is again fixed for a given level of jammer noise, and the code rate and processing gain $\{R_o, C; \eta\}$ are allowed to vary. For each code rate-processing gain combination, the final step of the optimization is performed by allowing $a = \rho r \lambda_J$ to vary in order to obtain a minimum value of m (i.e., the jammer has the final say). The last two steps of the optimization yield $\hat{m}$ values for which the corresponding throughputs are known from step one. Each value of throughput is then normalized and the maximim normalized value is selected.

Finally, when jamming is present, we consider two cases. The first case assumes that λ_J is constant, regardless of the processing gain. This means that the jammer will offset any relative increase in the processing gain, by increasing its total power ᵇʸ the same relative amount. Therefore, an increase in the processing gain only reduces the effect of multiple-access interference. We consider this case because it provides some insights into the behavior of the network that would otherwise go unnoticed.

The second case is more realistic, because it assumes that the total jammer power is constant. Therefore, if the spread-spectrum bandwidth is extended by a relative increase in

the processing gain, then the average bit energy-to-jammer noise ratio will be increased by the same relative amount. Consequently, an increase in the processing gain reduces both the effects of multiple-access interference and jamming. Define $\tilde{\lambda}_J$ as the bit energy-to-jammer noise ratio that would be obtained with unity processing gain, i.e., $\tilde{\lambda}_J = \lambda_J \mid_{\eta=1}$. With constant jamming power, $\tilde{\lambda}_J$ is also constant. Then if $\eta > 1$, the bit energy-to-jammer noise ratio will be $\lambda_J = \eta \tilde{\lambda}_J$. Therefore, the optimization in (4.18) is performed in exactly the same manner as in the constant λ_J analysis except that $\lambda_J = \eta \tilde{\lambda}_J$.

4.3.1 Throughput-Delay Performance at Constant Bit Energy-to-Jammer Noise Ratio

Figs. 4.2-4.3 and 4.4-4.7 are plots of maximin normalized throughput, $T_{\{R_o,C\}}$, against traffic intensity ν and against average delay D, respectively. Results are shown for population sizes $N = 10$ and 30 and for constant bit energy-to-jammer noise levels of $\lambda_J = \infty$ and $\lambda_J = 10.00$ dB. When jamming is present the effect of jammer state information is shown. In general, jammer noise has a greater effect on network performance than than background noise for all traffic intensities. This can be seen by comparing Figs. 4.2-4.7 with Figs. 3.5-3.7. If $\nu > \nu^{\{R_o,C\}}$, then throughput-delay performance in the presence of jamming ($\lambda_J = 10.0$ dB) is almost the same as in the presence of background noise ($\lambda_o = 10.34$ dB). Nearly equivalent performance occurs because the optimal jamming fraction is close to unity when $\lambda_J = 10.0$ dB. For the same reason, jammer state information has little effect on performance for $\nu > \nu^{\{R_o,C\}}$. If $\nu < \nu^{\{R_o,C\}}$, then jamming causes throughput-delay performance to be noticeably less than when the channel is subjected to background noise. Performance degrades because standard narrow-band ALOHA/Hybrid ARQ ($\eta = 1$) is being used for this range of traffic intensities. Note that the availability jammer of state information has a significant effect on performance, especially for the cutoff rate case.

Figs. 4.8-4.9 illustrate the effect of bit energy-to-jammer noise ratio λ_J, population size N, and jammer state information on the cutoff traffic intensity $\nu^{\{R_o,C\}}$. In general, $\nu^{\{R_o,C\}}$ increases to its maximum value (N) as λ_J decreases. Note that for each $\nu^{\{R_o,C\}}$ there is a corresponding λ_J which is defined as the jammer noise limit for that cutoff intensity, denoted by $\lambda_J^{\{R_o,C\}}$. Also, for each λ_J there is a corresponding cutoff traffic intensity. The

λ_J which $\nu^{\{R_o,C\}}$ is asymptotic to is defined as the network *asymptotic jammer noise limit*, and is denoted $\hat{\lambda}_J^{\{R_o,C\}}$. With jammer state information, $\hat{\lambda}_J^{\{R_o,C\}} = \{6.82 \text{ dB}, 4.81 \text{ dB}\}$. Without jammer state information, $\hat{\lambda}_J^{\{R_o,C\}} = \{7.39 \text{ dB}, 4.97 \text{ dB}\}$. The network cannot operate at bit energy-to-jammer noise ratios below these asymptotic jammer noise limits, because they represent the smallest λ_J that can be present for reliable coded communication in the absence of multiple-access interference [86].

Figs. 4.10-4.11 show how the optimal processing gain $\eta^{\{R_o,C\}}$ depends on the traffic intensity for various population sizes N, bit energy-to-jammer noise ratios λ_J, and jammer state availability. For the $N = \infty$ case, $\eta^{\{R_o,C\}}$ depends on ν in a nearly linear fashion. The effect of finite population size is a 'staircase' type curve which tends to the $N = \infty$ curve as $N \to \infty$. Note that for the cutoff rate case, systems with jammer state information require larger values of η^{R_o} than those without jammer state information, while for the capacity case, jammer state information has no impact at $\lambda_J = 10.00$ dB because $\rho^C = 1$.

Figs. 4.12-4.13 show how the optimal processing gain $\eta^{\{R_o,C\}}$ depends on the bit energy-to-jammer noise ratio λ_J for a particular traffic intensity, $\nu = 5.0$, and for $N = 10, 30$. In general, the optimal processing gain increases with decreasing λ_J. Note that the $N = 10$ curve overlies the $N = 30$ curve. Recall that, for a given traffic intensity, there is a corresponding jammer noise limit $\lambda_J^{\{R_o,C\}}$. Thus, for a given traffic intensity, as $\lambda_J \to \lambda_J^{\{R_o,C\}}$, $\eta^{\{R_o,C\}}$ increases to some finite maximum value at $\lambda_J^{\{R_o,C\}}$. Observe how $\eta^{\{R_o,C\}}$ increases drastically as λ_J nears $\lambda_J^{\{R_o,C\}}$. Should λ_J be less than the noise limit for a given value of ν, then $\nu < \nu^{\{R_o,C\}}$ and CDMA is no longer the optimal protocol. For this case, $\hat{\lambda}_J^{\{R_o,C\}} < \lambda_J < \lambda_J^{\{R_o,C\}}$, the optimal processing gain is unity. By using Figs. 4.8-4.13, it is possible to estimate $\eta^{\{R_o,C\}}$ for any values of λ_J, ν, and N, because of the nearly linear dependency of $\eta^{\{R_o,C\}}$ on ν.

Fig. 4.14-4.15 summarize the dependency of the optimal code rate $\{R_o^*, C^*\}$ on the bit energy-to-jammer noise ratio λ_J, with and without jammer state information, respectively. Note that the selection of the optimal code rate depends primarily upon ν, λ_J and the availability of jammer state information, and does not directly depend on N. In fact, the same results are obtained for all population sizes [29,86]. When $\lambda_J = \infty$ and $\nu < \nu^{\{R_o,C\}}$, the optimal code rate $\{R_o^*, C^*\}$ is unity. Hence, the optimal protocol is plain ARQ. In

fact, plain ARQ is used *only* when $\lambda_J = \infty$ and $\nu < \nu^{\{R_o,C\}}$. When $\lambda_J < \infty$ and $\nu < \nu^{\{R_o,C\}}$, $\{0.454, 0.500\} < \{R_o^*, C^*\} < 1.0$ when jammer state information is available, and $\{0.247, 0.379\} < \{R_o^*, C^*\} < 1.0$ when it is not. In either case, Hybrid ARQ is used. For $\lambda_J \leq \infty$ and $\nu > \nu^{\{R_o,C\}}$, $0.454 < R_o^* < 0.480$ and $C^* = 0.500$ when jammer state information is available, and $\{0.247, 0.379\} < \{R_o^*, C^*\} < \{0.480, 0.500\}$ when it is not. CDMA is the optimal protocol in this case. Note that for a given level of jammer noise, the optimal code rate can be determined as the traffic intensity varies by using Figs. 4.8-4.9 and 4.14-4.15 . For a given λ_J, Figs. 4.8-4.9 gives the corresponding $\nu^{\{R_o,C\}}$. As the traffic intensity varies above and below this particular $\nu^{\{R_o,C\}}$, the optimal code rate is given by the lower branch and upper branch of Figs. 4.14-4.15, respectively.

The dependency of $\rho^{\{R_o,C\}}$ on λ_J is shown in Figs. 4.16 and 4.18, with and without jammer state information, respectively. As with the code rate, the selection of the optimal jamming fraction depends primarily upon ν and λ_J, and the availability of jammer state information. The optimal jamming fraction does not depend on the population size. Observe that if $\nu < \nu^{\{R_o,C\}}$, then $\rho^{\{R_o,C\}} \to 0$ as $\lambda_J \to \infty$. If $\nu > \nu^C$, then $\rho^C \to 1$ as $\lambda_J \to \infty$ with or without jammer state information. If $\nu > \nu^{R_o}$, then $\rho^{R_o} \to 1$ as $\lambda_J \to \infty$ with jammer state information. However, without jammer state information, $\rho^{R_o} \to 0$ as $\lambda_J \to \infty$ with a scalloped appearance.

Finally, it should be noted that for each of the optimal jamming fractions given in Figs. 4.16 and 4.18, there actually exist a range of jamming fractions about $\rho^{\{R_o,C\}}$ which result in the same network performance. This range of ρ values occurs because $\hat{m} = \lfloor m \rfloor$ where m is a convex cup function in ρ over this range of ρ. The lower and upper bounds on the range for the optimal jammming fraction $\rho_{L,U}^{\{R_o,C\}}$ are shown in Figs. 4.17 and 4.19 for the cases of with and without jammer state information, respectively, and for $\nu > \nu^{\{R_o,C\}}$. For $\nu < \nu^{\{R_o,C\}}$, standard narrow-band ALOHA is used ($\hat{m} = 1$) with just enough coding ($\{R_o, C\} < 1.0$) to overcome the effects of jamming. For this case, any nonzero value for the jamming fraction ($0.0 < \rho \leq 1.0$) results in $\hat{m} = 1$ and produces the same results. Similar nonzero ranges for ρ occurs when CDMA is used, but only at high bit energy-to-jammer noise ratios, $\lambda_J > 10.0$ dB.

4.3.2 Throughput-Delay Performance at Constant Jammer Power

Fig. 4.20 is a plot of the maximin normalized throughput T_{R_o} against traffic intensity for the case of constant jammer power. Results are showned for $N = 10$ and ∞, with jammer state information, and for $\tilde{\lambda}_J^{\{R_o,C\}}$ ranging from -10 dB to ∞ dB. Results for $N = \infty$ provide a lower limit on performance. If $\tilde{\lambda}_J < \hat{\lambda}_J^{\{R_o,C\}}$, then a cutoff intensity does not exist and the throughput increases gradually with the traffic intensity. In this case, both coding ($r < 1.0$) and processing gain ($\eta > 1.0$) are necessary to achieve a nonzero throughput for all traffic intensities. Recall that for the constant λ_J analysis, when $\lambda_J < \hat{\lambda}_J^{\{R_o,C\}}$ then throughput was zero because $\hat{\lambda}_J^{\{R_o,C\}}$ represented the smallest jammer noise level that can be present for reliable coded communication in the absence of multiple-access interference. If $\tilde{\lambda}_J \geq \hat{\lambda}_J^{\{R_o,C\}}$, then a cutoff intensity exists and the throughput-traffic intensity characteristic takes on a form similar to that obtained in the constant λ_J analysis. For $\tilde{\lambda}_J \geq \hat{\lambda}_J^{\{R_o,C\}}$ and $\nu < \nu^{\{R_o,C\}}$, coding alone is sufficient to overcome the effects of jamming ($\eta = 1$).

Fig. 4.22 summarizes the dependency of $\hat{m}$ on the traffic intensity ν and the bit energy-to-jammer noise ratio $\tilde{\lambda}_J$, for a population size of $N = 10$. This diagram is very useful because it inherently summarizes the dependency of the optimal processing gain, code rate, and jamming fraction on ν and $\tilde{\lambda}_J$. To see this, observe that for a given $\tilde{\lambda}_J$, $\hat{m}$ remains constant over a certain range of ν. For each $\{\tilde{\lambda}_J, \hat{m}\}$, there is a corresponding $\eta^{\{R_o,C\}}$, $\{R_o^*, C^*\}$, and $\rho^{\{R_o,C\}}$ which also remain constant over the same range of traffic intensity. Note that for a given value of $\hat{m}$, the corresponding $\eta^{\{R_o,C\}}$, $\{R_o^*, C^*\}$, and $\rho^{\{R_o,C\}}$ do not depend on the population size. These results are shown in Figs. 4.23-4.25. As with the constant λ_J case, there are upper and lower bounds for $\rho^{\{R_o,C\}}$. These are shown in Figs. 4.26-4.27.

Results for the capacity case with jammer state information are shown in Figs. 4.28-4.35. Results for the cutoff rate and capacity cases without jammer state information closely follow the results with jammer state information, and are not given here. Partial results for the cutoff rate case without jammer state information are shown in [30] .
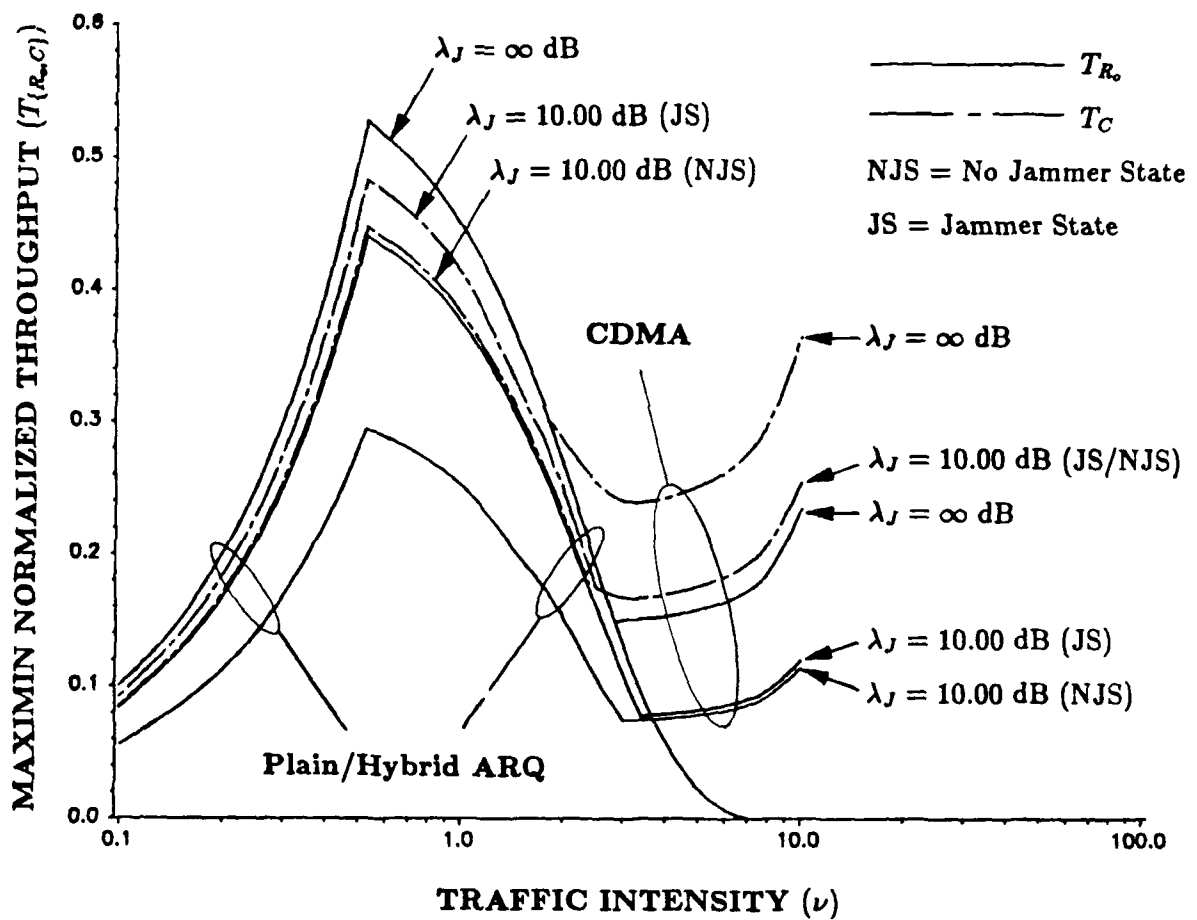
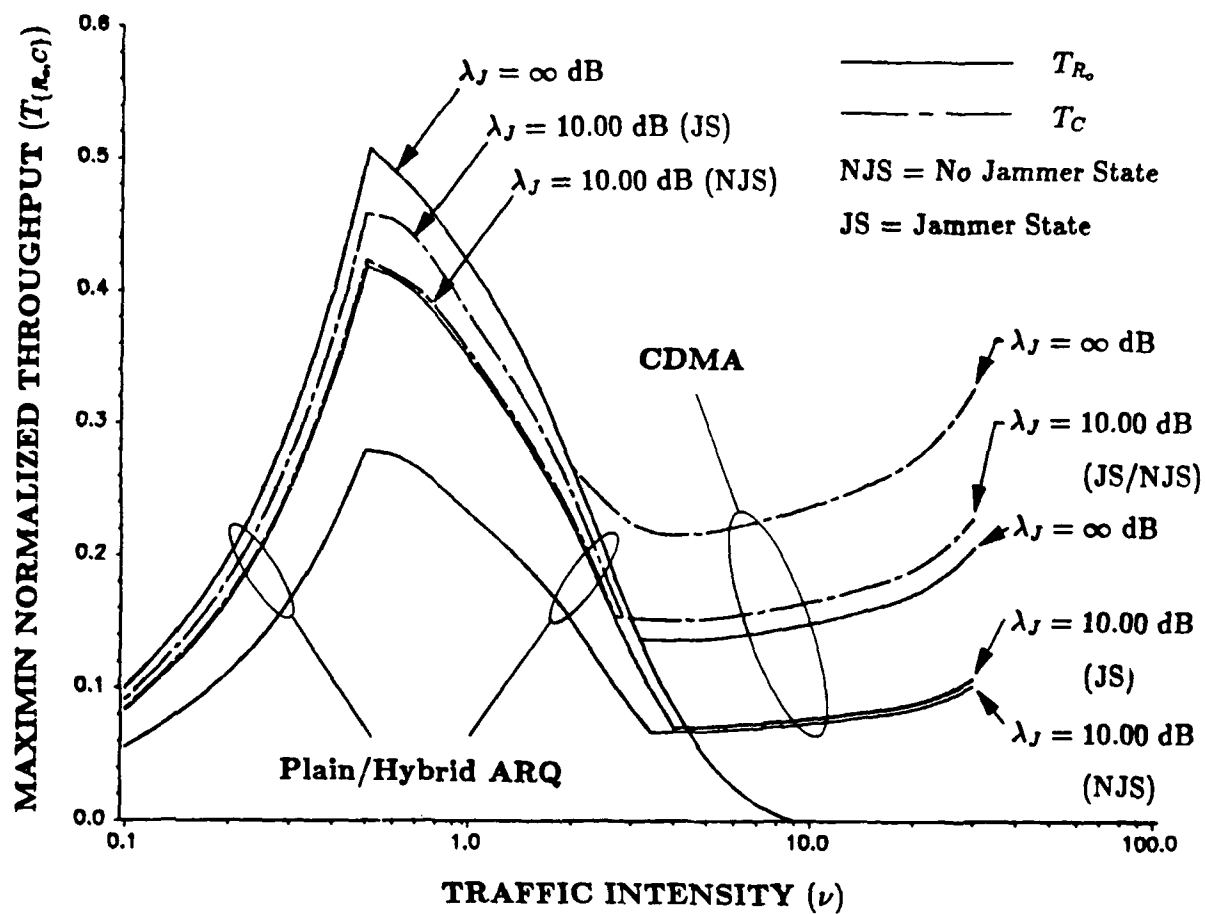Figure 4.2: Maximin Normalized Throughput ($T_{\{R_o,C\}}$) versus Traffic Intensity (ν) for $N = 10$

Figure 4.3: Maximin Normalized Throughput $(T_{\{R_o,C\}})$ versus Traffic Intensity (ν) for $N = 30$
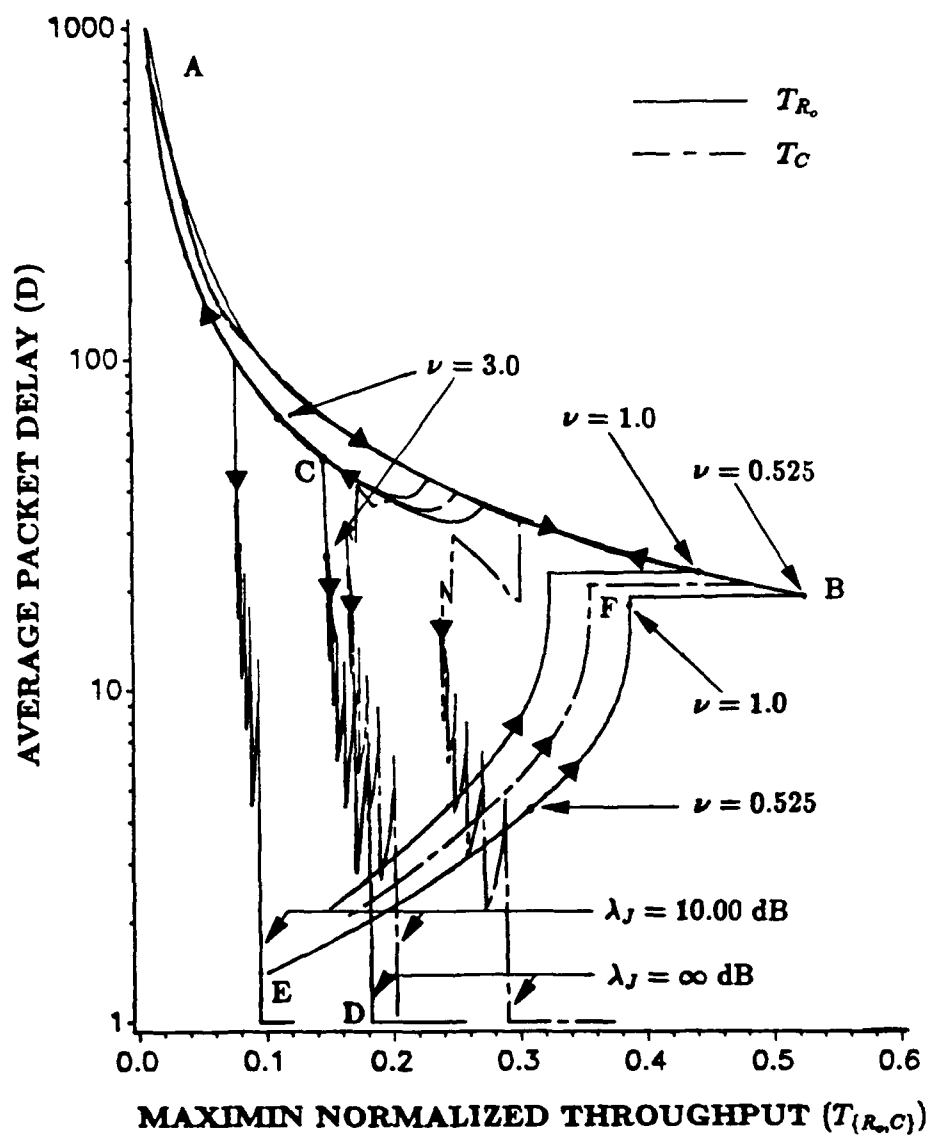
Figure 4.4: Average Packet Delay (D) versus Maximin Normalized Throughput ($T_{\{R_o,C\}}$) for $N = 10$ (Jammer State Information)
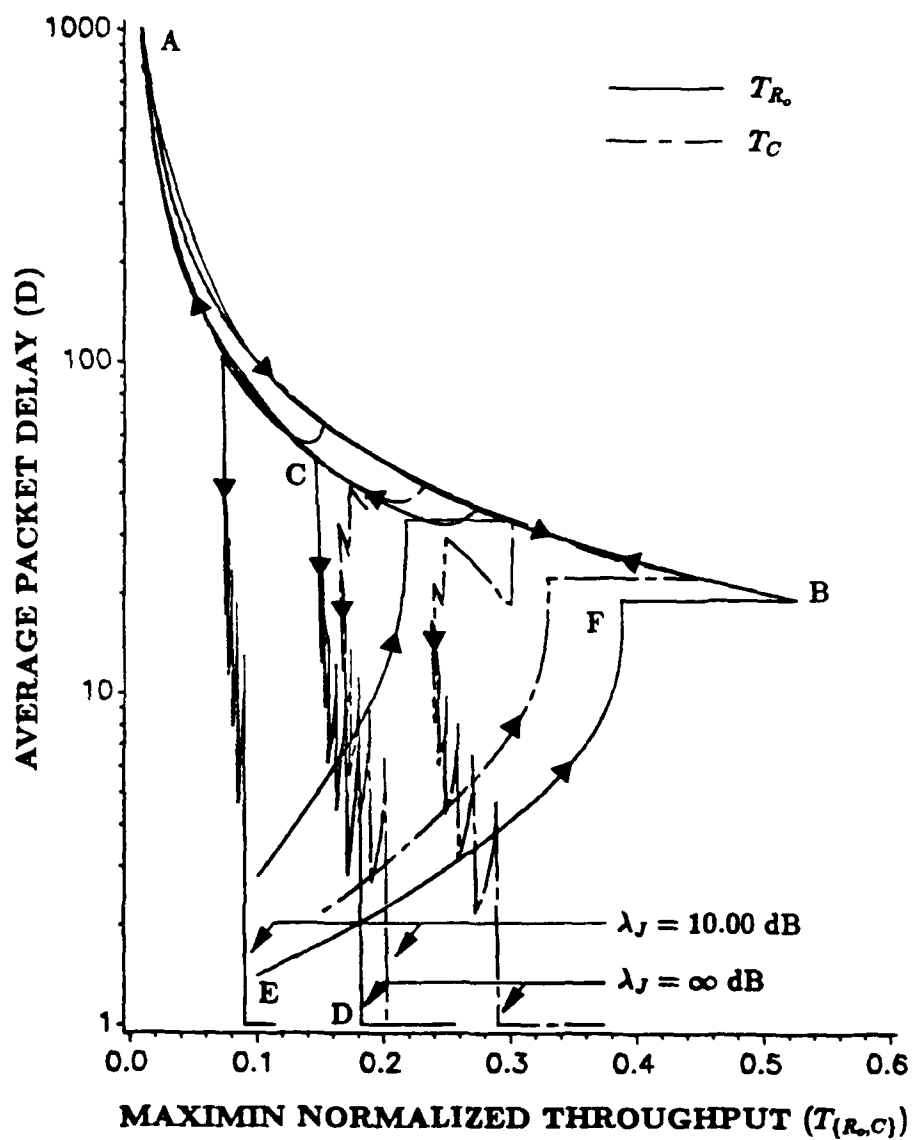
Figure 4.5: Average Packet Delay (D) versus Maximin Normalized Throughput ($T_{\{R_o,C\}}$) for $N = 10$ (No Jammer State Information)
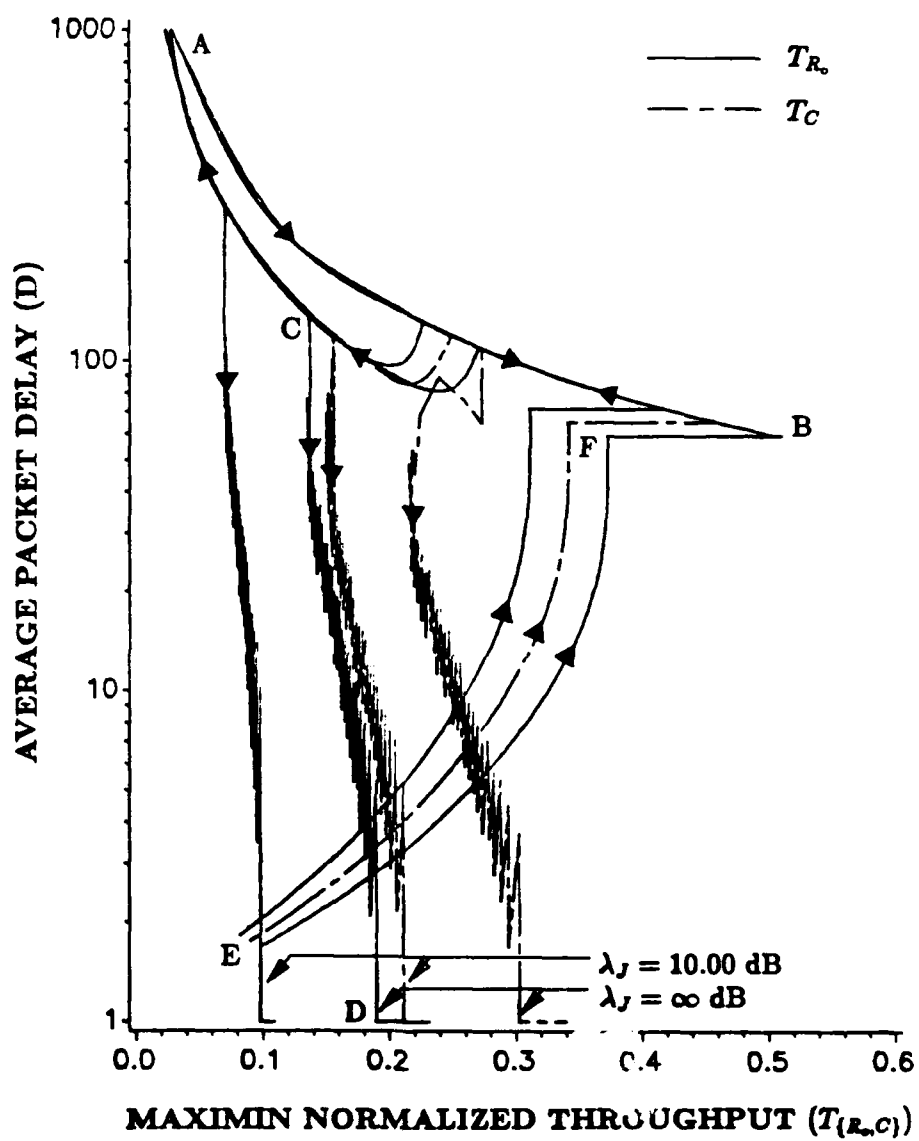
Figure 4.6: Average Packet Delay (D) versus Maximin Normalized Throughput $(T_{\{R_o,C\}})$ for $N = 30$ (Jammer State Information)
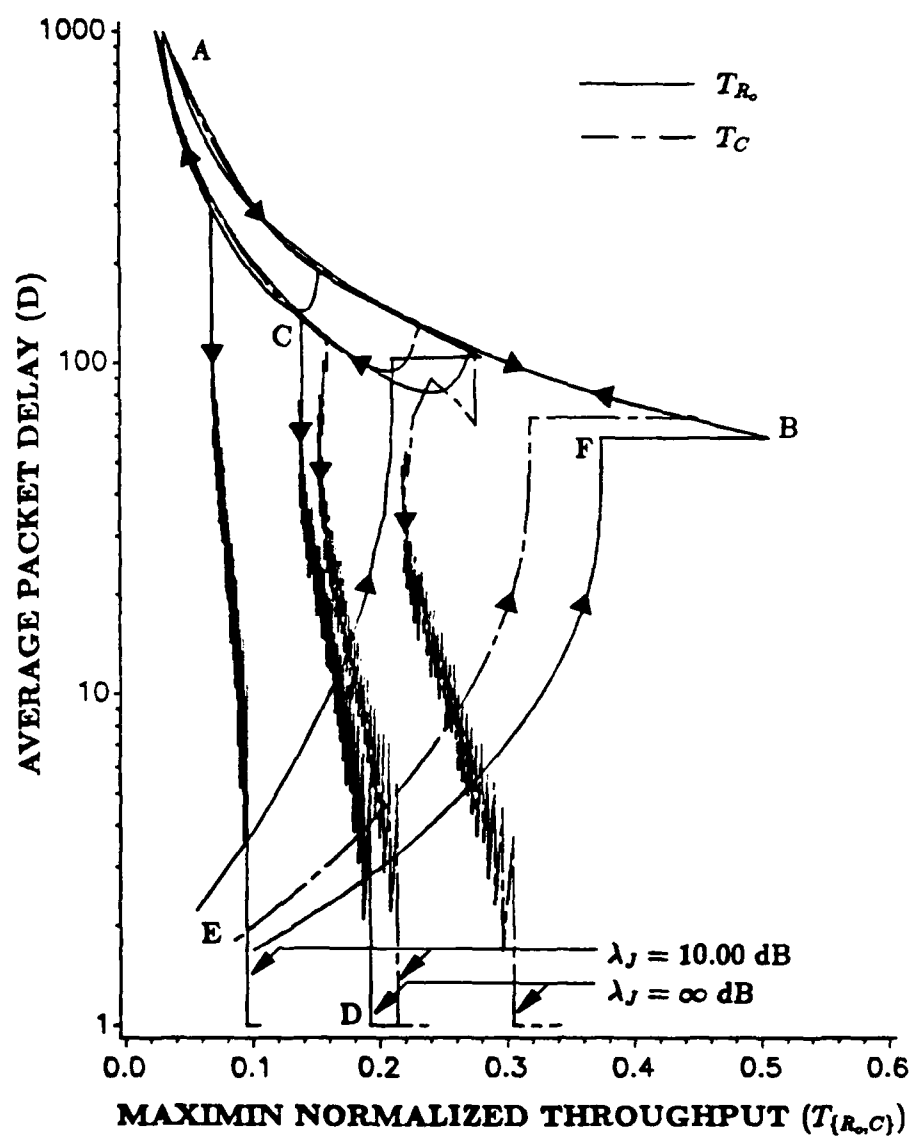
Figure 4.7: Average Packet Delay (D) versus Maximin Normalized Throughput $(T_{\{R_o,C\}})$ for $N = 30$ (No Jammer State Information)
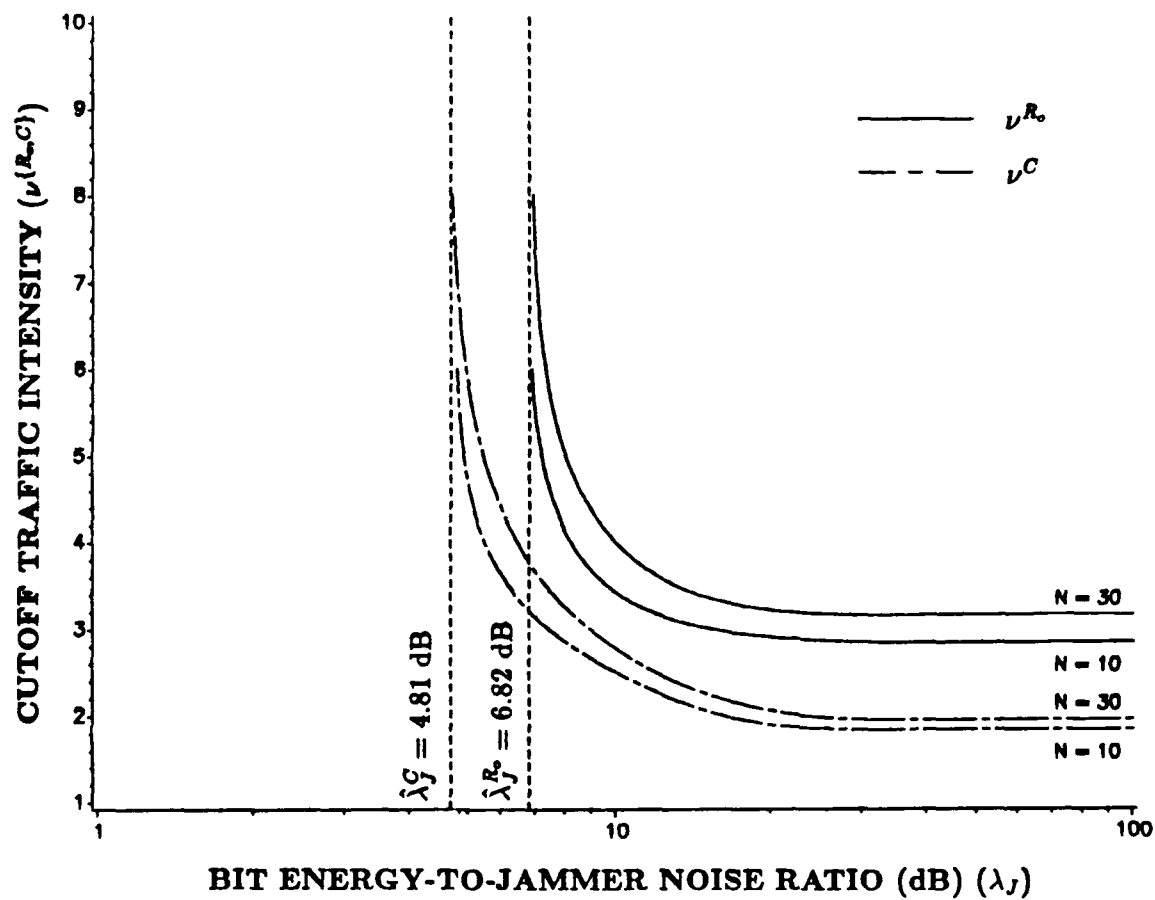
Figure 4.8: Cutoff Traffic Intensity ($\nu^{\{R_o,C\}}$) versus Bit Energy-to-Jammer Noise Ratio (λ_J) (Jammer State Information)
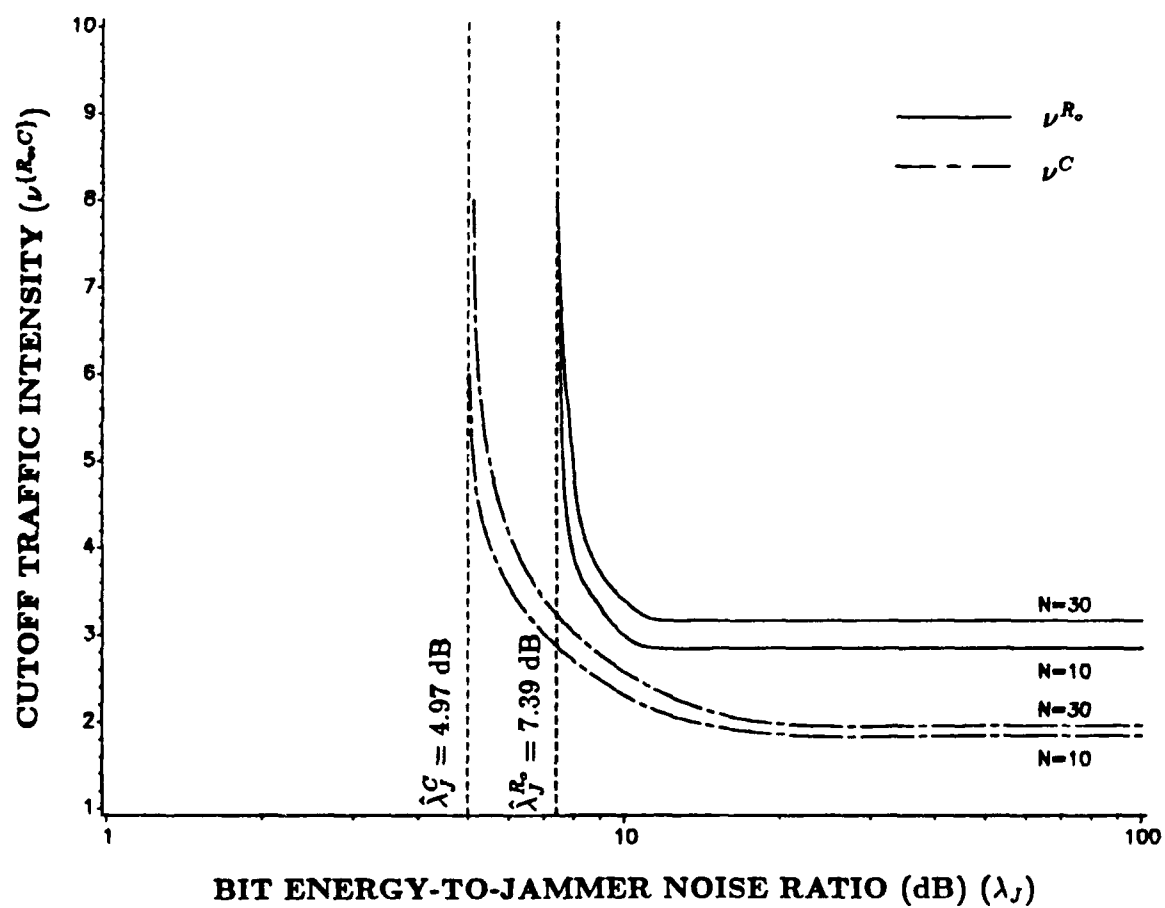
Figure 4.9: Cutoff Traffic Intensity ($\nu^{\{R_o,C\}}$) versus Bit Energy-to-Jammer Noise Ratio (λ_J) (No Jammer State Information)

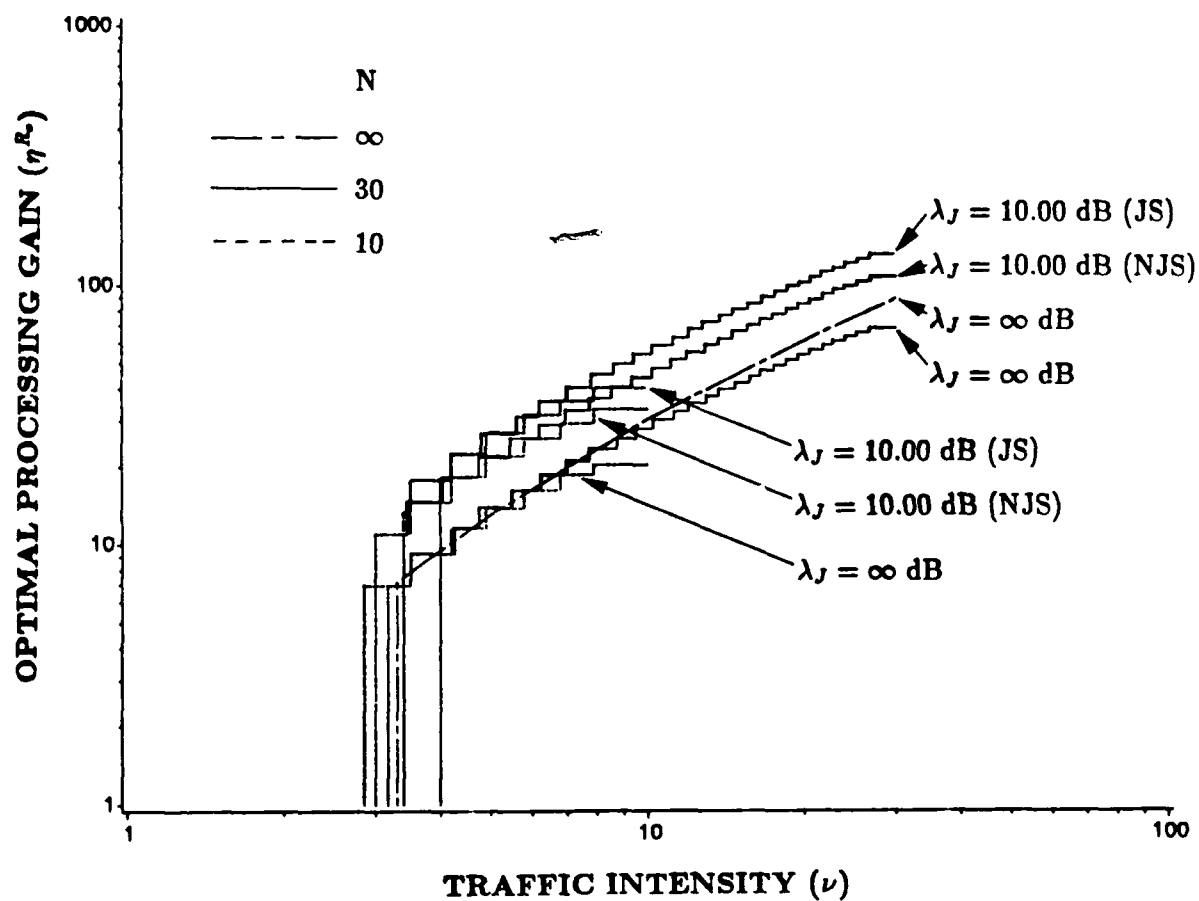Figure 4.10: Optimal Processing Gain (η^{R_o}) versus Traffic Intensity (ν) for the Cutoff Rate Case

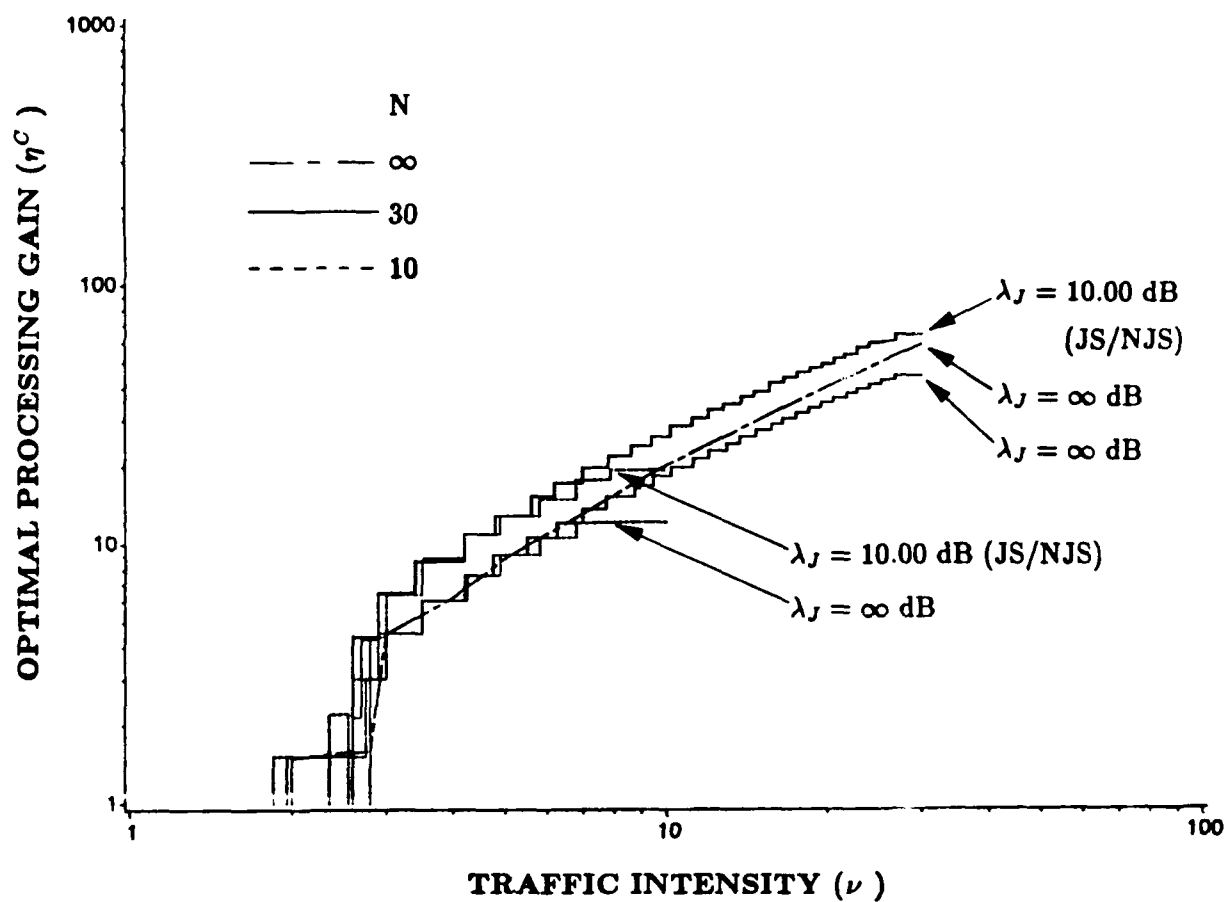Figure 4.11: Optimal Processing Gain (η^C) versus Traffic Intensity (ν) for the Capacity Case

Figure 4.12: Optimal Processing Gain ($\eta^{\{R_o,C\}}$) versus Bit Energy-to-Jammer Noise Ratio (λ_J) (Jammer State Information) ($\nu = 5.0$)
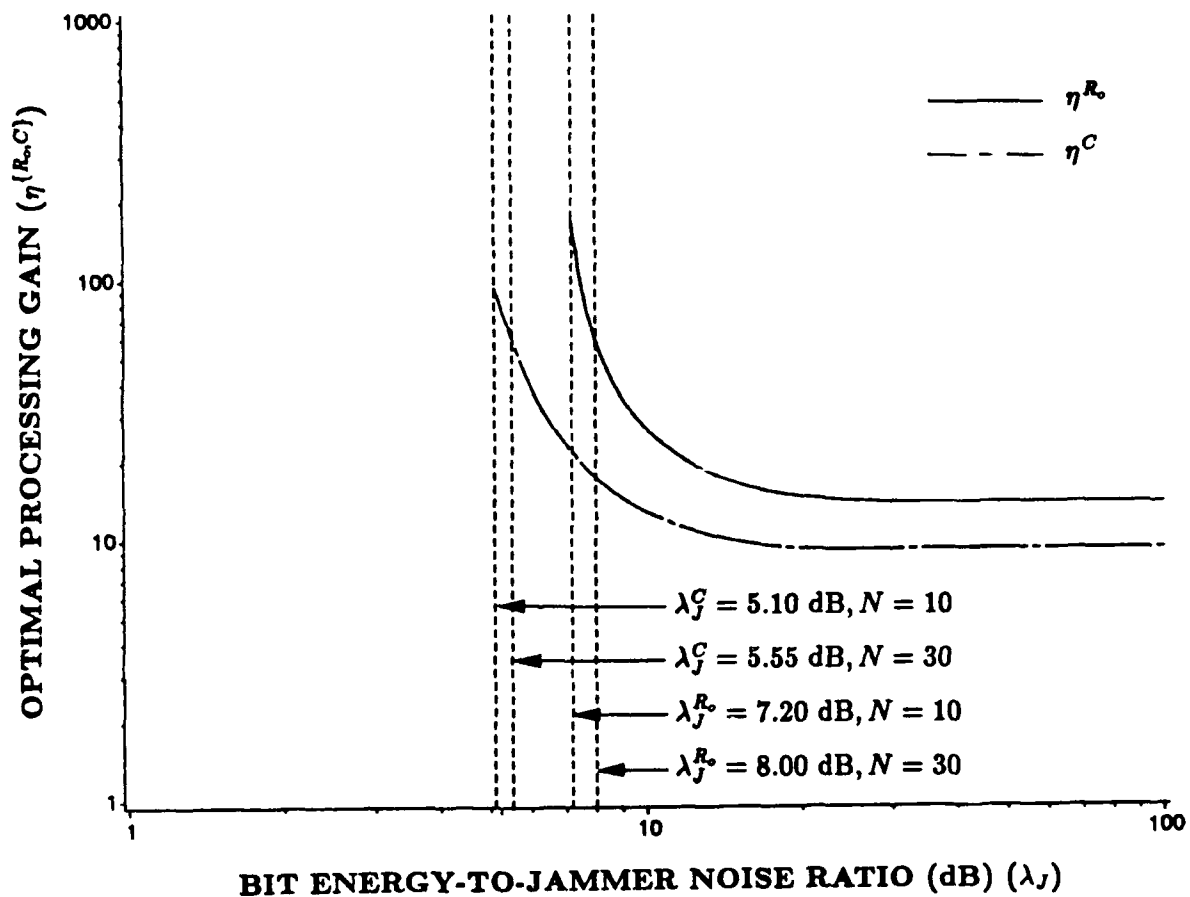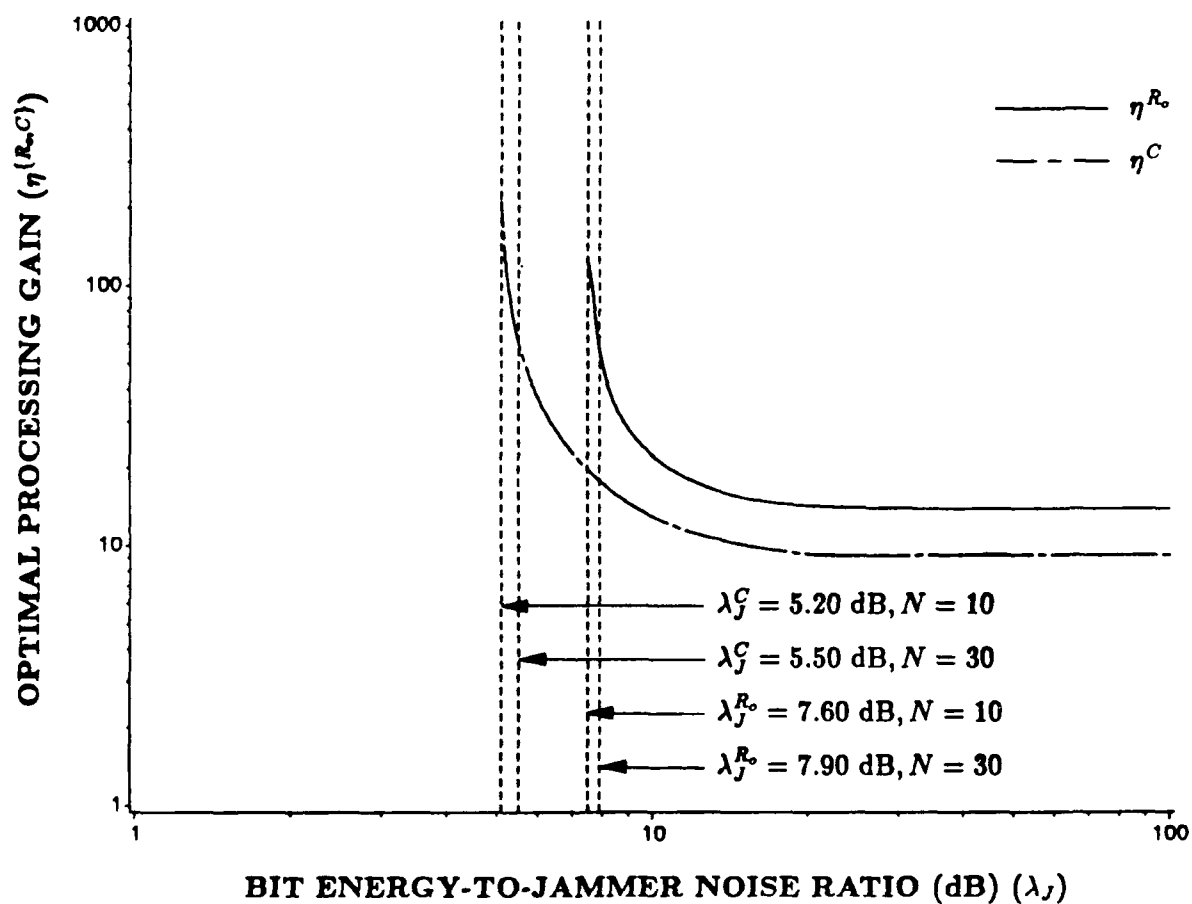
Figure 4.13: Optimal Processing Gain $(\eta^{\{R_o,C\}})$ versus Bit Energy-to-Jammer Noise Ratio (λ_J) (No Jammer State Information) $(\nu = 5.0)$
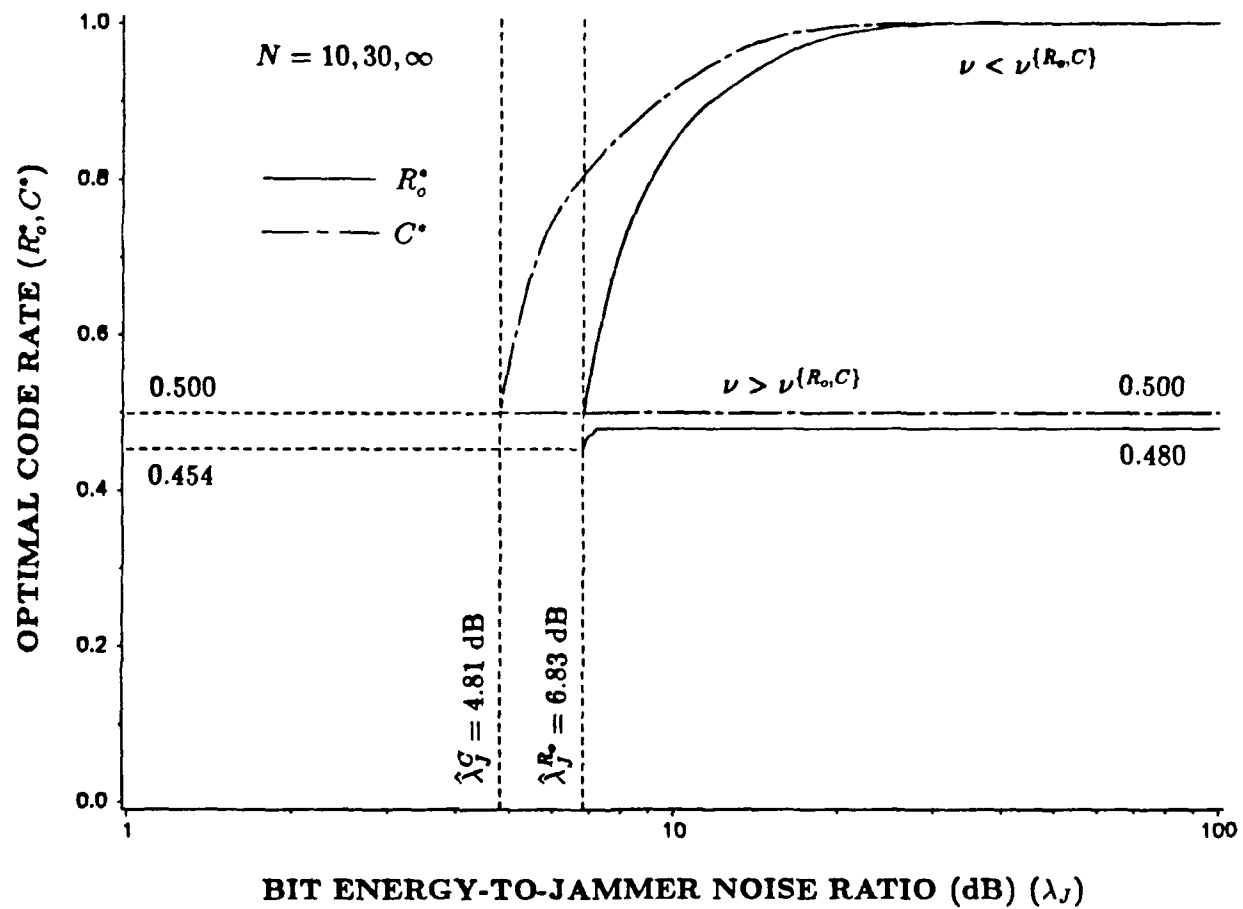
Figure 4.14: Optimal Code Rate (R_o^*, C^*) versus Bit Energy-to-Jammer Noise Ratio (Jammer State Information)
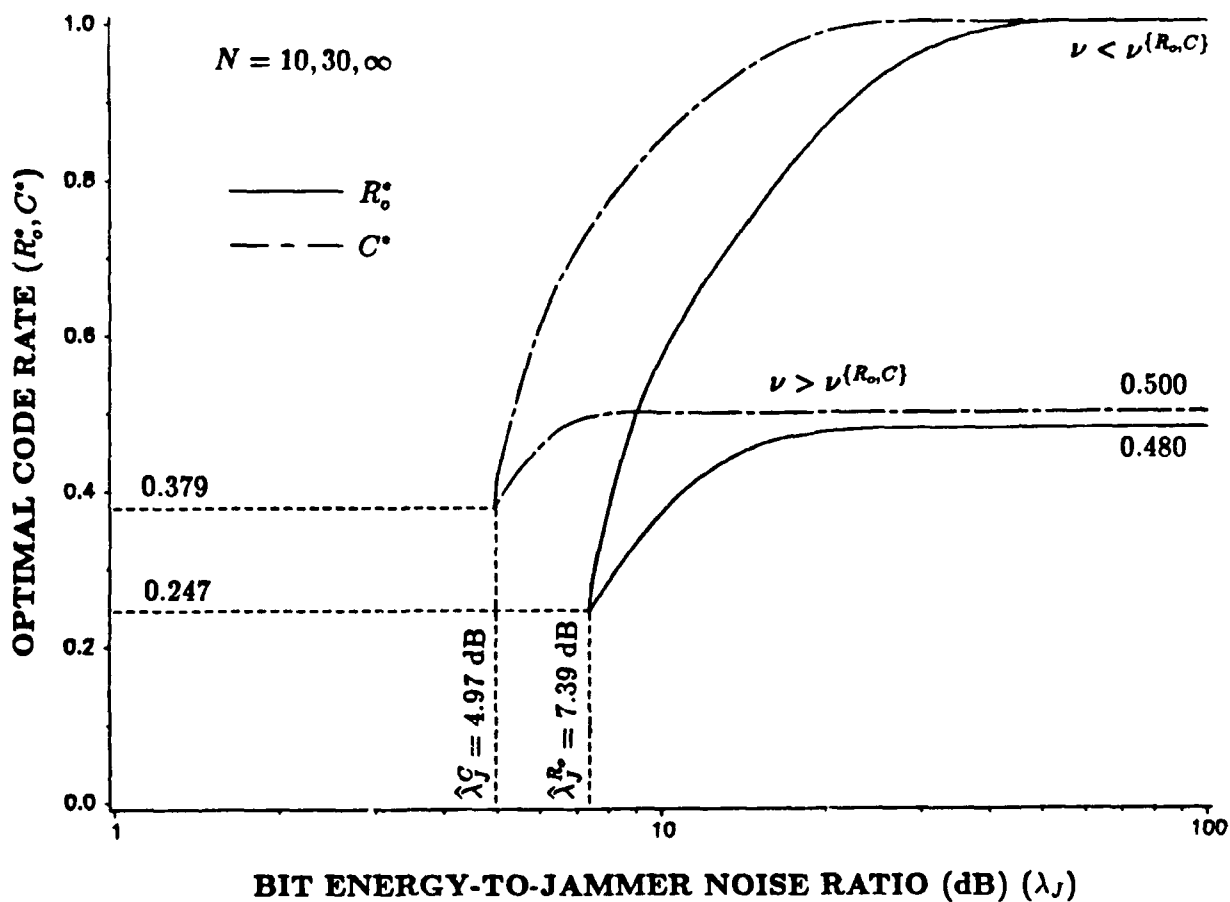
Figure 4.15: Optimal Code Rate (R_o^*, C^*) versus Bit Energy-to-Jammer Noise Ratio (No Jammer State Information)
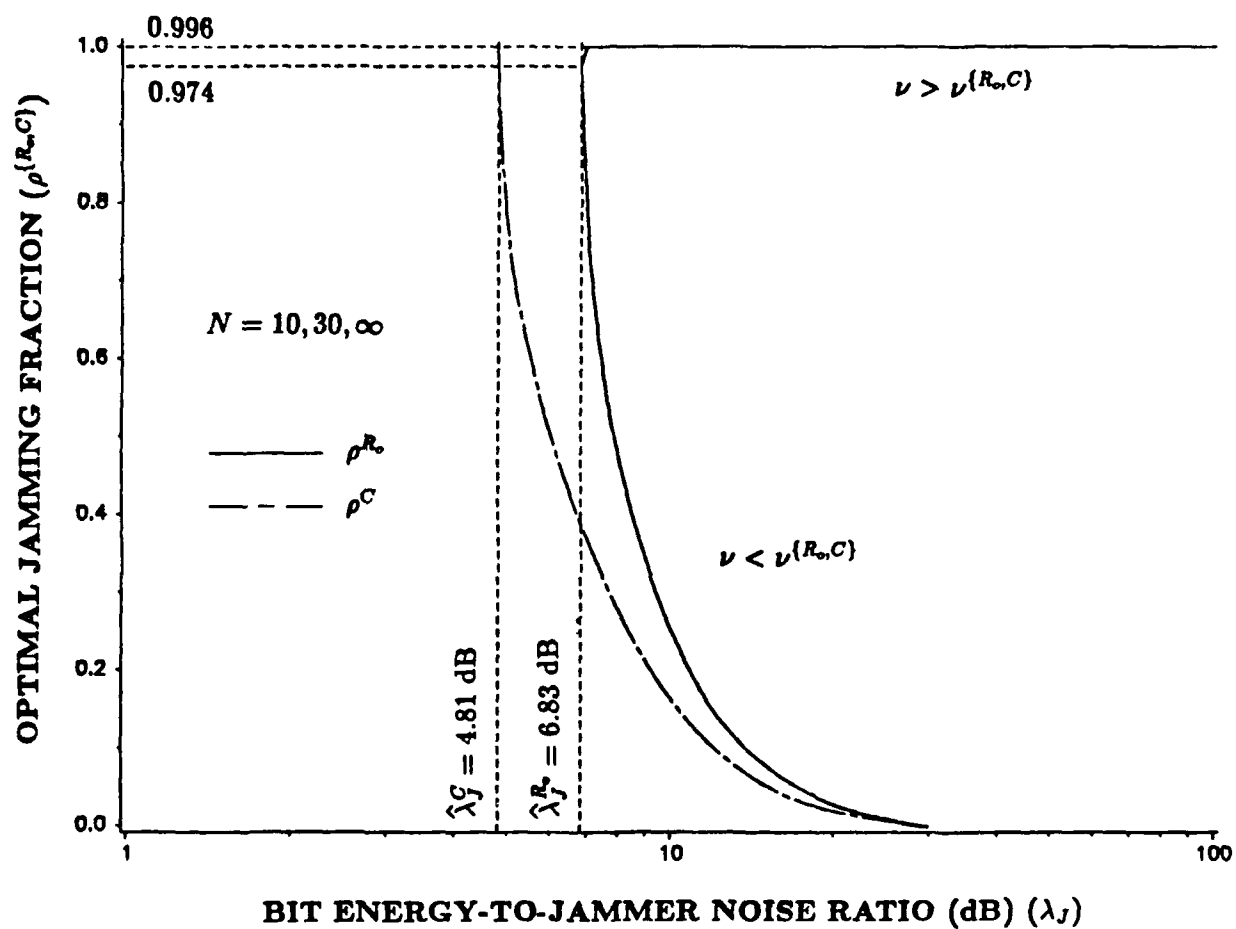
Figure 4.16: Optimal Jamming Fraction ($\rho^{\{R_o, C\}}$) versus Bit Energy-to-Jammer Noise Ratio (Jammer State Information)
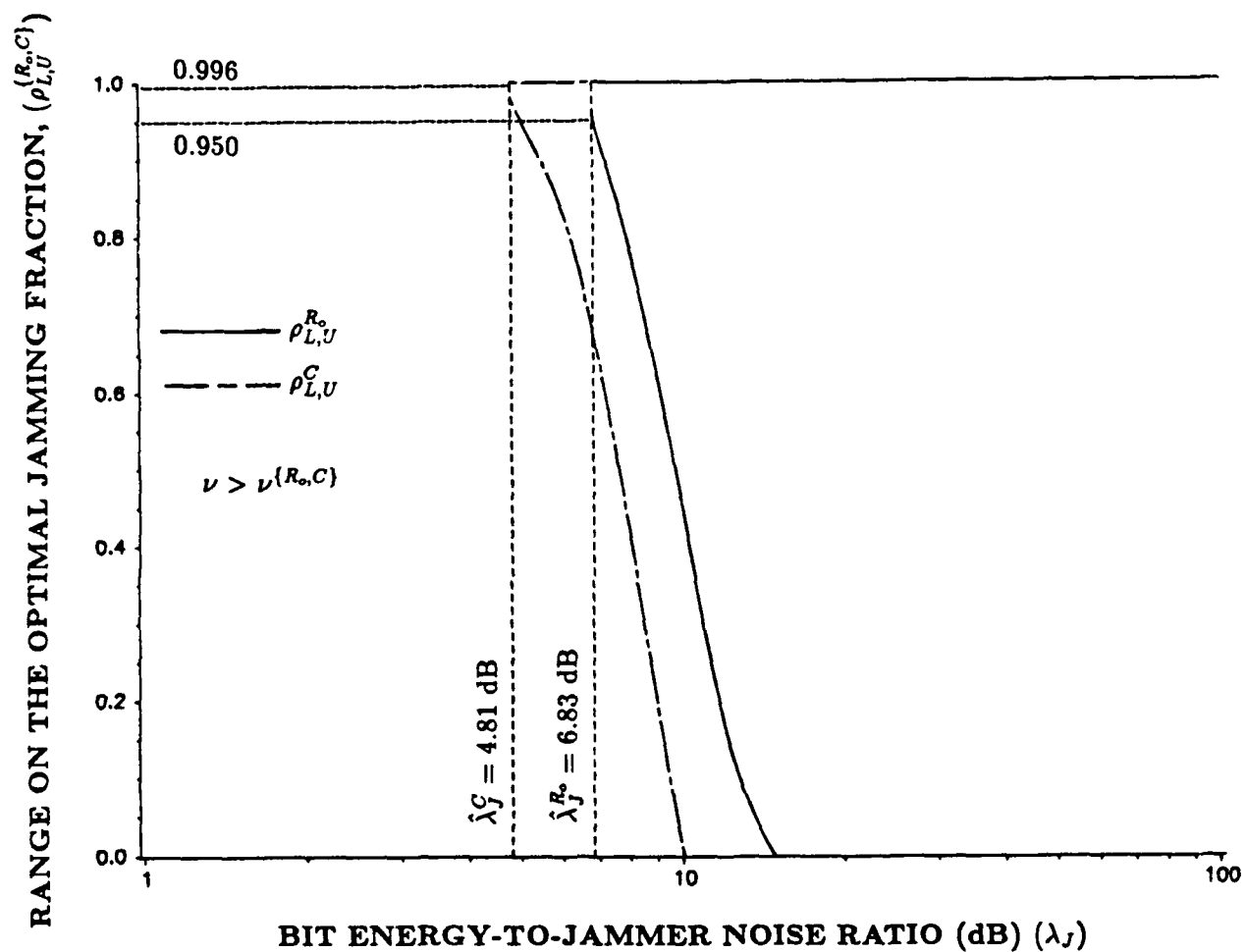
Figure 4.17: Lower and Upper Bounds on the Range for the Optimal Jamming Fraction $(\rho_{L,U}^{\{R_o,C\}})$ versus Bit Energy-to-Jammer Noise Ratio (Jammer State Information)
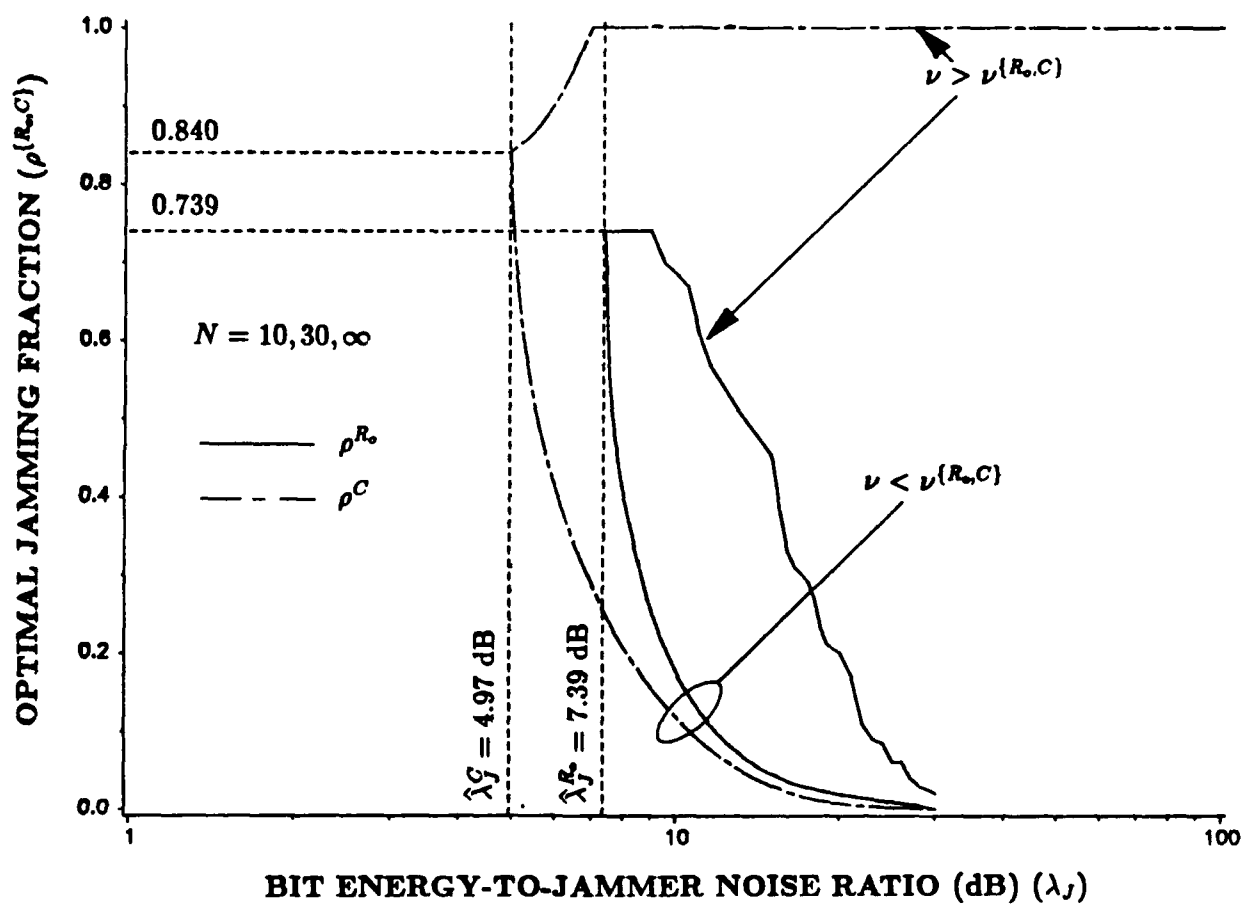
Figure 4.18: Optimal Jamming Fraction ($\rho^{\{R_o,C\}}$) versus Bit Energy-to-Jammer Noise Ratio (No Jammer State Information)
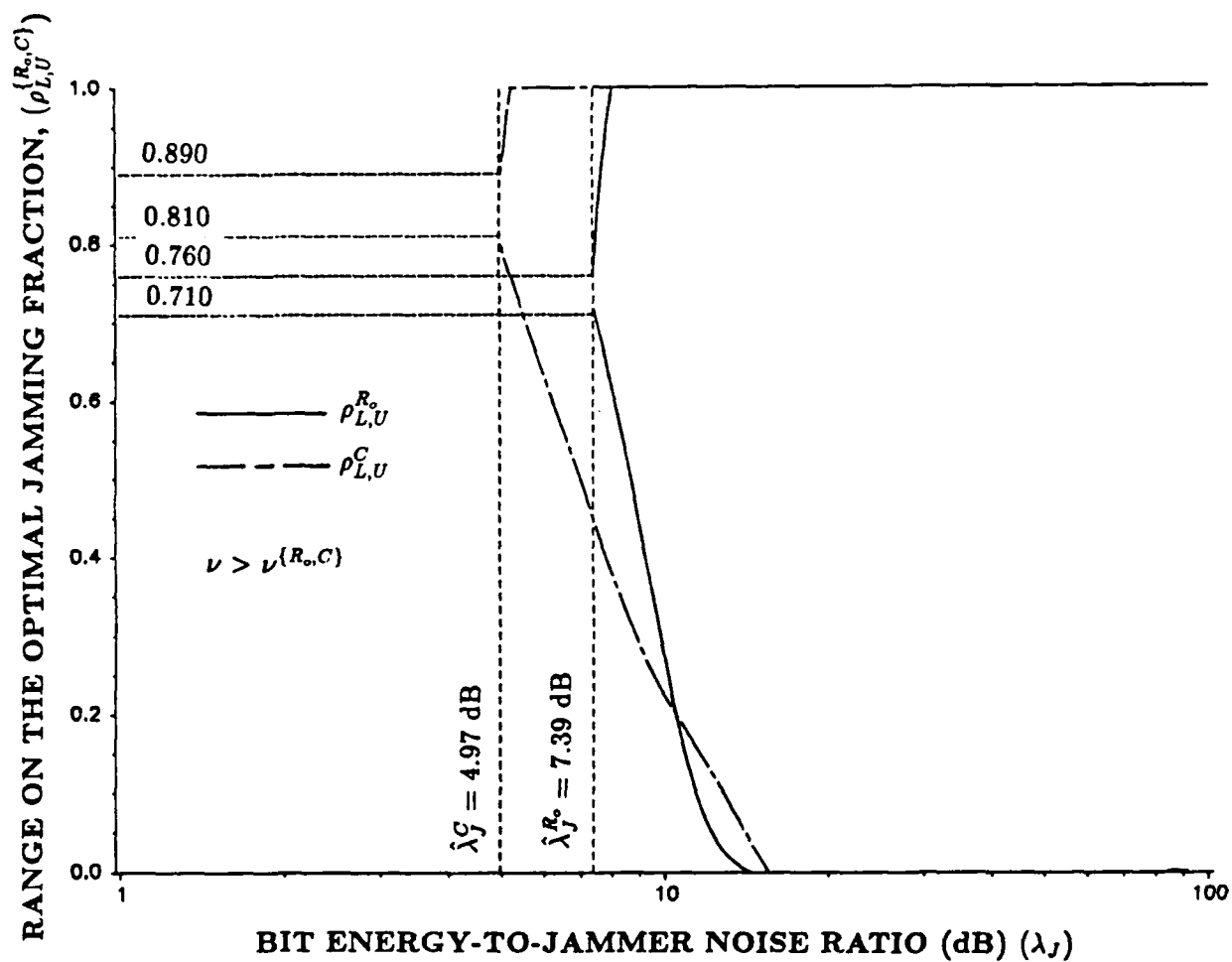
Figure 4.19: Lower and Upper Bounds on the Range for the Optimal Jamming Fraction $(\rho_{L,U}^{\{R_o,C\}})$ versus Bit Energy-to-Jammer Noise Ratio (No Jammer State Information)

Figure 4.20: Maximin Normalized Throughput (T_{R_o}) versus Traffic Intensity (ν) (Constant Jammer Power, Cutoff Rate Case, Jammer State Information)

Figure 4.21: Average Packet Delay (D) versus Maximin Normalized Throughput (T_{R_o}) for $N = 10$ (Constant Jammer Power, Cutoff Rate Case, Jammer State Information)

Figure 4.22: Number of Simultaneous Users ($\hat{m}$) versus Traffic Intensity (ν) versus Bit Energy-to-Jammer Noise Ratio ($\tilde{\lambda}_J$) for $N = 10$ (Constant Jammer Power, Cutoff Rate Case, Jammer State Information)

Figure 4.23: Optimal Processing Gain (η^{R_o}) versus Traffic Intensity (ν) versus Bit Energy-to-Jammer Noise Ratio ($\tilde{\lambda}_J$) for $N = 10$ (Constant Jammer Power, Cutoff Rate Case, Jammer State Information)

Figure 4.24: Optimal Code Rate (R_o^*) versus Traffic Intensity (ν) versus Bit Energy-to-Jammer Noise Ratio $(\tilde{\lambda}_J)$ for $N = 10$ (Constant Jammer Power, Cutoff Rate Case, Jammer State Information)
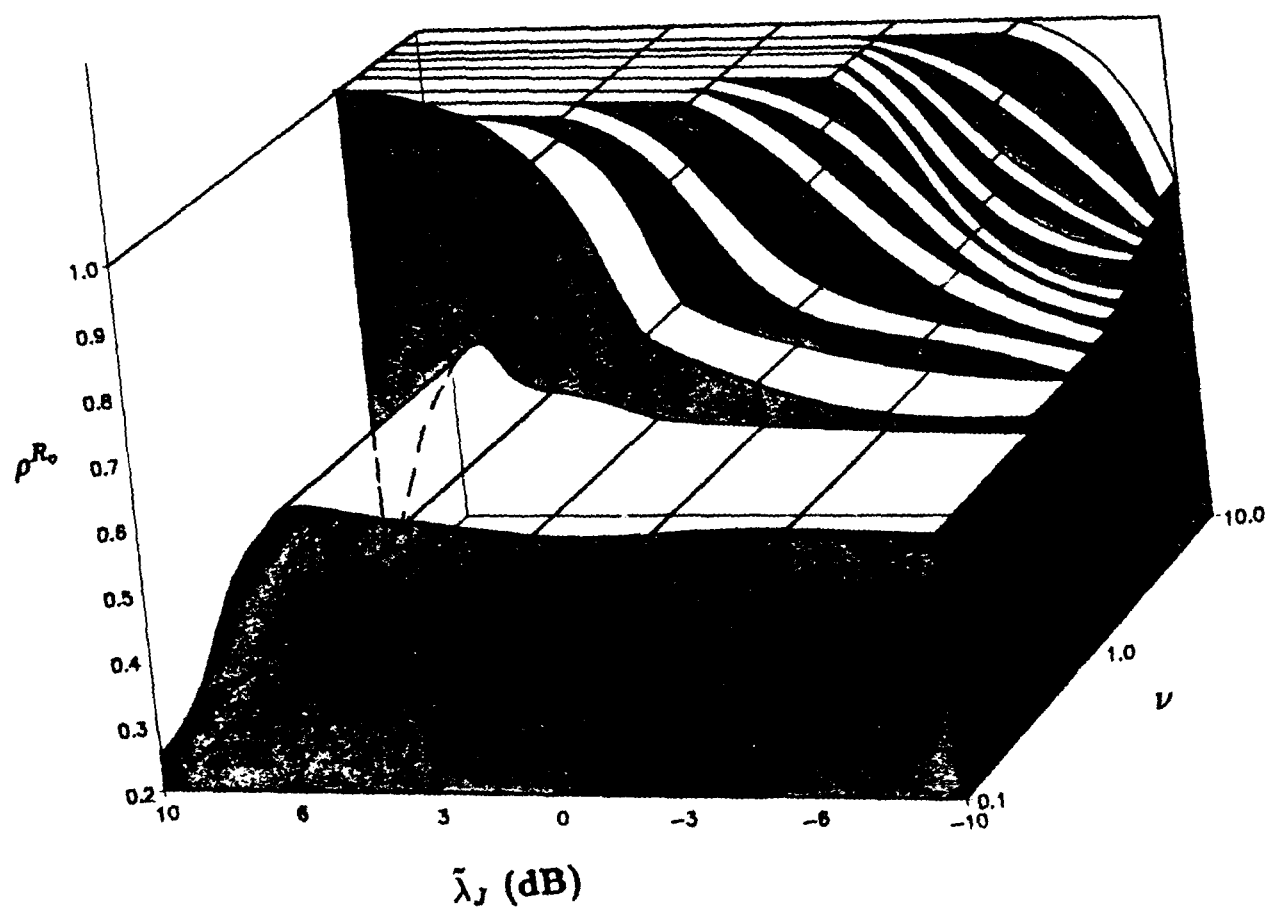
Figure 4.25: Optimal Jamming Fraction (ρ^{R_o}) versus Traffic Intensity (ν) versus Bit Energy-to-Jammer Noise Ratio ($\tilde{\lambda}_J$) for $N = 10$ (Constant Jammer Power, Cutoff Rate Case, Jammer State Information)
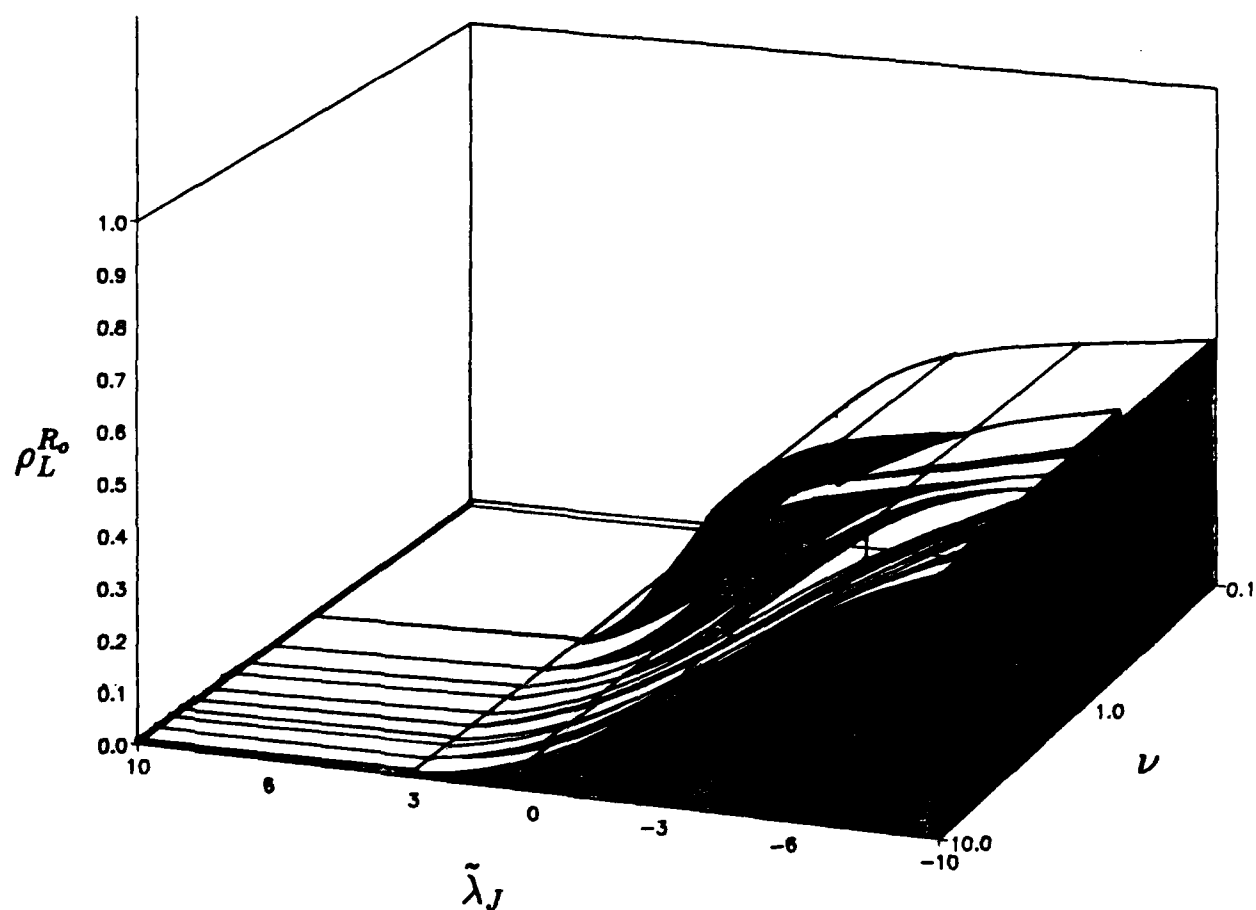
Figure 4.26: Lower Bound on the Range for the Optimal Jamming Fraction $(\rho_{L,U}^{R_o})$ versus Traffic Intensity (ν) versus Bit Energy-to-Jammer Noise Ratio $(\tilde{\lambda}_J)$ for $N = 10$ (Constant Jammer Power, Cutoff Rate Case, Jammer State Information)
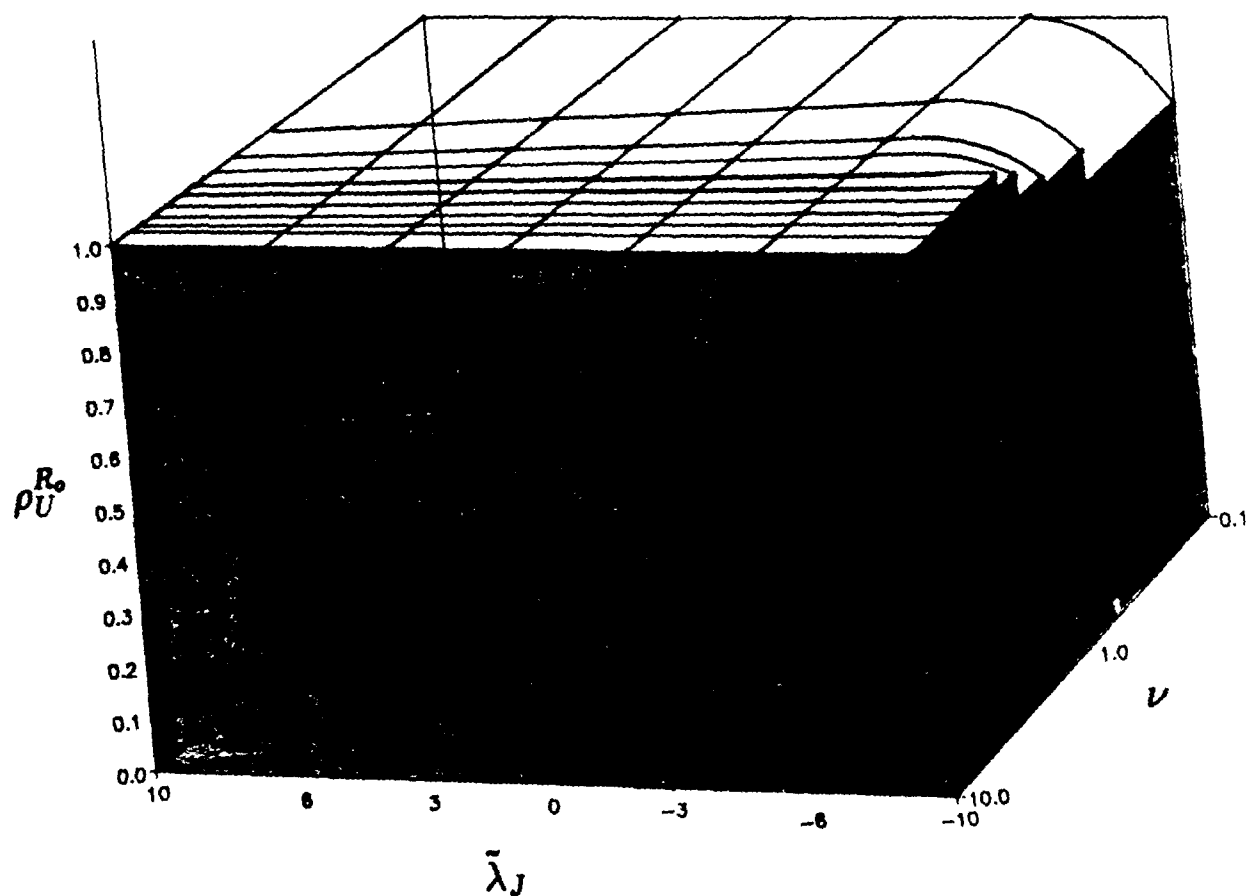
Figure 4.27: Upper Bound on the Range for the Optimal Jamming Fraction $(\rho_{L,U}^{R_o})$ versus Traffic Intensity (ν) versus Bit Energy-to-Jammer Noise Ratio $(\tilde{\lambda}_J)$ for $N = 10$ (Constant Jammer Power, Cutoff Rate Case, Jammer State Information)
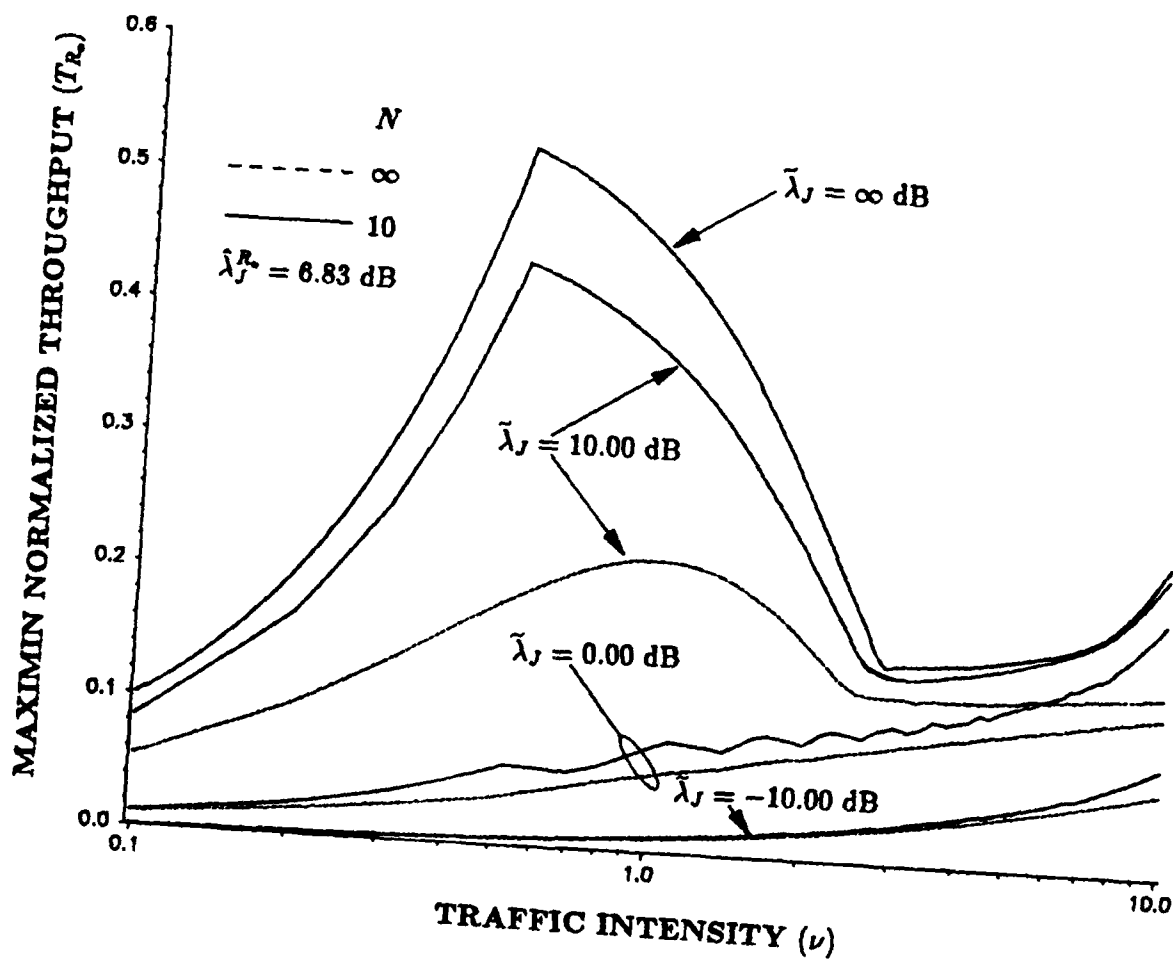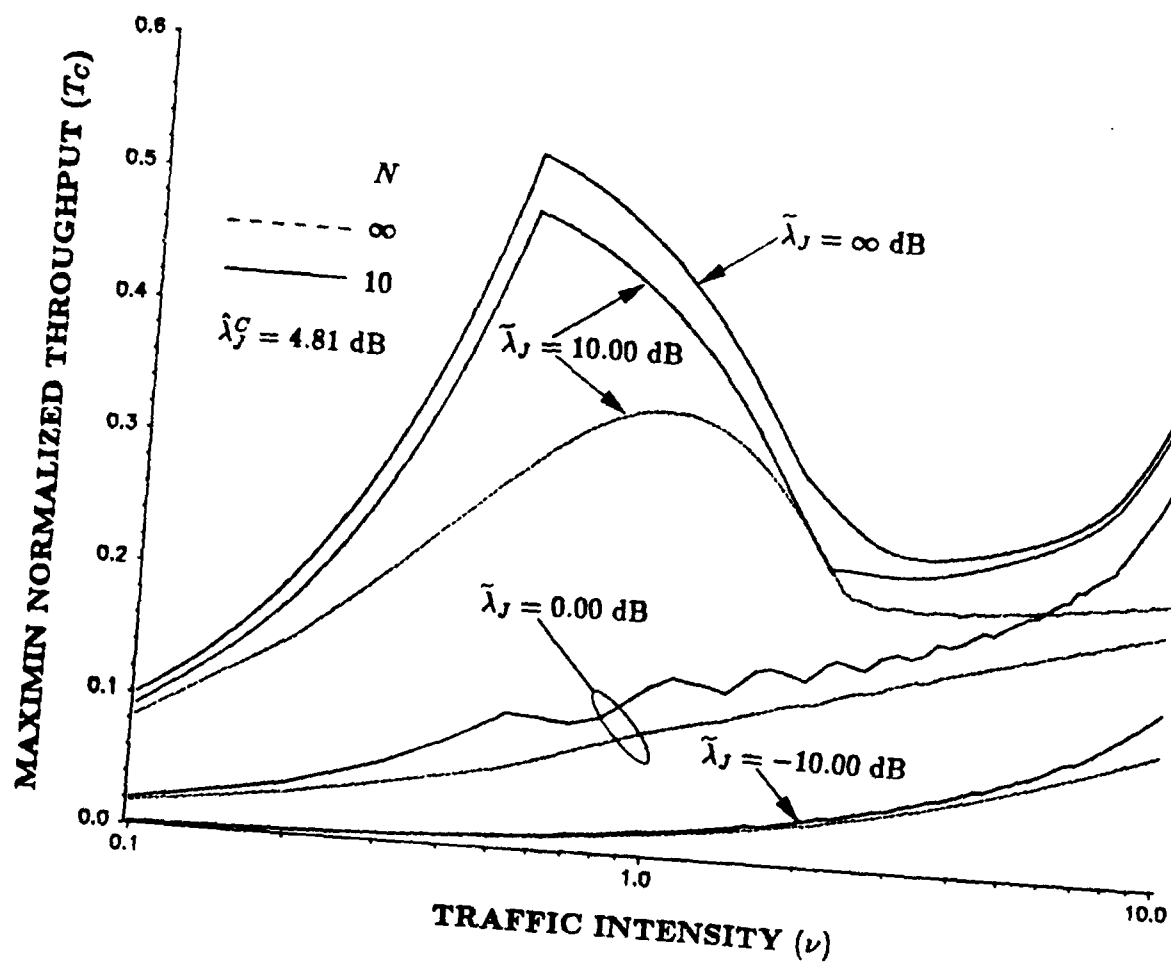
Figure 4.28: Maximin Normalized Throughput (T_C) versus Traffic Intensity (ν) (Constant Jammer Power, Capacity Case, Jammer State Information)
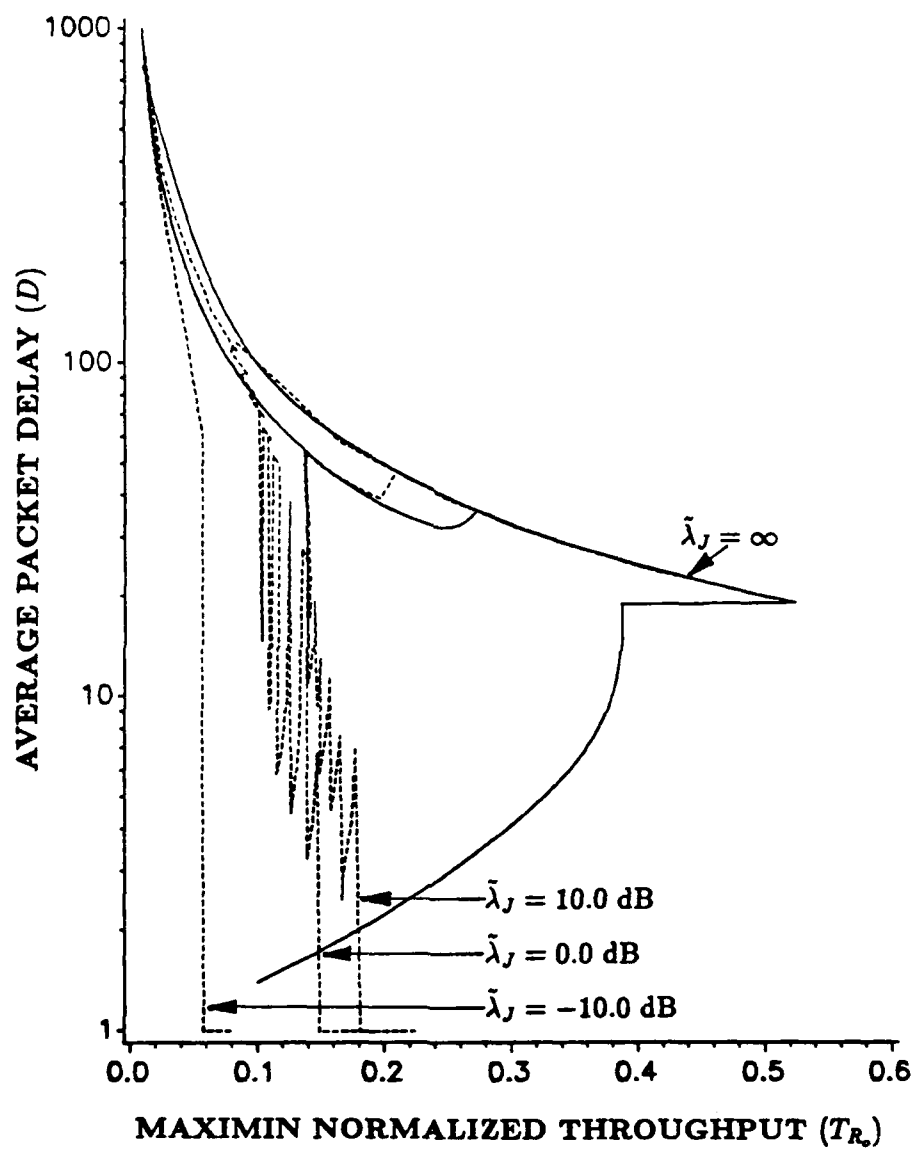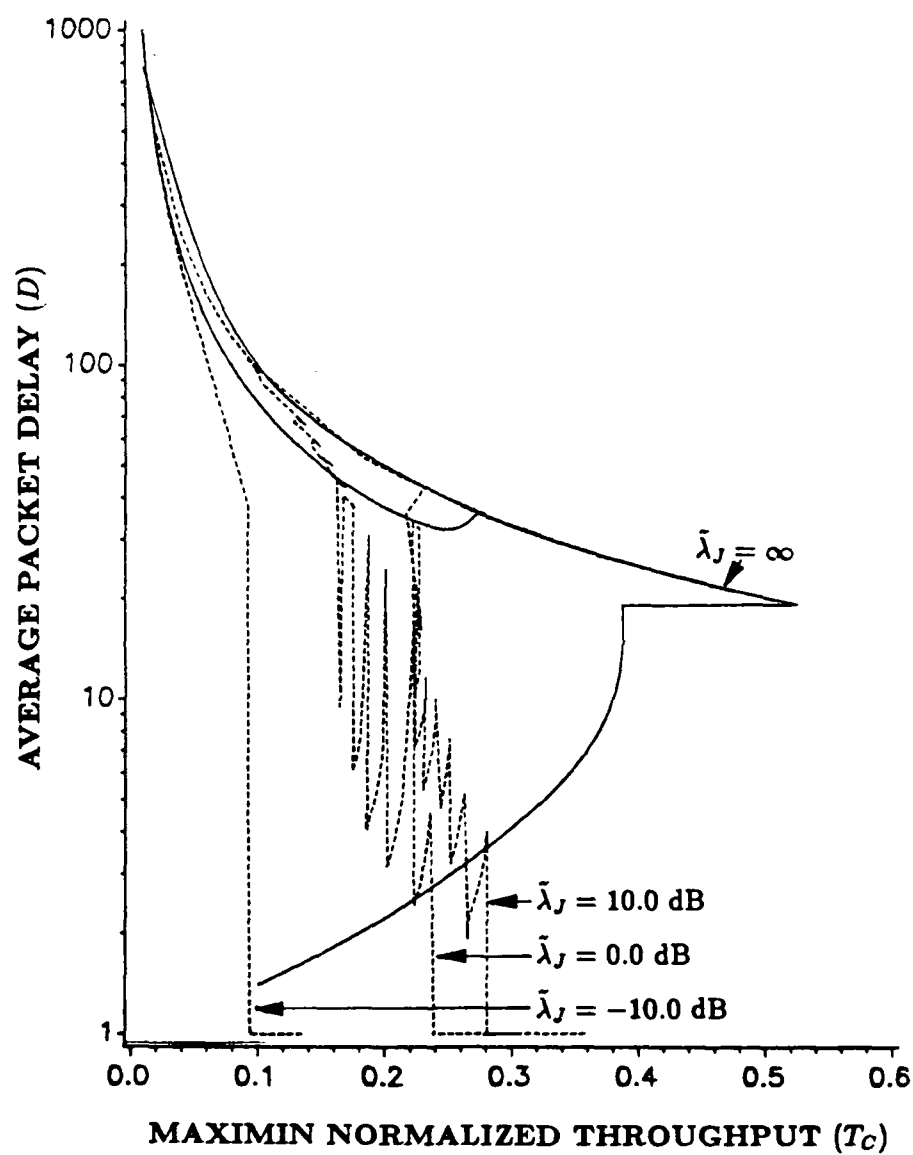
Figure 4.29: Average Packet Delay (D) versus Maximin Normalized Throughput (T_C) for $N = 10$ (Constant Jammer Power, Capacity Case, Jammer State Information)
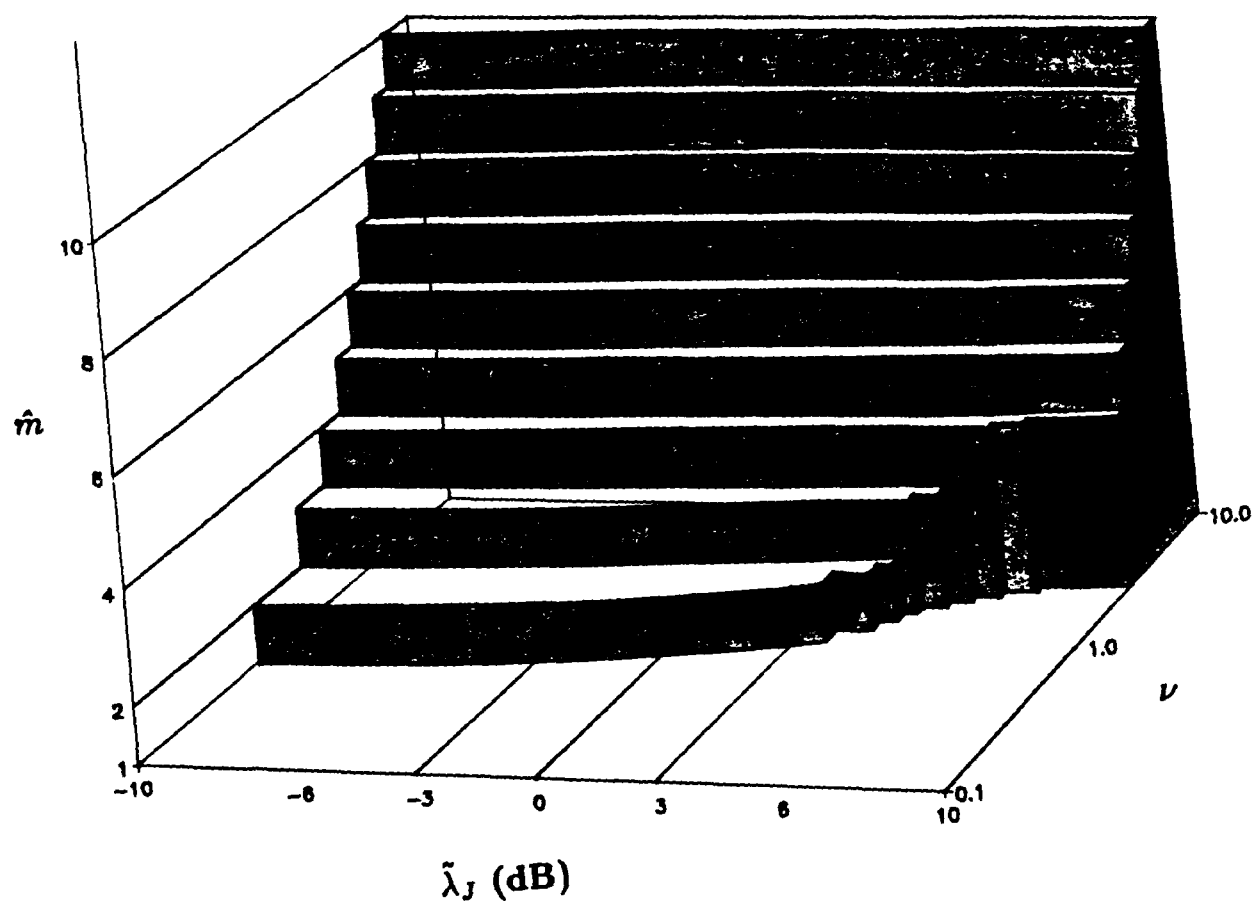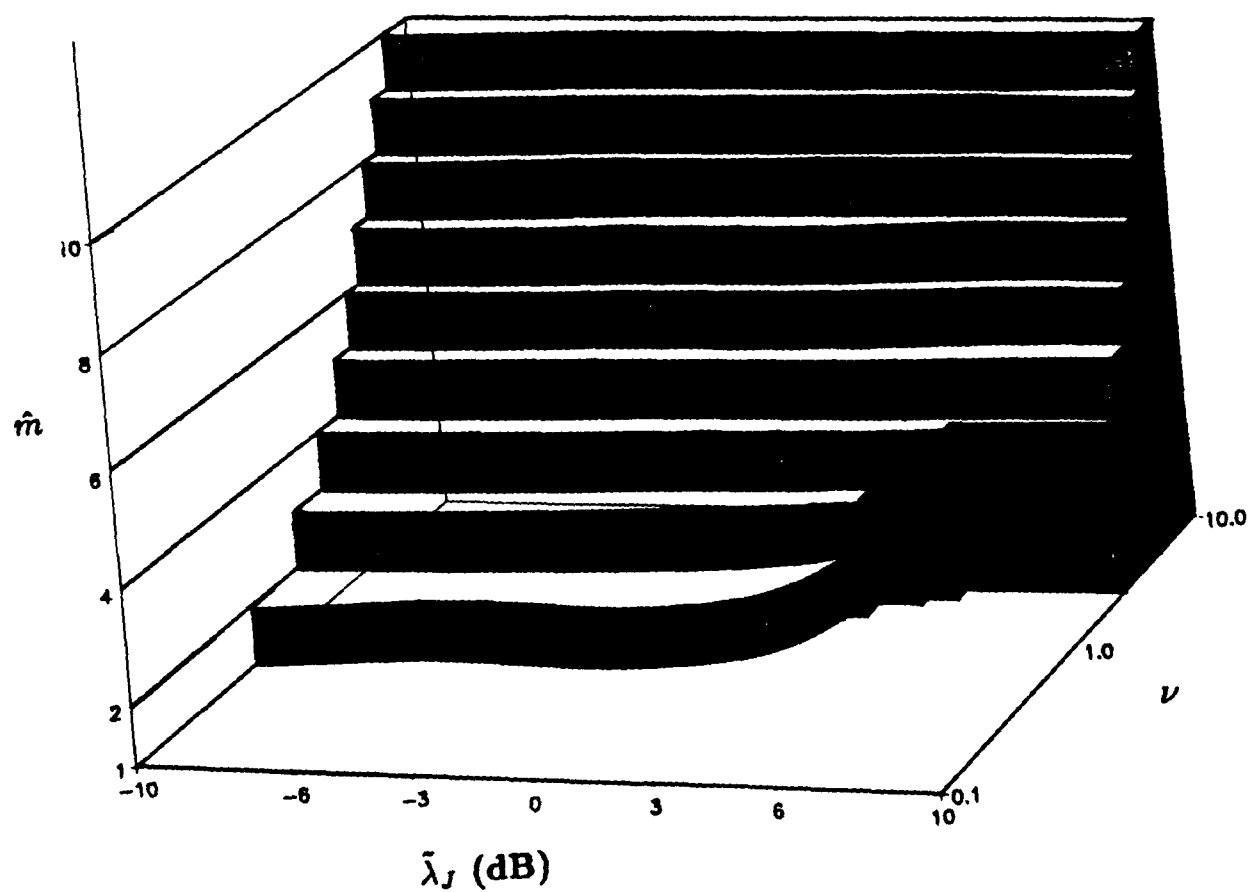
Figure 4.30: Number of Simultaneous Users ($\hat{m}$) versus Traffic Intensity (ν) versus Bit Energy-to-Jammer Noise Ratio ($\tilde{\lambda}_J$) for $N = 10$ (Constant Jammer Power, Capacity Case, Jammer State Information)
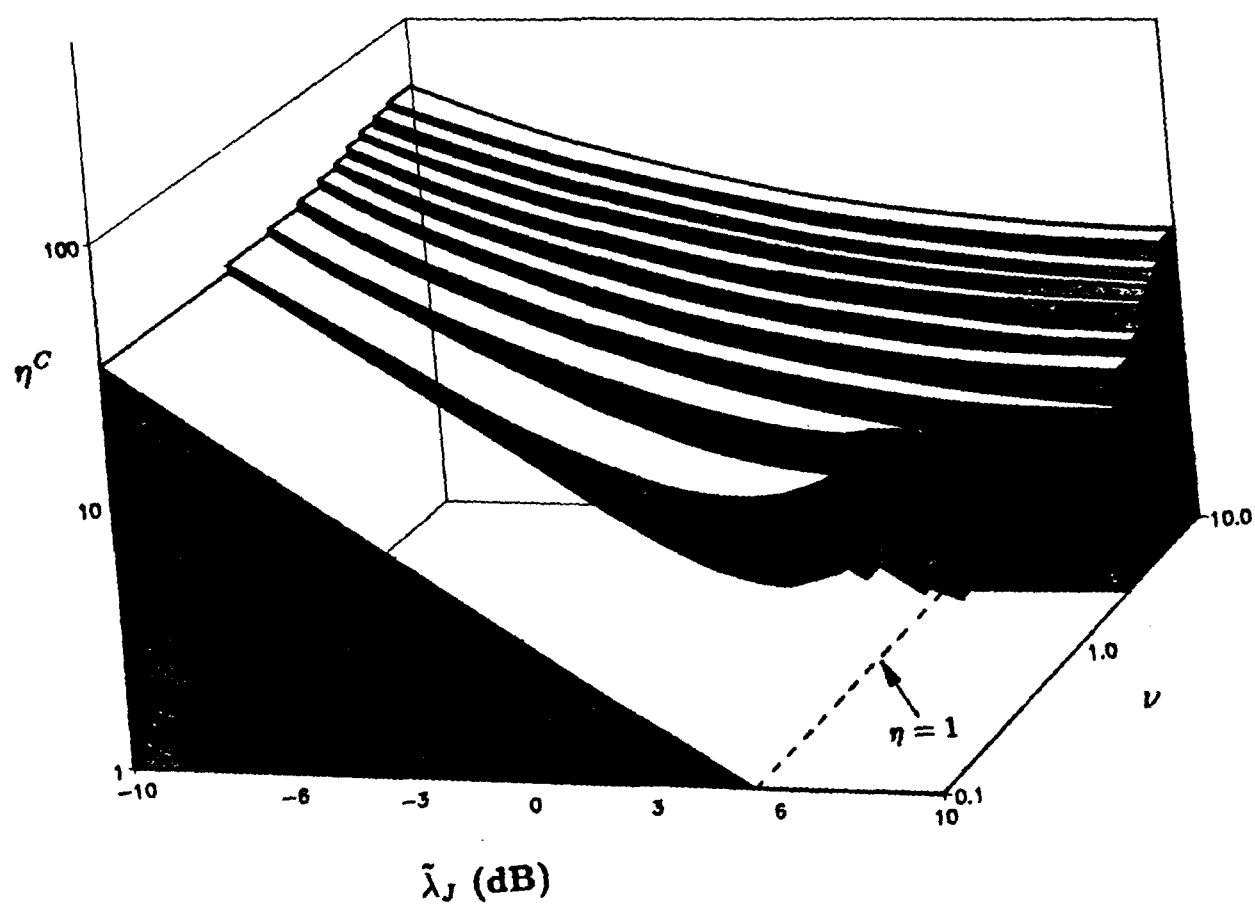
Figure 4.31: Optimal Processing Gain (η^C) versus Traffic Intensity (ν) versus Bit Energy-to-Jammer Noise Ratio ($\tilde{\lambda}_J$) for $N = 10$ (Constant Jammer Power, Capacity Case, Jammer State Information)
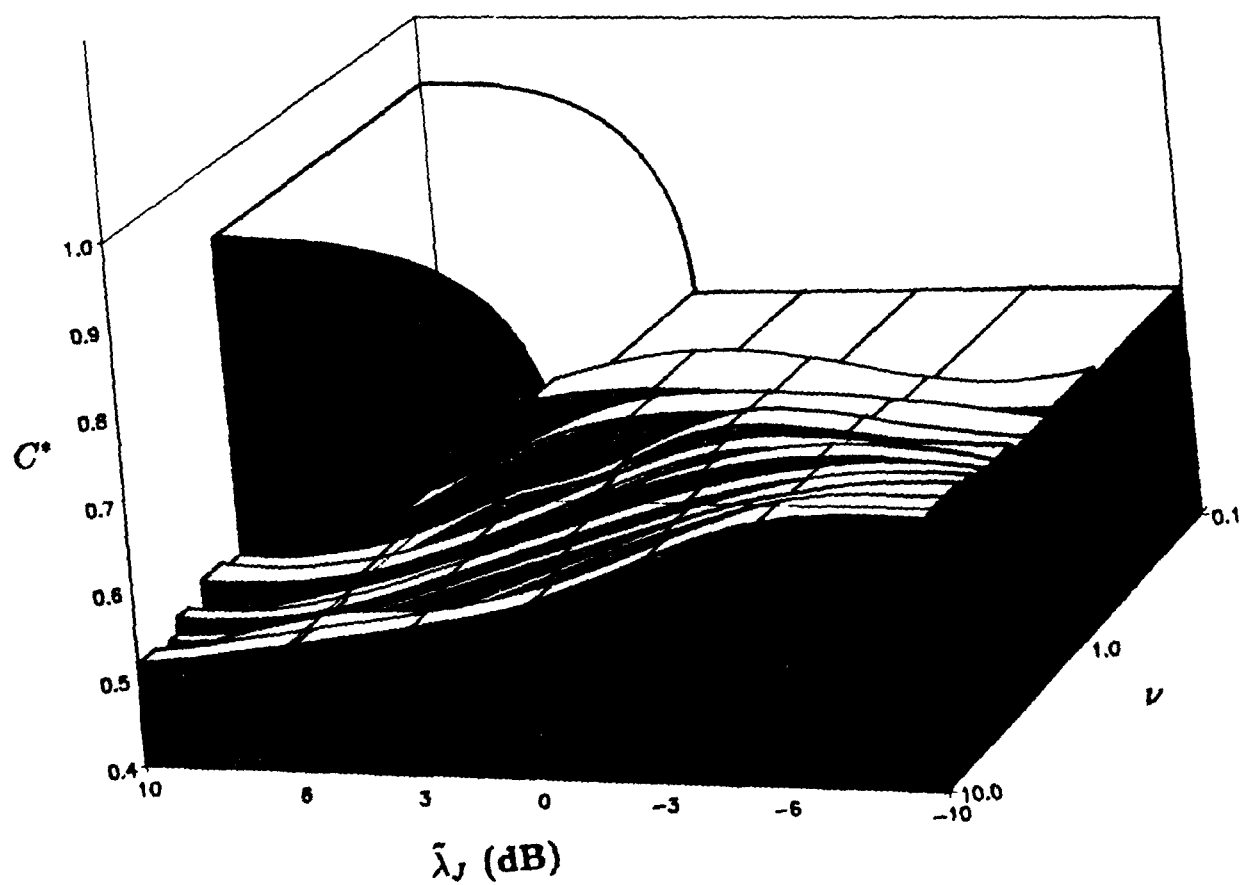
Figure 4.32: Optimal Code Rate (C^*) versus Traffic Intensity (ν) versus Bit En-ergy-to-Jammer Noise Ratio $(\tilde{\lambda}_J)$ for $N = 10$ (Constant Jammer Power, Capacity Case, Jammer State Information)
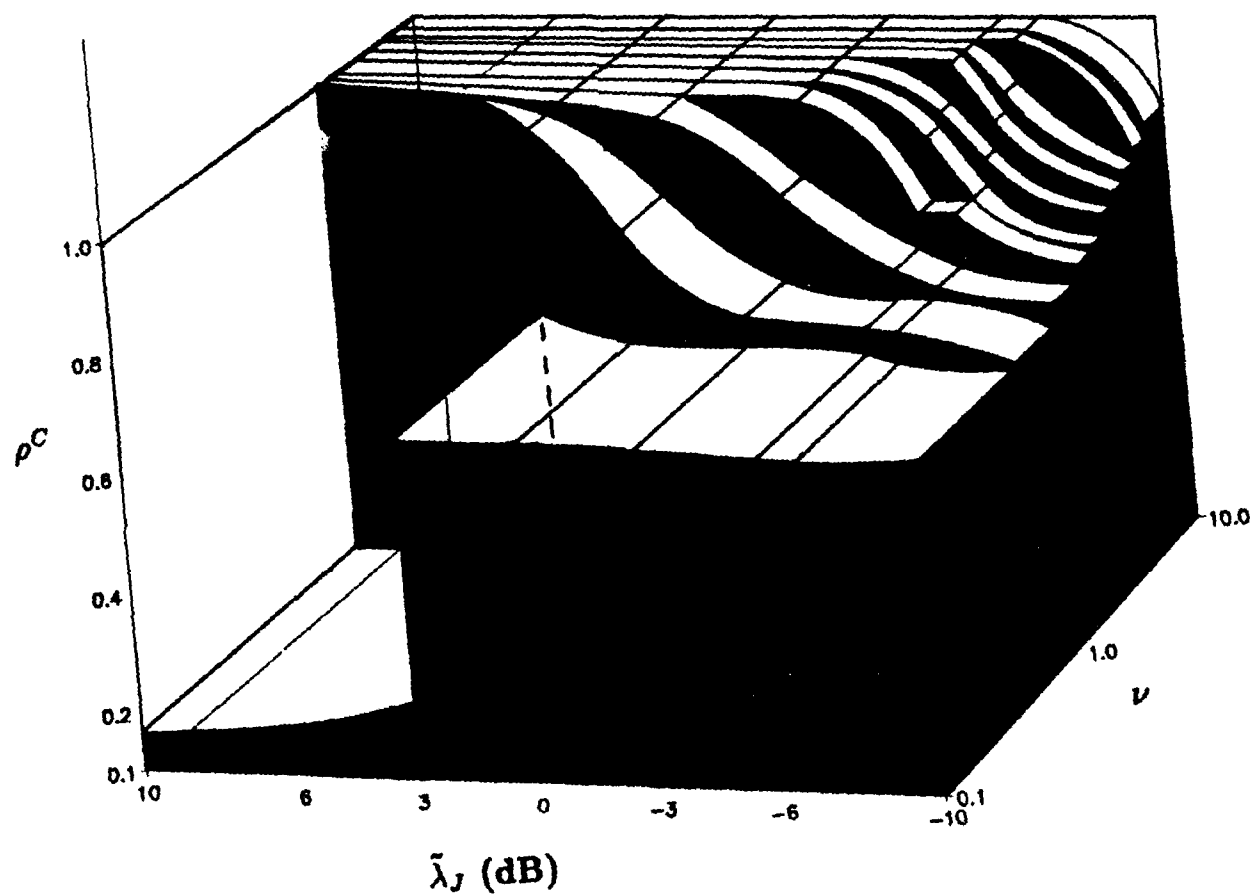
Figure 4.33: Optimal Jamming Fraction (ρ^C) versus Traffic Intensity (ν) versus Bit Energy-to-Jammer Noise Ratio ($\tilde{\lambda}_J$) for $N = 10$ (Constant Jammer Power, Capacity Case, Jammer State Information)
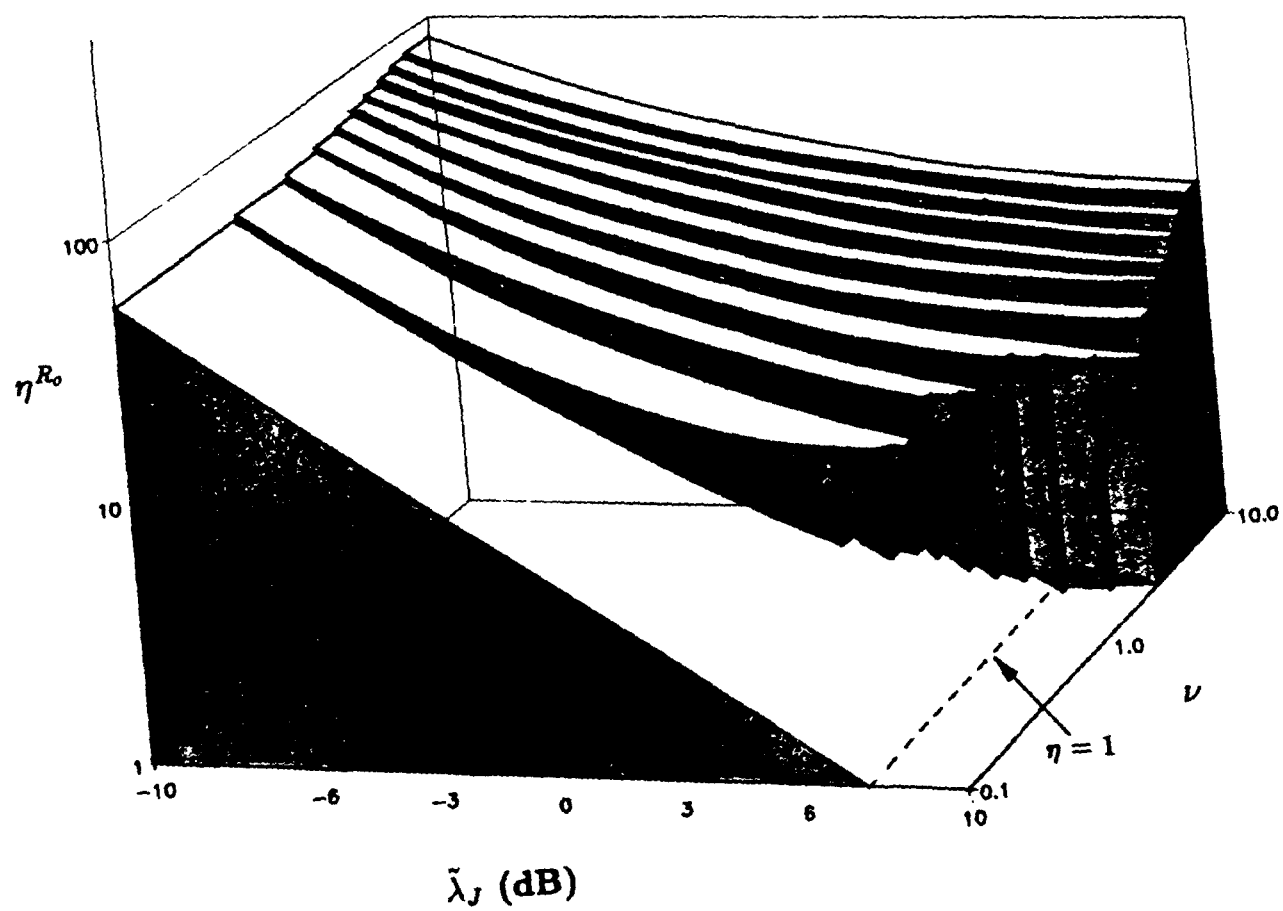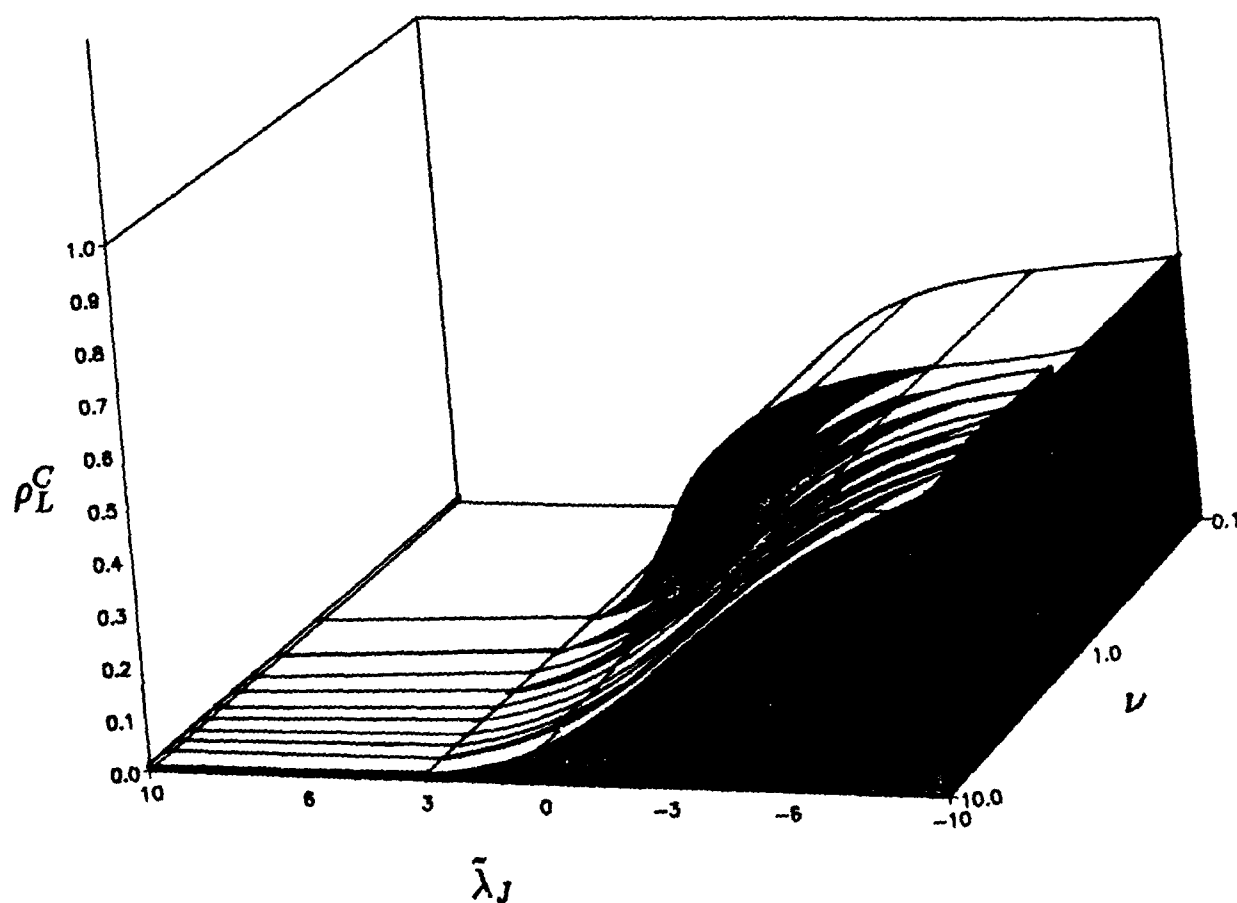
Figure 4.34: Lower Bound on the Range for the Optimal Jamming Fraction ($\rho_{L,U}^C$) versus Traffic Intensity (ν) versus Bit Energy-to-Jammer Noise Ratio ($\tilde{\lambda}_J$) for $N = 10$ (Constant Jammer Power, Capacity Case, Jammer State Information)
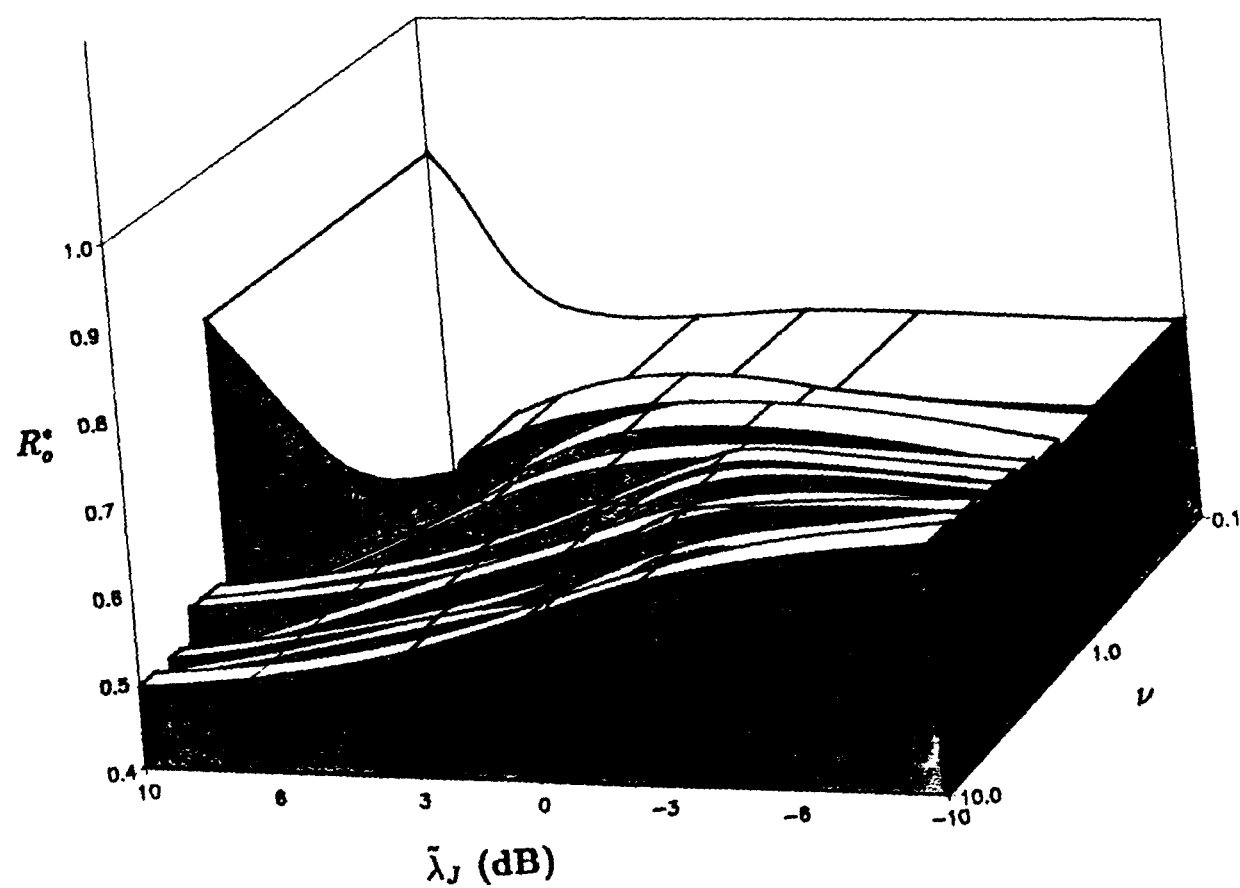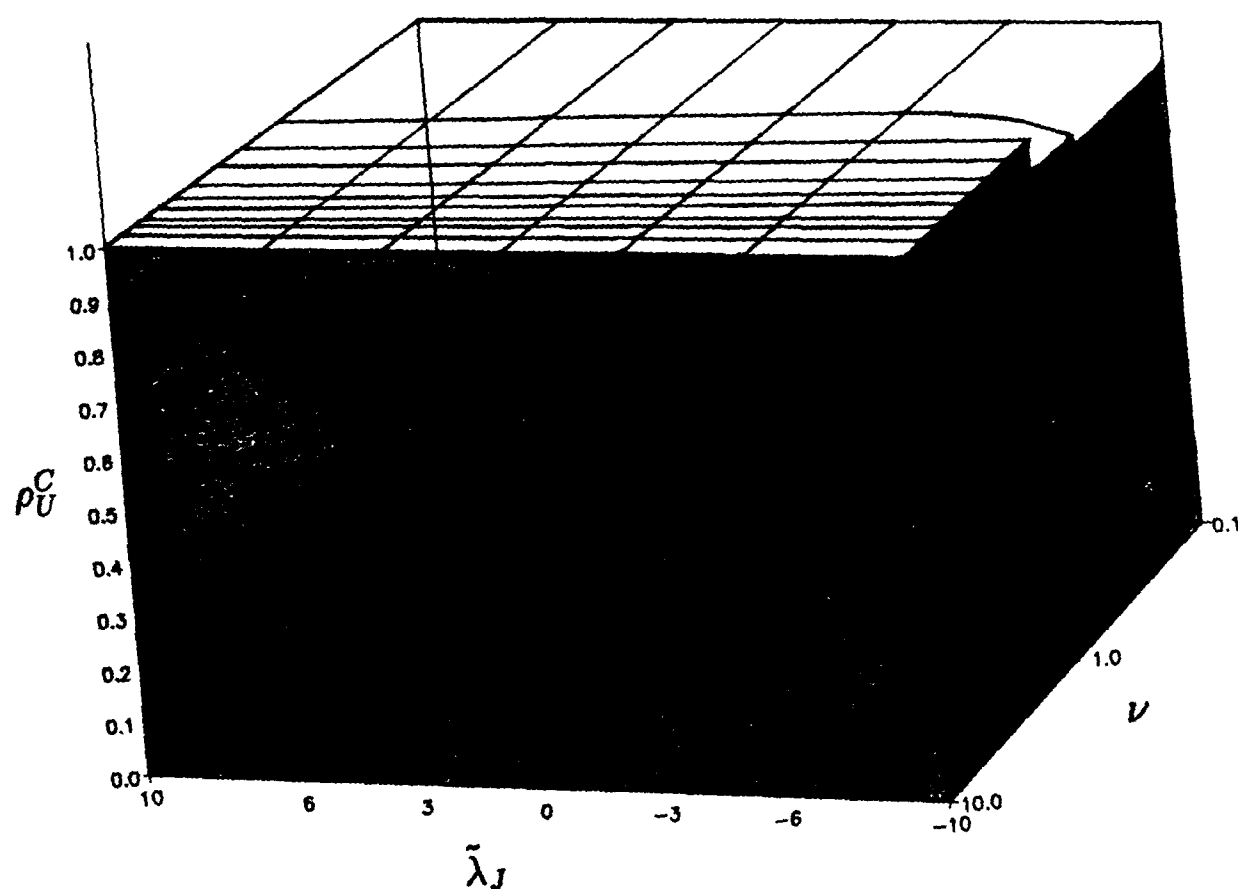
Figure 4.35: Upper Bound on the Range for the Optimal Jamming Fraction ($\rho_{L,U}^C$) versus Traffic Intensity (ν) versus Bit Energy-to-Jammer Noise Ratio ($\tilde{\lambda}_J$) for $N = 10$ (Constant Jammer Power, Capacity Case, Jammer State Information)

CHAPTER 5

Operational Considerations

This chapter discusses general network operation under ideal conditions and practical issues which must be considered when implementing the theoretical results developed in this study.

5.1 General Network Operation

The results presented in Chapters 3 and 4 suggest that the network will operate in one of three modes: plain ARQ, Hybrid ARQ, or CDMA. The mode of operation selected depends primarily upon the traffic intensity ν, the noise level $\lambda_{o,J}$, and, to a lesser degree, upon the population size N and the availability of jammer state information. Ideally, each transmitter and receiver knows the exact network state $[\nu, \lambda_{o,J}, N,$ Jammer State] and the corresponding optimal design parameter values $[p_r^*, \{R_o^*, C^*\}, \eta^{\{R_o,C\}}]$, and the network is homogeneous. As such, the same *optimal* code rate and processing gain are used for transmitting (encoding) and receiving (decoding) a packet, and optimum network performance is achieved.

Under the above ideal operating conditions, two situations are possible: $\tilde{\lambda}_{o,J} > \hat{\lambda}_{o,J}^{\{R_o,C\}}$ or $\tilde{\lambda}_{o,J} < \hat{\lambda}_{o,J}^{\{R_o,C\}}$. If $\tilde{\lambda}_{o,J} > \hat{\lambda}_{o,J}^{\{R_o,C\}}$ and the traffic intensity is low enough to permit stable network operation (eg., $\nu < 0.5$), the network will operate in the plain ARQ mode when $\tilde{\lambda}_{o,J} = \infty$ and in Hybrid ARQ mode when $\tilde{\lambda}_{o,J} < \infty$. In this case, a transmitter will have to decide whether it wants to operate with minimal delay, maximum (maximin) throughput, or some non-optimal throughput-delay combination in between by choosing the appropriate probability of retransmission in Fig. 3.8. For $\tilde{\lambda}_{o,J} > \hat{\lambda}_{o,J}^{\{R_o,C\}}$, the probability of retransmission is adjusted according to variations in the traffic intensity and the population size

(Fig. 3.8), and the code rate is adjusted to changes in the noise level (Fig. 3.15) depending upon the availability of jammer state information (eg., Figs. 4.14,4.15). When the traffic intensity reaches a certain level ($0.5 \leq \nu \leq 1.0$), the network becomes unstable. As the traffic intensity continues to increase, a cutoff intensity is eventually reached where the optimal protocol becomes CDMA. The employment of CDMA stabilizes the network. While in the CDMA mode of operation, the probability of retransmission is adjusted according to variations in the traffic intensity and population size (Fig. 3.8), the processing gain is adjusted according to changes in the traffic intensity, the noise level, and the population size (eg., Figs. 4.8,4.13), and code rate is adjusted to changes in the noise level (eg., Figs. 4.14-4.15). When jamming is present, code rate and processing gain adjustments depend on the availablity of jammer state information.

For the situation where $\tilde{\lambda}_{o,J} < \hat{\lambda}_{o,J}^{\{R_o,C\}}$, CDMA is optimal for all traffic intensities. For this case, optimal design parameter values are selected as they are for the CDMA case described above.

5.2 Practical Operational Issues

Consider a satellite relay network. The up-link portion of this network can be modeled as having a 'centralized' paired-off topology (Fig. 3.1.b.). Each terrestrial transmitter is paired with a particular satellite receiver by means of a seperate code channel (explained latter). The homogeneous network assumption applies in this case because all packets arrive at the satellite receivers with equal power levels (otherwise power control can be used), and all satellite receivers are affected by the same jamming strategy. Thus, the analysis of this study applies to the up-link portion of the network.

At the satellite, an attempt is made to despread and/or decoded all arriving packets. Should the code rate and processing gain be insufficient for the current network conditions (i.e., $M > \hat{m}$), then all packets will be incorrectly decoded and will be subsequently NACKed by the satellite. Otherwise, all packets are relayed to their intended terrestrial receivers.

In general, the analysis of this study does not apply to the down-link portion of the network because the topology is not paired-off. Ordinarily, the possibility exists for multiple packets to be addressed to the same receiver. This violates the paired-off assumption.

However, should the probability for multiple addressees be negligible, then the down-link is paired-off and the analysis applies. In either case, note that when transmitting on the down-link(s), the satellite knows the number of simultaneous packets being relayed so that it can select just enough (optimal) coding and processing gain to overcome the effects of multiple-access interference experienced at the terrestrial receiver. As long as the enemy jammer's strategy is to jam the satellite instead of the terrestrial portion of the network, then the homogeneity assumption applies to the down-link because the satellite broadcasts its composite signal to all terrestrial receivers.

For optimum network performance, it is critical that each transmitter-receiver pair have an accurate and compatible estimate of the network state $[\nu, \lambda_{o,J}, N,$ Jammer State]. An accurate network state estimate is necessary so that *optimal* design parameter values $[p_r, \eta^{\{R_o, C\}}, \{R_o, C\}]$, such as those determined in Chapters 3 and 4, are selected for the existing network conditions. Inaccurate network estimates result in either insufficient packet coding which increases packet retransmissions (delay) or overly coded packets which decreases throughput. A compatible estimate is necessary so that receivers use the correct (transmitted) code rate and processing gain to decode the received packet. In the current example, the satellite and terrestrial receivers do not necessarily experience the same network state (e.g., multiple-access interference, jammer noise). This makes it difficult for terrestrial transmitters to select design parameters values (code rates and processing gain) which are optimal for reception at the satellite. Techniques for network state estimation and dissemination are discussed more fully below.

There are numerous techniques available for estimating the network state. Estimates of λ_o can be obtained by measuring the background noise during quiet (no traffic) periods, or by measuring background noise in an adjacent unused frequency band. These estimates of λ_o can be used for both the narrow-band and CDMA modes of operation. Estimates of λ_J are more difficult to generate. For narrow-band operation, the presence of an enemy jammer is easily detected by the resulting sudden increase in received energy. A measurement of the instantaneous signal-to-noise ratio can be used to make a reasonably accurate estimate of λ_J [56]. For CDMA operation, however, there is no clear way to estimate λ_J in the presence of multiple-access interference. This is a subject for further research.

$\nu <$	2.85	3.5	4.2	4.9	5.8	6.8	7.9	10.0
R_o^*	1.0	0.5	0.5	0.5	0.5	0.5	0.5	0.5
η^{R_o}	1	7	10	12	14	17	19	21

Table 5.1: Optimal Code Rate R_o^* and Processing Gain η^{R_o} Values for $\lambda_{o,J} = \infty$ and $N = 10$

The traffic intensity can be estimated either directly or indirectly. For narrow-band operation, ν can be estimated directly by simply counting the number of successful packet transmissions over a certain number of slots periods. For CDMA operation ν can be estimated directly by monitoring the pseudonoise level (eg., the receiver front end automatic gain control voltage) [90]. Indirect methods for estimating ν during narrow-band operation typically involve an estimate of the number of backlogged users $\hat{n}$ $[\hat{\nu} = p_o(N - \hat{n}) + p_r\hat{n}]$. Estimates of $\hat{n}$ are derived from the statistics of the acknowledgement channel [28,34,45,65]. Another technique for indirectly estimating the traffic intensity is to monitor the number of errors corrected by the forward error correction hardware. The number of errors corrected within a packet gives the probability of symbol error which, with an estimate of the noise level, can be used in equations (3.21) or (4.15) to give an estimate of the number of simultaneous users per slot. This estimation technique can be used for both the narrow-band and CDMA modes of operation. For the present network example, assume that any one or a combination of the above estimation techniques are used to derive an estimate of the network state. Furthermore, assume that estimate inaccuracies fall within the design safety margin of the design parameter tables discussed below. Finally, regardless of the technique used, estimates can be made to adapt over time by windowing the estimate over an appropriate number of time slots.

Optimal values of the network design parameters $[p_r^*, \{R_o^*, C^*\}, \eta^{\{R_o,C\}}]$ versus the network state $[\tilde{\lambda}_{o,J}, \nu, N, \text{Jammer State}]$ are available in a 'table look-up' fashion at each receiver and transmitter. Due to the discrete nature of $\hat{m}$ and the spreading sequences, optimal design parameter values for the code rate and processing gain remain fixed over various ranges of ν for a given $\lambda_{o,J}$ and N. For example, Table 5.1 gives the cutoff rate results for $\tilde{\lambda}_{o,J} = \infty$ and $N = 10$. Note that processing gains have been increased

to the next higher integer value (eg., 5.25 becomes 6) because spread spectrum coding requires an integer number of spreading chips. Processing gains can be further increased to provide greater design safety margins, but at the expense of operating farther from optimal performance. Larger ranges in system parameters can be used for a given set of design parameter values (coarser grain) to save on memory space, again, at the expense of performance. Optimal retransmission probabilities are not shown in Tabel 5.1, but are available at each receiver and transmitter. Recall that p_r^* varys continuously with ν for a given N, and depends on $\tilde{\lambda}_{o,J}$ only through ν^{R_o}.

Because networks are rarely homogeneous throughout, as in the current example, transmitters will not know the network state at the corresponding receiver. Therefore, for the current network example, the following protocol is used to disseminate network state information between transmitter-receiver pairs. Initially, the transmitter uses an estimate of its own network state as an estimate of the receiver's network state. Design parameters are selected and the packet is encoded accordingly. The transmitted packet's header contains the transmitter's network state and the design parameter values which were used to encode the data portion of the packet. At the receiver, the packet header is decoded and the packet decoding instructions and the transmitter network state information are recovered. The receiver uses the decoding instructions to decode the data portion of the packet and inverts the transmitter's network state information to obtain optimal encoding parameter values for encoding the next data packet to that transmitter. Note that additional coding may be used to further ensure successful reception of the data packet, but at the expense of less than optimal performance. Recall that very large processing gains are used instead of optimal code rate-processing gain combinations for encoding acknowledgement packets. Acknowledgement packet headers will, however, contain receiver network state information and decoding instructions. When the initial transmitter decodes this acknowledgement, it recovers the current estimate of the receiver's network state and uses this estimate to encode the next data packet transmission to that receiver. All subsequent packet transmissions between the transmitter and receiver contain updated network state information which is used to maintain optimum network performance as the network conditions vary. For this discussion, assume that the network state does not vary within the slot period, and does

not vary drastically from slot to slot.

For the slotted operation considered in this analysis, assume that the duration of a packet equals one time slot. Each packet is composed of a packet header followed by the data. The packet header is encoded with the spreading sequence (address) of the intended receiver and is used by the receiver for packet sychronization. Note that the packet header is encoded with the spreading sequence regardless of which mode of network operation. The packet header also contains packet decoding instructions which are the design parameter values used by the transmitter to encode the packet, the transmitter's network state, and the packet's destination.

Each packet is comprised of a single codeword. Error correction/detection is achieved by using a low rate ($r = 0.5$), high constraint length (e.g., 32) punctured convolutional code. Code puncturing provides for a variable rate code which uses the same basic encoder/decoder structure for all possible code rates. A punctured code is a high rate code ($r = (v - 1)/v$) obtained by periodically deleting certain symbols from the output stream of a low rate ($r = 1/v$) encoder. Depending on the original low rate code and the number and positions of the punctured symbols, code rates within the range $1/v \leq r \leq (v - 1)/v$ can be obtained. Punctured codes have been shown to perform nearly as well (i.e., within 0.1 to 0.2 dB) as the best known convolutional codes for the given rate [26,27,32]. Fano sequential decoding is used with a time-out algorithm [52]. With the time-out algorithm, retransmissions are requested when the decoding time exceeds the decoder time limit. The decoder time limit is yet another design parameter over which performance can be optimized. Packet lengths on the order of 1000 bits are used so that the decoding tail (eg., 32 bits) is negligible.

Gold code sequences are used for spreading (address) sequences. They have been shown to exhibit good autocorrelation (peak value of $\eta = 2^l - 1$) and crosscorrelation (bounded maximum peak value of $1 + 2^{(l+2)/2}$) properties and sufficiently large family size ($\eta + 2$). Here, l is the shift register(s) length used to generate the sequence [19,80]. Sequence lengths on the order of several thousand chips (eg., $l = 15$) are used to provide ample processing gain and code family size. Longer code lengths are avoided so that crosscorrelation bounds are not unnecessarily large. When in the CDMA mode of operation, transmitters encode the

entire packet with the spreading code of the intended receiver (receiver-directed). Variable amounts of processing gain are obtained by using sufficiently long segments of the basic spreading code. Again, packet headers are always encoded with a portion of the appropriate spreading sequence to aid in packet synchronization.

As a final note on performance comparison, assume that there is a certain amount of available transmission bandwidth, and that the network transmission rate remains fixed using this entire bandwidth regardless of which mode of operation, narrow-band or CDMA. When operating in the narrow-band mode, the data (information) rate depends only on the code rate r, excluding the overhead due to the packet header, the decoding tail of the convolutional code, etc., $(T_B = \frac{1}{r}T_S = \frac{1}{r}T_C)$. When no coding is used ($r = 1.0$), the duration of a data bit, a code symbol, and a spreading chip are equal ($T_B = T_S = T_C$). In this case, the data rate equals the network transmission rate. When operating in the CDMA mode, the data rate is reduced by a factor of r/η to account for the coding and the processing gain being used ($T_B = \frac{1}{r}T_S = \frac{\eta}{r}T_C$). Alternately, a comparison of the amount of bandwidth required to support a certain fixed data rate could be made. In this case, CDMA would require approximately η/r more bandwidth than uncoded narrow-band ALOHA. Although CDMA uses more bandwidth (or a slower data rate) than narrow-band ALOHA, recall that CDMA is still more efficient in terms of network utilization than narrow-band ALOHA for the existing network conditions (.e.g, $\nu > \nu^{\{R_o,C\}}$). In fact, when the network is stressed (e.g., $\tilde{\lambda}_{o,J} < \hat{\lambda}_{o,J}^{\{R_o,C\}}$), CDMA may be required in order to obtain any reasonable throughput.

CHAPTER 6

Conclusions

The objective of this research was to examine and optimize the performance of a slotted direct-sequence random access CDMA network. Performance was evaluated in terms of link-level throughput-delay for networks stressed by multiple-access interference, background noise, and jammer noise. Performance was optimized over network design parameters such as the retransmission probability, code rate, and processing gain in the presence of a worst case enemy pulse jammer. Performance results were obtained for the network operating with complete and partial side information. These results are summarized below.

6.1 Summary of Results

6.1.1 Performance Results for Background Noise with Complete Side Information

The following results help to characterize the general behavior of CDMA networks, and provide useful guidelines for their design.

- A key result of this study is that, at high traffic intensities, it is more efficient in terms of network utilization to use CDMA in conjunction with Type I Hybrid ARQ than to use Type I Hybrid ARQ alone. For slotted narrow-band ALOHA systems, throughput falls off dramatically as the traffic intensity increases beyond unity. Delay becomes very large. However, when CDMA is used, throughput initially decreases to some minimal value, at a particular traffic intensity, and then increases again. The corresponding delay decreases. The traffic intensity at which CDMA achieves

this improved performance over the Hybrid ARQ was defined as the *cutoff traffic intensity*. The cutoff traffic intensity designates when CDMA should or should not be used. When operating at traffic intensities above the cutoff traffic intensity, it is more efficient to use CDMA, while below it Hybrid ARQ should be used.

- Lower performance limits based on the bit energy-to-background noise ratio were determined. These were defined as the *asymptotic noise limits*. They represent the smallest level of background noise that can be present for reliable coded communications in the absence of multiple-access interference. Network operation is not possible below these limits.

- The retransmission probability plays a critical role in the throughput-delay-stability tradeoff. Numerical results showed that the optimal retransmission probability depends primarily on the traffic intensity, to a lesser degree on the population size, and only indirectly on the level of background noise. For low traffic intensities (i.e., less that unity), there are two possible values for p_r^*. One value corresponds to operating with maximal throughput and nonminimal delay, and the other value corresponds to operating with minimal delay and nonmaximal throughput. Values of retransmission probability between these these two optimal values may be used to trade off throughput for delay, or vice-versa. For the higher traffic intensities, CDMA is used and, in general, $p_r^* = p_o = \nu/N$. Here again, the choice can sometimes be made between maximal or nonmaximal throughput by choosing $p_{r,BN}$ or $p_{r,NBN}$. Also, some other nonoptimal p_r within the range of the optimal p_r values can be selected in order to trade off throughput for delay.

- The optimal processing gain and code rate depend strongly on the traffic intensity and the level of background noise, respectively. There is a stepwise linear dependency between optimal processing gain and traffic intensity. Population size has little effect on the optimal processing gain and has no effect on the optimal code rate. For traffic intensities less than the cutoff traffic intensity, the optimal processing gain is unity and the optimal code rate varies between unity and approximately one-half. Hybrid ARQ is the optimal protocol in this case. For traffic intensities greater than the cutoff

traffic intensity, the optimal processing gain is greater the unity and the optimal code rate is constant at approximately one-half. CDMA is the optimal protocol in this case.

- In general, optimal design parameter values are insensitive to the population size.

- CDMA has a stabilizing effect at high traffic intensities.

6.1.2 Performance Results for Jammer Noise with Partial and Complete Side Information

- Constant Bit Energy-to-Jammer Noise Ratio (λ_J):

  - Comments made concerning the background noise analysis apply here for the case of constant λ_J. At high traffic intensities, it is more efficient to use CDMA that to use hybrid ARQ. Notions of a cutoff traffic intensity and an asymptotic jammer noise limit also exist.

  - For a given traffic intensity and population size, pulse jamming has a more severe effect on network performance than background noise. As such, pulse jamming tends to increase the required optimal processing gain and decrease the required optimal code rate. The absence of jammer state information accentuates these effects.

  - Optimal values of the jamming fraction depend primarily on the jammer noise level, the traffic intensity, and the availability of jammer state information. They do not depend on population size. At traffic intensities above cutoff, there exists a range of jamming fractions about the optimal jamming fraction which when used by the enemy jammer result in the same throughput-delay performance.

- Constant Jammer Power ($\tilde{\lambda}_J$):

  - With constant power jamming, two situations arise. If $\tilde{\lambda}_J < \hat{\lambda}_J^{\{R_o, C\}}$, then a cutoff intensity does not exist and the throughput increases gradually with the traffic intensity. In this case, both coding ($r < 1.0$) and processing gain ($\eta >$

1.0) are necessary to achieve a optimum performance. If $\tilde{\lambda}_J > \hat{\lambda}_J^{\{R_o,C\}}$, then a cutoff intensity exists and the throughput-traffic intensity characteristic takes on a form similar to that obtained in the constant λ_J analysis. For $\tilde{\lambda}_J > \hat{\lambda}_J$ and $\nu < \nu^{\{R_o,C\}}$, coding alone is sufficient to overcome the effects of jamming $(\eta = 1)$.

- For a given $\tilde{\lambda}_J$, the maximum allowable number of packets transmissions in a time slot $\hat{m}$ remains constant over a certain range of ν. This 'staircase' dependency of $\hat{m}$ on ν and $\tilde{\lambda}_J$ inherently summarizes the dependency of the optimal processing gain, code rate and jamming fraction on ν and $\tilde{\lambda}_J$. For each $\{\tilde{\lambda}_J, \hat{m}\}$, there is a corresponding $\eta^{\{R_o,C\}}$, $\{R_o^*, C^*\}$, and $\rho^{\{R_o,C\}}$ which also remain constant over that range of traffic intensity. For a given $\hat{m}$, the corresponding $\eta^{\{R_o,C\}}$, $\{R_o^*, C^*\}$, and $\rho^{\{R_o,C\}}$ do not depend on the population size.

- In general, the use of CDMA tends to force the enemy jammer to choose a jamming fraction of one.

CHAPTER 7

Suggestions for Future Research

Many research questions have arisen during the course of this research which are worthy of further study.

- Adaptive Hybrid ARQ protocol. Examine the performance of an adaptive hybrid ARQ protocol. With adaptive hybrid ARQ, packets are transmitted by using a code that has a relatively high initial rate r_i. This ensures that the throughput is not unnecessarily supressed due to excessive coding redundancy. If the initial code rate exceeds the cutoff rate (capacity) of the channel during a particular slot interval, then the packet will be eroneously decoded and a retransmission will be requested. If the retransmitted packet, coded with rate r_i, also exceeds the cutoff rate (capacity), then the two codewords are combined to form a code with rate $r_i/2$. This lower rate code may have a rate that does not exceed the composite channel cutoff rate (capacity), hence allowing correct decoding. If not, more retransmissions are required. Multiple packet retransmissions are combined to obtain a sufficiently lower rate code $r_i/(w+1)$, where w is the number of retransmissions. For the adaptive hybrid ARQ case, the availability of packet side information provides the receiver with knowledge of the number of packets transmitted in each slot or, equivalently, the level of multiple-access interference associated with each packet (codeword) reception. This information can then be used as a measure of the packet reliability (codeword) so that codewords can be appropriately weighted during the decoding process.

- Channel state estimation. Develop techniques for estimating the bit energy-to-jammer noise ratio and jammer state in the presence of multiple-access interference.

- <u>Channel state dissemination</u>. Determine more efficient and reliable algorithms for disseminating channel state information. The stability of these algorithms is critical for proper network operation.

- <u>Alternate network topologies</u>. The star topology, for example, represents an alternative topology which could be investigated within the framwork of this study. The effects of capture significantly effect network performance in this case. Additionally, the effects of the effects of pathloss, shadowing, multipath fading, as well as multiple-access interference, background noise, and jammer noise, could be studied.

- <u>Alternate acknowledgement schemes</u>. The current analysis assumes that acknowledgements are cost free and completely reliable. For network operation in the presence of jamming, an entire time slot is used for each (N)ACK. This permits the (N)ACK packet power level to be adjusted low enough so that its multiple-access interference has a negligible effect on the data packets. Techniques for determining when, and by how much, (N)ACK packet power levels can be reduced are necessary to implement such a scheme. Also, the effect of transmitting (N)ACK packets at power levels equal to the data packets could be investigated. Additionally, the analysis could be generalized and performance potentially improved by the use of alternate acknowledgement schemes (eg., minislots).

- <u>Pure ALOHA</u>. The performance analysis of asynchronous ALOHA would generalize the results obtained so far for slotted channel operation.

- <u>Soft Decision Decoding</u>. With jammer state information, soft decision decoding yields better performance than the hard decision decoding assumed in this study.

APPENDIX A

Appendix

In this appendix, the state transition probabilities p_{ij} are derived for the Markov model discussed in Chapter 3. Recall that we view the network as a discrete-time system where $n(t)$ represents the number of backlogged users n during a particular slot interval. For a population size of N, the network may be in any one of $N + 1$ possible states. The state transition probability p_{ij} is defined as the probability of moving from a state having i backlogged users in a given time slot to a state having j backlogged users in the next time slot or

$$p_{ij} = \text{Prob}\{n(t+1) = j \mid n(t) = i\}. \tag{A.1}$$

In one step, $n(t)$ may decrease by an amount up to $\hat{m}$, remain the same, or increase in size up to N.

Case I : A decrease in backlog.

An $l = i - j$ decrease in $n(t)$ occurs when l retransmissions are successful. In the present system, this can occur only when l retransmissions occur together with up to $\hat{m} - l$ new transmissions. Any combination of new transmissions greater than $(\hat{m} - l)$ plus l retransmissions would be blocked by the network. Any combinations involving fewer or greater than l retransmissions would represent a different state transition probability. Thus,

$$
\begin{aligned}
p_{i,i-l} &= \text{Prob[up to } (\hat{m} - l) \text{ NTX]} \cdot \text{Prob[}l \text{ RTX]} \\
&= \sum_{k=0}^{\min(\hat{m}-l,N-i)} b(k, N - i, p_o) b(l, i, p_r), \tag{A.2}
\end{aligned}
$$

where the terms in the summation represent the binomial distribution function such that

$$b(\alpha, n, p) = \binom{n}{\alpha} p^{\alpha}(1 - p)^{n-\alpha}, \tag{A.3}$$

and NTX and RTX are abbreviations for new packet transmissions and packet retransmissions, respectively. Note that $\hat{m}$ limits the size in which decreases in the number of backlogged users can be made. That is

$$p_{i,i-l} = 0, \qquad \text{for } l > \hat{m} \tag{A.4}$$

Case II : Backlog remains constant.

Remaining at the same number of backlogged users can occur in three ways. Transmissions may involve neither NTXs nor RTXs, only NTX, or only RTXs. Note that transmissions involving both NTXs and RTXs necessarily increase or decrease $n(t)$.

A. A transmission involving neither NTXs nor RTXs occurs with probability

$$
\begin{aligned}
p_{ii} &= \text{Prob[no NTX]} \cdot \text{Prob[no RTX]} \\
&= b(0, N - i, p_o) b(0, i, p_r).
\end{aligned} \tag{A.5}
$$

B. A transmission involving only NTXs can maintain the same number of backlogged users only if the number of NTXs are less than or equal to $\hat{m}$. This occurs with probability

$$
\begin{aligned}
p_{ii} &= \text{Prob[no RTX]} \cdot \text{Prob[up to } \hat{m} \text{ NTX]} \\
&= (1 - p_r)^i \sum_{k=0}^{\min(N-i,\hat{m})} b(k, N - i, p_o).
\end{aligned} \tag{A.6}
$$

C. A transmission involving only RTXs can maintain a constant backlog size if more than $\hat{m}$ RTXs are attempted. This occurs with probability

$$
\begin{aligned}
p_{ii} &= \text{Prob[no NTX]} \cdot \text{Prob[more than } \hat{m} \text{ RTX]} \\
&= b(0, N - i, p_o) \sum_{k=\hat{m}+1}^{i} b(k, i, p - r).
\end{aligned} \tag{A.7}
$$

Using (A.5), (A.6), and (A.7) and accounting for the relative sizes of the current number of backlogged users i, $\hat{m}$, and N, p_{ii} can be expressed as

$$p_{ii} = \begin{cases} \sum_{k=0}^{\min(N-i,\hat{m})} b(k, N-i, p_o) b(0, i, p_r), & i \leq \hat{m} \\ \\ \sum_{k=0}^{\min(N-i,\hat{m})} b(k, N-i, p_o) b(0, i, p_r) \\ \quad + \sum_{k=\hat{m}+1}^{i} b(k, i, p_r) b(0, N-i, p_o), & \hat{m} < i < N \\ \\ \sum_{k=\hat{m}+1}^{N} b(k, N, p_r) + b(0, N, p_r), & i = N \end{cases} \qquad (A.8)$$

<u>Case III</u> : An increase in backlog.

An l increase in the number of backlogged users occurs when l NTXs occur together with more than $(\hat{m} - l)$ RTXs. This occurs with probability

$$\begin{aligned} p_{ii} &= \text{Prob}[l \text{ NTX}] \cdot \text{Prob}[\text{more than } (\hat{m} - l) \text{ RTX}] \\ &= b(l, N-i, p_o)[1 - \sum_{k=0}^{\hat{m}-l} b(k, i, p_r)]. \end{aligned} \qquad (A.9)$$

Note that as opposed to the decrease in backlog case, a one-step increase in backlog is limited by the quantity $N - i$. Note also that increases in backlog are impossible for combinations of NTXs and RTXs totaling less than or equal to $\hat{m}$.

Combining (A.2), (A.8), and (A.9), the state transition probabilities p_{ij} become:

$$
p_{ij} = \begin{cases}
& \text{(for } j < i\text{)} \\[4pt]
0, & i - j > \hat{m} \\[4pt]
\sum_{k=0}^{\min(\hat{m}-i+j,N-i)} b(k, N-i, p_o) b(i-j, i, p_r), & i - j \le \hat{m} \\[10pt]
& \text{(for } j = i\text{)} \\[4pt]
\sum_{k=0}^{\min(N-i,\hat{m})} b(k, N-i, p_o) b(0, i, p_r), & i \le \hat{m} \\[4pt]
\sum_{k=0}^{\min(N-i,\hat{m})} b(k, N-i, p_o) b(0, i, p_r) & \\
\quad + \sum_{k=\hat{m}+1}^{i} b(k, i, p_r) b(0, N-i, p_o), & \hat{m} < i < N \\[6pt]
\sum_{k=\hat{m}+1}^{N} b(k, N, p_r) + b(0, N, p_r), & i = N \\[10pt]
& \text{(for } j > i\text{)} \\[4pt]
0, & j \le \hat{m}, j - i \le \hat{m} \\[4pt]
b(j-i, N-i, p_o)[1 - \sum_{k=0}^{\hat{m}-j+i} b(k, i, p_r)], & \hat{m} < j \le N, j - i \le \hat{m} \\[4pt]
b(j-i, N-i, p_o), & \hat{m} < j \le N, j - i > \hat{m}
\end{cases} \tag{A.10}
$$

Note that for $\hat{m} = 1$, (A.10) reduces to the state transition probabilities for the conventional narrow-band slotted ALOHA [39], and that (A.10) is a special case of the state transition probabilities derived in [75] for random access CDMA networks.

Bibliography

[1] A. H. Abdelmonem and T. N. Saadawi. Effect of Non-Perfect Codes on the Throughput-Delay Performance of Spread Spectrum Packet Network. *in Proc Int. Conf. Commun.*, 177–183, 1988.

[2] N. Abramson. The ALOHA System - Another Alternative for Computer Communications. *in AFIPS Conf. Proc. 1970 Fall Joint Computer Conference*, 37:281–285, 1970.

[3] J. C. Arnbak and et. al. Capacity of Slotted ALOHA in Rayleigh Fading Channels. *IEEE Journal on Selected Areas in Communications*, 5(2):261–269, Feb. 1987.

[4] G. Benelli. An ARQ Scheme with Memory and Soft Error Detectors. *IEEE Transactions on Communications*, 33(3):285–288, Mar. 1985.

[5] R. J. Benice and A. H. Frey. An Analysis of Retransmission Systems. *IE. '? Transactions of Communications Technology*, 12:135–145, Dec. 1964.

[6] R. J. Benice and A. H. Frey. Comparisons of Error Control Techniques. *IEEE Transactions of Communications Technology*, 12:146–154, Dec. 1964.

[7] K. Brayer. Error Control Techniques Using Binary Symbol Burst Codes. *IEEE Transactions on Communications*, 16:199–214, Apr. 1968.

[8] J. I. Capetanakis. Tree Algorithms for Packet Broadcasting Channels. *IEEE Transactions on Information Theory*, 25:505–515, Sept. 1979.

[9] A. B. Carleial and M. E. Hellman. Bistable Behavior of ALOHA Type Systems. *IEEE Transactions on Communications*, 23(4):401–409, Apr. 1975.

[10] D. Chase. Application of Code Combining to a Selective-Repeat ARQ Link. *MILCOM Conference Record*, 1:247–252, August 1985.

[11] D. Chase and et. al. Code Combining - A Maximum Likelihood Decoding Approach for Combining an Arbitrary Number of Noisy Packets. *IEEE Transactions on Communications*, COM-33(5):385–393, May 1985.

[12] G. C. Clark and J. B. Cain. *Coding for Error Control*. Plenum Press, New Jersey, 1981.

[13] A. Cohen and et. al. A New Coding Technique for Asynchronous Multiple Access Communications. *IEEE Transactions on Communications*, 19(5):849–855, Oct. 1971.

[14] R. A. Comroe and D. J. Costello. ARQ Schemes for Data Transmission in Mobile Radio Systems. *IEEE Transactions on Vehicular Technology*, VT-33(3):88–97, August 1984.

[15] D. H. Davis and S. A. Gronemeyer. Performance of Slotted ALOHA Random Access with Delay Capture and Randomized Time of Arrival. *IEEE Transactions on Communications*, COM-28(5):703–710, May 1980.

[16] J. C. Dill and J. A. Silvester. A Dedicated Channel Acknowledgement Protocol for Multihop CDMA Packet Radio Networks. *in Proc. MILCOM'88*, 36.7.1–5, 1988.

[17] A. Drukarev and D. J. Costello, Jr. A Comparison of Block and Convolutional Codes in ARQ Error Control Schemes. *IEEE Transactions on Information Theory*, 30:2449–2455, Nov. 1982.

[18] A. Drukarev and D. J. Costello, Jr. Hybrid ARQ Error Control Using Sequential Decoding. *IEEE Transactions on Information Theory*, 29:521–535, July 1983.

[19] S. El-Khamy and A. Balameshi. Selection of Gold and Kasami Code Sets for Spread Sprectrum CDMA Systems of Limited Number of Users. *Int. J. Satellite Commun.*, 5:23–32, Jan-Mar 1987.

[20] M. Y. Elsanadidi and W. W. Chu. Study of Acknowledgement Schemes in a Star Multiaccess Network. *IEEE Transactions on Communications*, 30(7):1657–1667, July 1982.

[21] M. J. Ferguson. On the Control, Stability, and Waiting Time in a Slotted ALOHA Random-Access System. *IEEE Transactions on Communications*, Nov. 1975.

[22] C. Fujiwara and et. al. Evaluation of Error Control Techniques in Both Independent Error and Dependent Error Channels. *IEEE Transactions on Communications*, 26:785–793, June 1978.

[23] R. G. Gallager. Conflict Resolution in Random Access Broadcasts Networks. *Proc. AFOSR Workshop Commun. Theory Appl., Provincetown, MA*, 74–76, Sept. 1978.

[24] E.A. Geraniotis. Performance of Noncoherent Direct Sequence Spread-Spectrum Multiple-Access Communications. *IEEE Journal on Selected Areas in Communications*, 3:687–694, Sep. 1985.

[25] E.A. Geraniotis and M.B. Pursley. Error Probabilities for Direct-Sequence Spread-Spectrum Multiple-Access Communications – Part II. *IEEE Transactions on Communications*, 30:985–995, May 1982.

[26] J. Hagenauer. Hybrid ARQ/FEC Protocols on Fading Channels Using Rate Compatible Punctured Convolutional Codes. *in Proc Int. Conf. Commun.*, 21.4.1–21.4.5, 1987.

[27] J. Hagenauer. Rate Compatible Punctured Convolutional Codes. *in Proc Int. Conf. Commun.*, 29.1.1–29.1.5, 1987.

[28] B. Hajek and T. Van Loon. Decentralized Dynamic Control of a Multiaccess Broadcast Channel. *IEEE Transactions on Automatic Control*, 27:559–569, 1982.

[29] J. M. Hanratty and G. L. Stuber. Asymptotic Performance Anaysis of Hybrid ARQ Protocols in Slotted Direct-Sequence Code Division Multiple-Access Networks. *in Proc. INFOCOM'89*, II:574–583, Apr. 1989.

[30] J. M. Hanratty and G. L. Stuber. Performance Analysis of Hybrid ARQ Protocols in Slotted Direct-Sequence Code Division Multiple-Access Networks: Jamming Analysis. *to appear in MILCOM'89, also submitted to IEEE Selected Areas in Communications*, 1989.

[31] J. Hui. Throughput Analysis for Code Division Multiple Accessing of the Spread Spectrum Channel. *IEEE Journal on Selected Areas in Communications*, 2(4):482–486, July 1984.

[32] G. C. Clark, and J. M. Geist J. B. Cain. Punctured Convolutional Codes of Rate $(n-1)/n$ and Simplified Maximum Likelihood Decoding. *IEEE Transactions on Information Theory*, IT-25(1):97–100, Jan. 1979.

[33] F. Jelinek. A Fast Sequential Decoding Algorithm Using a Stack. *IBM Journal. Res. Dev.*, 13:675–685, Nov. 1969.

[34] Y. C. Jenq. Optimal Retransmission Control of Slotted ALOHA Systems. *IEEE Transactions on Communications*, 29(6):891–895, June 1981.

[35] M. Kaplan. A Sufficient Condition for Nonergodicity of a Markov Chain. *IEEE Transactions on Information Theory*, IT-25(4):470–471, July 1979.

[36] T. Kasami and et. al. Error Detection with Linear Block Codes. *IEEE Transactions on Information Theory*, 29(1):131–136, Jan. 1983.

[37] L. Kleinrock and Y. Yemini. An Optimal Adaptive Scheme for Multiple Access Broadcast Communications. *in Proc Int. Conf. Commun.*, 7.2.1–7.2.5, 1978.

[38] L. Klienrock. *Queueing Systems*. John Wiley & Sons, Inc., New York, 1975.

[39] L. Klienrock and S. S. Lam. Packet Switching in a Multiaccess Broadcast Channel: Performance Evaluation. *IEEE Transactions on Communications*, COM-23(4):410–421, Apr. 1975.

[40] V. I. Korzhik. Bounds on the Undetected Error Probability and Optimum Group Codes in a Channel with Feedback. *Telecommun. and Radio Eng.*, 2:87–92, Jan. 1965.

[41] H. Krishna and S. Morgera. A Computational Complexity Approach to the Design of Linear Codes. *IEEE Transactions on Communications*, submitted for publication 1987.

[42] H. Krishna and S. Morgera. A New Error Control Scheme for Hybrid ARQ Systems. *IEEE Transactions on Communications*, 35(10):981–989, Oct. 1987.

[43] F. Kuperus and J. C. Arnbak. Packet Radio in a Rayleigh Channel. *Electron. Lett.*, 18:506–507, June 1982.

[44] S. S. Lam. *Packet Switching in a Multi-access Broadcast Channel with Application to Satellite Communication in a Computer Network*. PhD thesis, Dep. Comput. Sci., Univ. Calif., Los Angeles, 1974.

[45] S. S. Lam and L. Klienrock. Packet Switching in a Multiaccess Broadcast Channel: dynamic Control Procedures. *IEEE Transactions on Communications*, COM-23(9):891–905, September 1975.

[46] C. Lau and C. Leung. Performance Analysis of a Memeory ARQ Scheme with Soft Decision Detectors. *IEEE Transactions on Communications*, 34(8):827–832, Aug. 1986.

[47] C. C. Lee. Random Signal Levels for Channel Access in Packet Broadcast Networks. *IEEE Journal on Selected Areas in Communications*, 5(6):1026–1034, July 1987.

[48] S. S. Lee and J. A. Silvester. The Effect of Acknowledgements on the Performance of Distributed Spread Spectrum Packet Radio Networks. *in Proc Int. Conf. Commun.*, 1986.

[49] J.S. Lehnert and M.B. Pursley. Error Probabilities for Binary Direct-Sequence Spread-Spectrum Communications with Random Signature Sequences. *IEEE Transactions on Communications*, 35:87–98, Jan. 1987.

[50] C. S. K. Leung and A. Lam. Forward Error Correction for an ARQ Scheme. *IEEE Transactions on Communications*, 29(10):1514–1519, Oct. 1981.

[51] V. I. Levenshtein. Bounds on the Probability of Undetected Error. *Problem of Information Transmission*, 13(1):1–12, 1978.

[52] S. Lin and D. J. Costello, Jr. *Error Control Coding: Fundamentals and Applications*. Prentice-Hall, New Jersey, 1983.

[53] S. Lin and P. S. Yu. A Hybrid ARQ Scheme with Parity Retransmission for Error Control of Satellite Channels. *IEEE Transactions on Communications*, 30(7):1701–1719, July 1982.

[54] S. Lin and P. S. Yu. SPEC - An Effective Hybrid-ARQ Scheme. *IBM Res. Rep. 7591 (32852)*, Apr. 1979.

[55] L. R. Lugand and D. J. Costello, Jr. A Comparison of Three Hybrid ARQ Schemes Using Convolutional Codes on a Nonstationary Channel. *in GLOBECOM'82 Conf. Rec.*, C8.4, Dec. 1982.

[56] J. K. Omura, R. A. Scholtz, and B. K. Levitt M. K. Simon. *Spread Spectrum Communications*. Computer Science Press, 1985.

[57] F. J. MacWillaims and N. J. A. Sloane. *Theory of Error-Correcting Codes*. North Holland, Amsterdam, 1977.

[58] D. M. Mandelbaum. Adaptive-Feedback Coding Scheme Using Incremental Redundancy. *IEEE Int. Symp. Inform. Theory, Ithaca, NY*, 10–14, Oct. 1977.

[59] J. Massey. Coding Techniques for Digital Data Networks. *in Proc. Int. Conf. Inform. Theory and Syst.*, 1978.

[60] J.L. Massey. Coding and Modulation in Digital Communications. *Proc. Int. Zurich Sem. Digital Commun.*, E2(1)–E2(4), 1974.

[61] R. J. McEliece and W. E. Stark. Channels with Block Interference. *IEEE Transactions on Information Theory*, IT-30(4):44–53, Jan. 1984.

[62] J. J. Metzner. Improvements in Block-Retransmission Schemes. *IEEE Transactions on Communications*, 27(2):525–532, Feb. 1979.

[63] J. J. Metzner. On Improving Utilization in ALOHA Networks. *IEEE Transactions on Communications*, 24(4):447–448, Apr. 1976.

[64] J. J. Metzner. A Study of an Efficient Retransmission Strategy for Data Links. *in NTC'77 Conf. Rec.*, 3B:1.1-5, 1977.

[65] V. A. Mikhailov. A Random Acess Algorithm for a Broadcast Channel. *in 5th Int. Symp. Inform. Theory, Moscow*, 3:83-86, 1979.

[66] M. J. Miller and S. Lin. The Analysis of Some Selective-Repeat ARQ Schemes with Finite Receiver Buffer. *IEEE Transactions on Communications*, 29:1307-1315, Sept. 1981.

[67] J. M. Morris. Optimal Blocklengths for ARQ Error Control Schemes. *IEEE Transactions on Communications*, 27:488-493, Feb. 1979.

[68] J. M. Musser and J. N. Daigle. Throughput Analysis of an Asynchronous Code Division Multiple Access (CDMA) System. *in Proc Int. Conf. Commun.*, 1:2F.2.1-7, June 1982.

[69] C. Namislo. Analysis of Mobile Radio in Slotted ALOHA Network. *IEEE Journal on Selected Areas in Communications*, 2(7):583-588, July 1984.

[70] A. Polydoros and J. Silvester. Slotted Random Access Spread-Spectrum Networks: An Analytical Framework. *IEEE Journal on Selected Areas in Communications*, SAC-5(6):989-1001, July 1987.

[71] M. B. Pursley. Frequency-Hop Transmission for Satellite Packet Switching and Terrestrial Packet Radio Networks. *IEEE Transactions on Information Theory*, 32(5):652-667, Sept. 1986.

[72] M. B. Pursley. Performance Evaluation for Phase-Coded Spread Spectrum Multiple-Access Communication - Part I: System Analysis. *IEEE Transactions on Communications*, 25(8):793-799, Aug. 1977.

[73] M. B. Pursley and D. V. Sarwate. Performance Evaluation for Phase-Coded Spread Spectrum Multiple-Access Communication - Part II: Code Sequence Analysis. *IEEE Transactions on Communications*, 25(8):800-803, Aug. 1977.

[74] M.B. Pursley. The Role of Spread Spectrum in Packet Radio Networks. *Proceedings of the IEEE*, 75:116-134, Jan. 1987.

[75] D. Raychaudhuri. Performance Analysis of Random Access Packet-Switched Code Division Multiple Access Systems. *IEEE Transactions on Communications*, COM-29(6):895–901, June 1981.

[76] L. G. Roberts. ALOHA Packet System With and Without Slots and Capture. *Comput. Commun. Rev.*, 5:28–42, Apr. 1975.

[77] L. G. Roberts. Dynamic Allocation of Satellite Capacity through Packet Reservation. *in AFIPS Conf. Proc., 1973 National Comput. Conf.*, 711–716, 1973.

[78] E. Y. Rocher and R. L. Pickholtz. An Analysis of the Effectiveness of Hybrid Transmission Schemes. *IBM J. Res. Develop.*, 426–433, July 1970.

[79] D. V. Sarwate and M. B. Pursley. Cross Correlation Properties of Pseudo-Random and Related Sequences. *Proceedings of the IEEE*, 68:598–619, May 1980.

[80] D. V. Sarwate and M. B. Pursley. Crosscorrelation Properties of Pseudorandom and Related Sequences. *Proceedings of the IEEE*, 68:593–619, May 1980.

[81] A. R. K. Sastry. Effect of Acknowledgment Traffic on the Performance of Slotted ALOHA-Code Division Multiple Access Systems. *IEEE Transactions on Communications*, 32(11):1219–1222, Nov. 1984.

[82] A. R. K. Sastry. Performance of Hybrid Error Control Schemes on Satellite Channels. *IEEE Transactions on Communications*, 23:689–694, July 1975.

[83] A. R. K. Sastry and L. N. Kanai. Hybrid Error Control Using Retransmission and Generalized Burst-Trapping Codes. *IEEE Transactions on Communications*, 24:385–393, Apr. 1976.

[84] P. S. Sindhu. Retransmission Error Control with Memory. *IEEE Transactions on Communications*, 25(5):473–479, May 1977.

[85] E. S. Sousa and J. A. Silvester. A Spreading Code Protocol for a Distributed Spread Spectrum Packet Radio Network. *in Proc. GLOBCOM'84*, 481–486, Nov. 1984.

[86] G. L. Stuber. Asymptotic Throughput in Slotted Direct-Sequence Code Division Multiple-Access Networks. *in Proc. MILCOM'88*, 44.6.1–44.6.5, October 1988.

[87] G. L. Stuber. Throughput Analysis of a Slotted Direct-Sequence Spread Spectrum Multiple-Access Network. *submitted to IEEE Transactions on Communications*, 1989.

[88] S. L. Su and V. Li. Performance Analysis of a Slotted Code Division Multiple Access (CDMA) Network. *in Proc. of 7th MIT/ONR C^3 Workshop on Distributed Information and Decision Systems, San Diego, CA*, 115–120, June 1984.

[89] F. A. Tobagi and L. Kleinrock. The Effect of Acknowledgement Traffic on the Capacity of Packet-Switched Radio Channels. *IEEE Transactions on Communications*, 26(6):815–825, June 1978.

[90] F. A. Tobagi and J. S. Storey. Improvements in Throughput of a CDMA Packet Radio Network Due to a Channel Load Sence Access Protocol. *in Proc. Allerton Conf.*, 40–49, 1984.

[91] Y. M. Wang and S. Lin. A Modified Selective-Repeat Type-II Hybrid ARQ System and its Performance Analysis. *IEEE Transactions on Communications*, 31(5):593–608, May 1983.

[92] Y. M. Wang and S. Lin. A Parity-Retransmission Hybrid ARQ Using a Convolutional Code and Viterbi Decoding for Error Control. *in GLOBECOM'82 Conf. Rec.*, E7.1, Dec. 1982.

[93] C. L. Weber and et. al. Performance Considerations of Code Division Multiple-Access Systems. *IEEE Transactions on Vehicular Technology*, VT-30(1):3–9, February 1981.

[94] E. J. Weldon. An Improved Selective-Repeat ARQ Strategy. *IEEE Transactions on Communications*, 30(3):480–486, Mar. 1982.

[95] S. B. Wicker. An Adaptive Type-I Hybrid-ARQ Technique Using the Viterbi Decoding Algorithm. *in MILCOM'88*, 1988.

[96] H. Yamamoto and K. Itoh. Veterbi Decoding Algorithm for Convolutional Codes with Repeat Request. *IEEE Transactions on Information Theory*, 26:540–547, Sept. 1980.

[97] K. Yoa. Error Probability of Asynchronous Spread Spectrum Multiple Access Communication Systems. *IEEE Transactions on Communications*, 25(8):803–809, Aug. 1977.

VITA

Joseph Michael Hanratty ███

He was raised in Aberdeen, Maryland and graduated from Aberdeen High School in 1967. Following graduation in 1972 from the United States Military Academy at West Point, New York, with a Bachelor of Science Degree, he was commissioned as a Second Lieutenant in the United States Army. Following assignments in Germany and Italy, he served with the 101st Airborne Division at Fort Campbell, Kentucky, where he received a Master of Science in Systems Management Degree from the University of Southern California in 1980. Subsequently, he attended the United States Naval Postgraduate School and received the Master of Science in Electrical Engineering in 1982. After serving as an assistant professor with the Department of Electrical Engineering at West Point, he was allowed to continue his graduate studies at the Georgia Institute of Technology in 1986.

He is currently a Major in the United State Army and a Professional Engineer in the state of Virginia.